

# SIEMENS

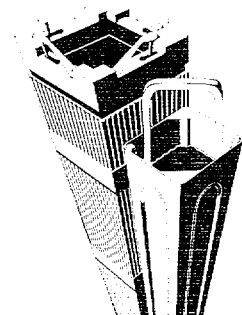
EMF-2361(NP)  
Revision 0

## EXEM BWR-2000 ECCS Evaluation Model

October 2000

Siemens Power Corporation  
Nuclear Division

---



Siemens Power Corporation

ISSUED IN SPC ON-LINE  
DOCUMENT SYSTEM  
DATE: 11/7/00

EMF-2361(NP)  
Revision 0

**EXEM BWR-2000 ECCS Evaluation Model**

Prepared:

N.R.  
S. E. Jensen, Team Leader  
Methods Development

\_\_\_\_\_  
Date

Contributors: J. D. Atchison (Sciencetech), S. C. Franz, M. M. Giles (Consultant), C. E. Hendrix, L. M. Koep, C. J. Lewis, J. A. Pumroy (Manpower), J. C. Rawlings (Consultant), K. D. Richert (Consultant), L. G. Riniker, and D. S. Rowe (Consultant).

Approved:

N.R.  
R. E. Collingham, Manager  
Methods Development

\_\_\_\_\_  
Date

Approved:

N.R.  
M. E. Garrett, Manager  
BWR Safety Analysis

\_\_\_\_\_  
Date

Approved:

J. F. Mallay  
J. F. Mallay, Director  
Regulatory Affairs

10/24/00  
Date

/lmk

**U.S. Nuclear Regulatory Commission  
Report Disclaimer**

**Important Notice Regarding Contents and Use of This Document**

***Please Read Carefully***

This technical report was derived through research and development programs sponsored by Siemens Power Corporation. It is being submitted by Siemens Power Corporation to the U.S. Nuclear Regulatory Commission as part of a technical contribution to facilitate safety analyses by licensees of the U.S. Nuclear Regulatory Commission which utilize Siemens Power Corporation fabricated reload fuel or technical services provided by Siemens Power Corporation for light water power reactors and it is true and correct to the best of Siemens Power Corporation's knowledge, information, and belief. The information contained herein may be used by the U.S. Nuclear Regulatory Commission in its review of this report and, under the terms of the respective agreements, by licensees or applicants before the U.S. Nuclear Regulatory Commission which are customers of Siemens Power Corporation in their demonstration of compliance with the U.S. Nuclear Regulatory Commission's regulations.

Siemens Power Corporation's warranties and representations concerning the subject matter of this document are those set forth in the agreement between Siemens Power Corporation and the Customer pursuant to which this document is issued. Accordingly, except as otherwise expressly provided in such agreement, neither Siemens Power Corporation nor any person acting on its behalf:

- a. makes any warranty, or representation, express or implied, with respect to the accuracy, completeness, or usefulness of the information contained in this document, or that the use of any information, apparatus, method, or process disclosed in this document will not infringe privately owned rights;
- or
- b. assumes any liabilities with respect to the use of, or for damages resulting from the use of, any information, apparatus, method, or process disclosed in this document.

### Abstract

This report describes a revised 10 CFR 50 Appendix K-based boiling water reactor (BWR) loss-of-coolant accident (LOCA) emergency core cooling system (ECCS) evaluation model (EXEM BWR-2000). This evaluation model is an evolution of the current SPC evaluation model, EXEM/BWR, and is applicable to both large- and small-break LOCA analyses. This report summarizes the features of the EXEM BWR-2000 evaluation model and provides a roadmap table to the references that make up the model.

This report describes the changes made to the current EXEM/BWR model to create the EXEM BWR-2000 evaluation model. These changes were made to EXEM/BWR to address issues raised regarding Siemens Power Corporation's (SPC) LOCA methodologies during a 1997 U.S. Nuclear Regulatory Commission (NRC) inspection and to correct known deficiencies in the methodology. The most significant change to the model was to replace the FLEX refill code with an extended RELAX code calculation. This replacement eliminates the need for data transfers from RELAX to FLEX and reduces the number of codes that must be maintained and reviewed. The other changes correct potential problems and address the pump degradation model and model validation concerns raised during the 1997 NRC inspection of SPC's BWR LOCA methodology.

This document presents the peak cladding temperature (PCT) results from the EXEM BWR-2000 model for large- and small-break BWR LOCA cases. The EXEM BWR-2000 model is generally expected to provide LBLOCA PCT results comparable to or below those of the EXEM/BWR model. The SBLOCA PCT results for the model, though generally lower than those calculated by EXEM/BWR, are believed to be more consistent with other vendor PCT results.

This document also provides results for a BWR-3 plant LOCA analysis using EXEM BWR-2000 and results from a series of sensitivity studies for time step variations, nodalization, and model change effects. The EXEM BWR-2000 model was validated against two-loop test apparatus (TLTA) test data and full integral simulation test (FIST) integral test results. The report also summarizes the conclusions drawn from these calculations. The Appendix K-based EXEM BWR-2000 model conservatively predicts LOCA behavior with results that fall within the 10 CFR 50.46 criteria.

### Nature of Changes

Item	Page	Description and Justification
1.		This is a new document.

## Contents

1.0	Introduction and Summary.....	1-1
2.0	SPC BWR LOCA Model References (Roadmap).....	2-1
2.1	Event Description.....	2-1
2.2	Methodology Overview.....	2-4
2.3	Blowdown Phase .....	2-6
2.3.1	Sources of Heat During the LOCA .....	2-7
2.3.2	Initial Stored Energy in the Fuel .....	2-7
2.3.3	Fission Heat.....	2-8
2.3.4	Decay of Actinides .....	2-8
2.3.5	Fission Product Decay .....	2-8
2.3.6	Metal-Water Reaction Rate .....	2-8
2.3.7	Reactor Internals Heat Transfer .....	2-9
2.3.8	Swelling and Rupture .....	2-9
2.3.9	Fuel Rod Thermal Parameters .....	2-9
2.3.10	Break Spectrum .....	2-9
2.3.11	Discharge Model .....	2-9
2.3.12	Noding Near the Break and ECCS Injection Points .....	2-10
2.3.13	Frictional Pressure Drops.....	2-10
2.3.14	Momentum Equation .....	2-10
2.3.15	Critical Heat Flux (CHF) .....	2-10
2.3.16	Post CHF Heat Transfer.....	2-10
2.3.17	Pump Modeling .....	2-11
2.3.18	Jet Pump Modeling .....	2-11
2.3.19	Single Failure .....	2-11
2.3.20	Containment Pressure .....	2-11
2.4	Refill or Spray Cooling Phase .....	2-11
2.4.1	Convective Heat Transfer Coefficients for Spray Cooling .....	2-12
2.4.2	The Boiling Water Reactor Channel Box Under Spray Cooling.....	2-12
2.5	Reflood Phase .....	2-13
3.0	Model Changes .....	3-1
3.1	Replacement of FLEX with RELAX .....	3-1
3.2	RELAX Code Changes .....	3-2
3.2.1	Extension of Ohkawa-Lahey Drift Flux Model.....	3-2
3.2.2	CHF Correlations .....	3-4
3.2.3	CE-EPRI Pump Degradation Model .....	3-8
3.2.4	RELAX Reflood Criteria .....	3-15
3.2.5	Enthalpy Injection Model .....	3-16
3.2.6	Other Changes.....	3-18
3.3	Applications Changes .....	3-18
3.3.1	Increased Jet Pump Noding and Modified Jet Pump Exit Description .....	3-21
3.3.2	Phase-Separation Model in the Bypass.....	3-23
3.3.3	Core Nodalization for LOCA Analysis.....	3-24
3.3.4	Upper Plenum Nodalization.....	3-27

4.0	Model Application and Sensitivities .....	4-1
4.1	BWR LOCA/ECCS Analysis Example Problems .....	4-1
4.1.1	Break Spectrum Example Problems .....	4-1
4.1.2	Large-Break LOCA Example Problem .....	4-7
4.1.3	Small-Break LOCA Example Problem .....	4-21
4.2	EXEM BWR-2000 Methodology Sensitivity Studies .....	4-35
4.2.1	RELAX Nodalization Sensitivity Studies .....	4-35
4.2.2	Time Step Convergence .....	4-44
5.0	Model Validation .....	5-1
5.1	FIST Benchmarks .....	5-2
5.1.1	Large-Break Test 6DB1B .....	5-6
5.1.2	Large-Break Test 4DBA1 .....	5-19
5.1.3	Small-Break Test 6SB2C .....	5-31
5.1.4	Summary of FIST Benchmarks .....	5-50
5.2	TLTA Benchmark .....	5-50
6.0	References .....	6-1
6.1	Model References (Roadmap) .....	6-1
6.2	Other References .....	6-2

### Tables

2.1	LOCA Model References .....	2-14
3.1	Value of Width of the Interpolation Band for the Enthalpy vs. Mass Flux Boundary .....	3-7
3.2	Head Difference Homologous Curves Based on CE-EPRI Data .....	3-13
3.3	Torque Difference Homologous Curves Based on CE-EPRI Data .....	3-14
3.4	Torque Difference Multiplier Table Based on CE-EPRI Data .....	3-14
4.1	EXEM BWR-2000 LOCA Methodology Demonstration Calculations .....	4-5
4.2	EXEM BWR-2000 Methodology LOCA Result Summary .....	4-6
4.3	Event Times for the BWR/3 0.8 DEG/PS SF-LPCI (LOCA) .....	4-8
4.4	Event Times for the BWR/3 0.5 Ft <sup>2</sup> /PD SF-LPCI (LOCA) .....	4-22
4.5	Core Nodalization Sensitivity Study Summary of Results .....	4-36
4.6	Upper Plenum Nodalization Sensitivity Study Summary of Results .....	4-39
5.1	Comparison of Events .....	5-8
5.2	Comparison of Events .....	5-21
5.3	Comparison of SBLOCA Events .....	5-35

## Figures

2.1	EXEM BWR-2000 Methodology.....	2-16
3.1	Effect of Drift Flux Models on Hot Channel Void Distribution .....	3-4
3.2	Boundaries of ANFB Applicability .....	3-7
3.3	Pump Types and Specific Speeds.....	3-15
3.4	Typical RELAX BWR System Model.....	3-20
3.5	RELAX Jet Pump Model.....	3-22
3.6	RELAX Average Core Model, Top Peaked .....	3-25
3.7	RELAX Hot Channel Model, Top Peaked .....	3-26
4.1	RELAX BWR System Model.....	4-3
4.2	RELAX Hot Channel Model, Top Peaked .....	4-4
4.3	Upper Plenum Pressure .....	4-9
4.4	Total Break Flow .....	4-9
4.5	Core Inlet Flow .....	4-10
4.6	Core Outlet Flow .....	4-10
4.7	Intact Loop Jet Pump Drive Flow .....	4-11
4.8	Intact Loop Jet Pump Suction Flow .....	4-11
4.9	Intact Loop Jet Pump Exit Flow .....	4-12
4.10	Broken Loop Jet Pump Drive Flow .....	4-12
4.11	Broken Loop Jet Pump Suction Flow .....	4-13
4.12	Broken Loop Jet Pump Exit Flow .....	4-13
4.13	ADS Flow .....	4-14
4.14	LPCS Flow .....	4-14
4.15	Lower Plenum Liquid Mass.....	4-15
4.16	Average Core Liquid Mass .....	4-15
4.17	Guide Tube Liquid Mass.....	4-16
4.18	Bypass Liquid Mass.....	4-16
4.19	Upper Plenum Liquid Mass.....	4-17
4.20	Hot Channel Inlet Flow .....	4-17
4.21	Hot Channel Outlet Flow.....	4-18
4.22	Hot Node Entrainment Flow.....	4-18
4.23	Hot Node Heat Transfer Coefficient (RELAX) .....	4-19
4.24	Hot Node Rod Temperature (RELAX) .....	4-19
4.25	HUXY Analysis .....	4-20
4.26	Upper Plenum Pressure .....	4-23
4.27	Total Break Flow .....	4-23
4.28	Core Inlet Flow .....	4-24
4.29	Core Outlet Flow .....	4-24
4.30	Intact Loop Jet Pump Drive Flow .....	4-25
4.31	Intact Loop Jet Pump Suction Flow .....	4-25
4.32	Intact Loop Jet Pump Exit Flow .....	4-26
4.33	Broken Loop Jet Pump Drive Flow .....	4-26
4.34	Broken Loop Jet Pump Suction Flow .....	4-27
4.35	Broken Loop Jet Pump Exit Flow .....	4-27
4.36	ADS Flow .....	4-28
4.37	LPCS Flow .....	4-28
4.38	HPCI Flow .....	4-29
4.39	Lower Plenum Liquid Mass.....	4-29



4.40	Average Core Liquid Mass.....	4-30
4.41	Guide Tube Liquid Mass.....	4-30
4.42	Bypass Liquid Mass.....	4-31
4.43	Upper Plenum Liquid Mass.....	4-31
4.44	Hot Channel Inlet Flow.....	4-32
4.45	Hot Channel Outlet Flow.....	4-32
4.46	Hot Node Entrainment Flow.....	4-33
4.47	Hot Node Heat Transfer Coefficient (RELAX).....	4-33
4.48	Hot Node Rod Temperature (RELAX).....	4-34
4.49	HUXY Analysis.....	4-34
4.50	RELAX 3 Node Average Core Model.....	4-37
4.51	Average Core Liquid Mass – Core Nodalization Sensitivity Study.....	4-38
4.52	RELAX Hot Node Surface Temperature - Core Nodalization Sensitivity Study.....	4-38
4.53	Lower Plenum Liquid Mass - Upper Plenum Nodalization Sensitivity Study.....	4-40
4.54	RELAX Hot Node Surface Temperature - Upper Plenum Nodalization Sensitivity Study (RELAX).....	4-40
4.55	RELAX 16-Node Hot Channel Model.....	4-42
4.56	Heat Flux and CHF - Hot Channel Nodalization Sensitivity Study.....	4-43
4.57	RELAX Hot Node Surface Temperature - Hot Channel Nodalization Sensitivity Study.....	4-43
4.58	RELAX Hot Node Surface Temperature - Time Step Convergence Sensitivity Study.....	4-45
5.1	RELAX Nodal Model for FIST.....	5-5
5.2	FIST BWR/6-DB1-B Jet Pump 1 Flow.....	5-9
5.3	FIST BWR/6-DB1-B Jet Pump 2 Flow.....	5-9
5.4	FIST BWR/6-DB1-B Pressure Response.....	5-10
5.5	FIST BWR/6-DB1-B Lower Downcomer Mass Inventory.....	5-10
5.6	FIST BWR/6-DB1-B Jet Pump 1 Mass Inventory.....	5-11
5.7	FIST BWR/6-DB1-B Jet Pump 2 Mass Inventory.....	5-11
5.8	FIST BWR/6-DB1-B Upper Plenum Mass Inventory.....	5-12
5.9	FIST BWR/6-DB1-B Bypass Region Mass Inventory.....	5-12
5.10	FIST BWR/6-DB1-B Lower Lower Plenum Mass Inventory.....	5-13
5.11	FIST BWR/6-DB1-B Upper Lower Plenum Mass Inventory.....	5-13
5.12	FIST BWR/6-DB1-B Bundle Mass Inventory.....	5-14
5.13	FIST BWR/6-DB1-B Temperature Response 75-Inch Elevation (1 of 4).....	5-14
5.14	FIST BWR/6-DB1-B Temperature Response 75-Inch Elevation (2 of 4).....	5-15
5.15	FIST BWR/6-DB1-B Temperature Response 75-Inch Elevation (3 of 4).....	5-15
5.16	FIST BWR/6-DB1-B Temperature Response 75-Inch Elevation (4 of 4).....	5-16
5.17	FIST BWR/6-DB1-B Temperature Response 87-Inch Elevation (1 of 4).....	5-16
5.18	FIST BWR/6-DB1-B Temperature Response 87-Inch Elevation (2 of 4).....	5-17
5.19	FIST BWR/6-DB1-B Temperature Response 87-Inch Elevation (3 of 4).....	5-17
5.20	FIST BWR/6-DB1-B Temperature Response 87-Inch Elevation (4 of 4).....	5-18
5.21	FIST BWR/4-DBA-1 Dome Pressure Response.....	5-22
5.22	FIST BWR/4-DBA-1 Jet Pump 1 Flow Comparison.....	5-22
5.23	FIST BWR/4-DBA-1 Jet Pump 2 Flow Comparison.....	5-23
5.24	FIST BWR/4-DBA-1 HPCI Flow Comparison.....	5-23
5.25	FIST BWR/4-DBA-1 LPCI Flow Comparison.....	5-24
5.26	FIST BWR/4-DBA-1 LPCS Flow Comparison.....	5-24

5.27	FIST BWR/4-DBA-1 Lower Downcomer Mass Inventory Response.....	5-25
5.28	FIST BWR/4-DBA-1 Jet Pump 1 Mass Inventory Response .....	5-25
5.29	FIST BWR/4-DBA-1 Jet Pump 2 Mass Inventory Response .....	5-26
5.30	FIST BWR/4-DBA-1 Lower Lower Plenum Mass Inventory Response.....	5-26
5.31	FIST BWR/4-DBA-1 Upper Lower Plenum Mass Inventory Response.....	5-27
5.32	FIST BWR/4-DBA-1 Hot Assembly Mass Inventory Response .....	5-27
5.33	FIST BWR/4-DBA-1 Bypass Region Mass Inventory Response .....	5-28
5.34	FIST BWR/4-DBA-1 Upper Plenum Mass Inventory Response .....	5-28
5.35	FIST BWR/4-DBA-1 Bundle Mid-Plane Temperature Response.....	5-29
5.36	FIST BWR/4-DBA-1 87-Inch Elevation Temperature Response .....	5-29
5.37	FIST BWR/4-DBA-1 111-Inch Elevation Temperature Response .....	5-30
5.38	FIST BWR/6-SB2-C SBLOCA Dome Pressure Response .....	5-36
5.39	FIST BWR/6-SB2-C SBLOCA Jet Pump 1 Flow .....	5-36
5.40	FIST BWR/6-SB2-C SBLOCA Jet Pump 2 Flow Response .....	5-37
5.41	FIST BWR/6-SB2-C SBLOCA Jet Pump 1 Mass Inventory.....	5-37
5.42	FIST BWR/6-SB2-C SBLOCA Jet Pump 2 Mass Inventory.....	5-38
5.43	FIST BWR/6-SB2-C SBLOCA Lower Downcomer Mass Inventory .....	5-38
5.44	FIST BWR/6-SB2-C SBLOCA Lower Lower Plenum Mass Inventory .....	5-39
5.45	FIST BWR/6-SB2-C SBLOCA Upper Lower Plenum Mass Inventory .....	5-39
5.46	FIST BWR/6-SB2-C SBLOCA Bundle Mass Inventory.....	5-40
5.47	FIST BWR/6-SB2-C SBLOCA Bypass Region Mass Inventory.....	5-40
5.48	FIST BWR/6-SB2-C SBLOCA Upper Plenum Mass Inventory.....	5-41
5.49	FIST BWR/6-SB2-C SBLOCA Temperature Response 75-Inch Elevation (1 of 3).....	5-41
5.50	FIST BWR/6-SB2-C SBLOCA Temperature Response 75-Inch Elevation (2 of 3).....	5-42
5.51	FIST BWR/6-SB2-C SBLOCA Temperature Response 75-Inch Elevation (3 of 3).....	5-42
5.52	FIST BWR/6-SB2-C SBLOCA Temperature Response 87-Inch Elevation (1 of 4).....	5-43
5.53	FIST BWR/6-SB2-C SBLOCA Temperature Response 87-Inch Elevation (2 of 4).....	5-43
5.54	FIST BWR/6-SB2-C SBLOCA Temperature Response 87-Inch Elevation (3 of 4).....	5-44
5.55	FIST BWR/6-SB2-C SBLOCA Temperature Response 87-Inch Elevation (4 of 4).....	5-44
5.56	FIST BWR/6-SB2-C SBLOCA Temperature Response 111-Inch Elevation .....	5-45
5.57	FIST BWR/6-SB2-C SBLOCA EM Temperature Response 75-Inch Elevation (1 of 3) .....	5-45
5.58	EM Temperature Response 75-Inch Elevation (2 of 3) .....	5-46
5.59	FIST BWR/6-SB2-C SBLOCA EM Temperature Response 75-Inch Elevation (3 of 3) .....	5-46
5.60	FIST BWR/6-SB2-C SBLOCA EM Temperature Response 87-Inch Elevation (1 of 4) .....	5-47
5.61	FIST BWR/6-SB2-C SBLOCA EM Temperature Response 87-Inch Elevation (2 of 4) .....	5-47
5.62	FIST BWR/6-SB2-C SBLOCA EM Temperature Response 87-Inch Elevation (3 of 4) .....	5-48

5.63	FIST BWR/6-SB2-C SBLOCA EM Temperature Response 87-Inch Elevation (4 of 4) .....	5-48
5.64	FIST BWR/6-SB2-C SBLOCA EM Temperature Response 111-Inch Elevation.....	5-49
5.65	TLTA Lower Plenum Mass.....	5-51
5.66	TLTA Steam Dome Pressure.....	5-51
5.67	TLTA Broken Loop Jet Pump Discharge Flow .....	5-52
5.68	TLTA Intact Loop Jet Pump Discharge Flow.....	5-52
5.69	Core Inlet Flow .....	5-53
5.70	Hottest Core Temperature .....	5-53

## 1.0 Introduction and Summary

This report describes revisions made to the SPC EXEM/BWR ECCS evaluation model (EM). This upgraded model, called EXEM BWR-2000, continues to meet the requirements of 10 CFR 50 Appendix K. Revisions made to the EXEM/BWR methodology to create EXEM BWR-2000 consist of relatively few changes. The system blowdown code (RELAX) in the methodology was upgraded and the core reflood code (FLEX) was eliminated. The remainder of the codes and methodology are unchanged from the EXEM/BWR model.

The NRC Core Performance Inspection (Inspection Report 99900081/97-01) of SPC in 1997 included an assessment of the EXEM/BWR LOCA methodology. The principal reasons for developing the EXEM BWR-2000 were to address the issues raised during this inspection and to address known deficiencies in the current methodology.

The EXEM/BWR model uses the FLEX code to compute the vessel refill and to define the time of core reflood. Although the use of the FLEX code saved computing time (when using mainframe computers), transferring the system calculation results from the RELAX system blowdown code to the FLEX system refill calculation required substantial data transfer and user intervention. With the aid of advanced computer workstations and the upgraded numerics installed in RELAX in 1991, it became logical to replace the FLEX code by extending the RELAX blowdown calculation through the refill period to predict the time of core reflood. This change eliminates the FLEX code and removes the attendant data transfer between RELAX and FLEX and user intervention.

[  
] Three additional full integral simulation test (FIST) comparisons were incorporated into the RELAX validation test suite to more fully demonstrate its performance.

Code and application changes were implemented to improve the RELAX model performance for refill and reflood and to achieve consistency with current SPC fuel design tools. These changes include:

- [ ]

- [ ]
- An upgrade of the two-phase pump degradation model based on Combustion Engineering - Electric Power Research Institute (CE-EPRI) data.
- Increased core, hot channel, and jet pump nodalization.
- Modification of other application options to improve code performance during refill and reflood including reflood criteria.
- An enthalpy injection model to ameliorate exaggerated condensation of subcooled core spray.

Section 2.0 covers the complete EXEM BWR-2000 model. A "roadmap" is provided which refers to the earlier evaluation models for features that have not been changed and indicates the appropriate sections of the report where the individual changes are described.

Section 3.0 discusses the code improvements and application changes to develop EXEM BWR-2000.

Section 4.0 provides the sensitivity studies and example calculations performed to demonstrate the adequacy of the revised evaluation model. Sensitivity studies include the effects of time-step variation, noding, and the incorporation of the [ ] CHF correlation into the EXEM/BWR heat transfer logic. Sections 4.1.1 and 4.1.2 contain the results for a typical BWR-3, including break spectrum results.

The EXEM BWR-2000 model results are expected to produce limiting transient PCTs between 1635°F to 1905°F. The PCTs for EXEM/BWR LOCA cases were between 1877°F to 1999°F.

Section 5 validates the EXEM BWR-2000 against test data for the standard TLTA benchmark, and against three FIST experiments. The FIST benchmarks include two LBLOCA tests and one SBLOCA test. Generally, the EXEM BWR-2000 model is shown to conservatively bound the test data for large breaks. The test results for small breaks show very low temperatures, and the EXEM BWR-2000 model using evaluation model options bounds the temperature data. The EXEM BWR-2000 model adequately predicts the important LOCA phenomena.

## 2.0 SPC BWR LOCA Model References (Roadmap)

This section provides an overview of and roadmap for SPC's Jet Pump BWR LOCA methodology. The roadmap comprises approved topical report references (Table 2.1) and computer code flow chart (Figure 2.1). The overview covers previously approved models, as well as references to model changes that are more thoroughly detailed in other sections of this report. The SPC BWR LOCA methodology consists of the NRC-approved methodology reports, codes, and guidelines that implement the methodology. The overview addresses the NRC-approved reports and the revisions used to develop EXEM BWR-2000. The roadmap documents the existing methodology approvals and is included to assist the reviewer in understanding the new evaluation model. As such, the roadmap is not intended to be reviewed for approval.

This section also presents an event description and methodology overview describing SPC's analysis approach to the various phases of the LOCA.

### 2.1 *Event Description*

A LOCA is defined as an instantaneous rupture of a reactor coolant system (RCS) pipe with break sizes ranging in cross-sectional area up to and including that of the largest pipe. For analysis purposes, the Jet Pump BWR LOCA event typically is described in three phases: blowdown, spray cooling or refill, and reflood. The blowdown phase covers the period from the beginning of the transient until the reactor coolant system pressure has decreased sufficiently that the ECCS low-pressure-core spray has activated and reached rated flow. Rated flow typically is reached at system pressures of 100 to 120 psig. The refill or spray cooling period begins when rated core spray is achieved and lasts until core reflood begins. Reflood occurs when the emergency core coolant (ECC) water injected into the system has created a mixture of liquid and steam that fills the reactor vessel lower plenum. At this time, the ECC mixture enters the bottom of the core and begins quenching the fuel rods. The time of reflood at a particular core location is defined as the time when a sustained steam flow containing a sufficient quantity of entrained liquid to cool the core is calculated to begin flowing past the plane of interest. Reflood lasts until the fuel rods are quenched. Cooling associated with the entrained liquid at the time of reflood is sufficient to terminate the LOCA temperature rise shortly after reflood begins and to eventually quench the core.

The scenario expected in a Jet Pump BWR during a LOCA is described in Section 4.2.5 of the Compendium of ECCS Research (NUREG 1230) (Reference 1). In this scenario, a large break is assumed to occur in the recirculation loop piping. The most limiting breaks occur either in the pump suction line between the reactor vessel and the recirculation pump (called a suction break) or in the pump discharge pipe from the recirculation pump to the jet pump header (called a discharge break). Coolant rapidly discharges through both sides of the break, with the greater flow coming from the side of the break connected directly to the reactor vessel. Flow from the jet pump side of the break typically is limited by choking of the reverse flow at the restricted jet pump drive nozzle. Flow from the vessel side of the break usually is limited by choking at the break location or at the suction line nozzle from the vessel.

As the reactor vessel begins to depressurize, a signal is quickly generated which initiates closure of the main steam isolation valves (MSIVs). A scram signal follows which inserts the control rods. With closure of the MSIVs, the energy transfer rate from the core often exceeds the removal rate from the break, resulting in a slight pressure rise. Once the reactor power is shut down and the stored energy removed, the system continues to depressurize.

As coolant is lost, the level of the fluid mixture in the vessel downcomer decreases. This level decrease initiates safety injection signals to start the ECC systems and to initiate a timer (usually 100 to 120 seconds) to activate the automatic depressurization system (ADS). Within a few seconds, the downcomer mixture level falls and uncovers the suction to the jet pumps. Uncovery of the jet pump suction has a marked effect on the discharge rate through the loop side of the break, which begins venting steam rather than a two-phase mixture. Also, the intact loop jet pumps, which continue to supply flow at coast down rates to the lower plenum and core, suddenly become ineffective as the suction fluid source becomes steam.

The downcomer level continues to fall and within a few more seconds reaches the level of the suction nozzle to the recirculation loop. At this time, flow from the vessel end of the break also changes from two-phase mixture to steam and the system depressurization rate increases. When the system pressure reaches saturation at the lower plenum fluid temperature, the lower plenum fluid begins flashing, which causes a swell and surge of fluid into the core. The flashing of lower plenum fluid provides a significant increase in core cooling until the flashing effect subsides.

Depending on the BWR design, ECC systems may include high-pressure core spray (HPCS) or high pressure coolant injection (HPCI), low-pressure core spray (LPCS), and low-pressure coolant injection (LPCI). The signal to initiate ECCS flow is received as the downcomer level passes the signal set points. The ECCS flow is delayed until emergency power is available and the ECC pumps have come up to speed, at which time ECCS flow is initiated. Flow rates from each of these systems depend on the system pressure against which the ECC must flow.

In large-scale systems, multi-dimensional effects have been shown to occur in the upper plenum and core during the injection of ECCS spray water into the upper plenum. The spray cooling event scenario is described in the compendium of ECCS research (Reference 1) and in SPC's approved spray cooling topical report, XN-NF-929(P)(A) and Supplements 1 through 4 (Reference 2). The following three different flow regimes have been observed in different fuel assemblies in the core.

- In the highest power core assemblies, steam flow is sufficient to cause counter-current flow limiting (CCFL) conditions to occur at the upper tie plate (UTP), which precludes spray flow from entering the bundle from above, and creates a co-current upward flow.
- In medium-power assemblies, spray liquid flows counter-current down against the upward flow of steam.
- In the low-power peripheral assemblies, the flow can be co-current downward.

In any event, some core cooling is observed throughout the core caused by fluid in the assembly, which is prevented from falling to the lower plenum by CCFL occurring at the side entry orifices. This fluid is supplemented by leakage flow into the assemblies from the bypass region.

The following occurs during spray cooling: The bypass region rapidly fills with ECC and the bypass fluid enters the bottom of the core via flow through the bypass region coolant holes in the lower tie plate and through the channel to tie plate seals. Because of steam updraft from lower plenum venting, the bypass fluid is retained in the fuel assembly and some cooling occurs. Fluid in the vessel lower plenum continues to depressurize and to boil off, which results in significant steam updraft through the core.

The upper plenum rapidly fills with ECC to the level of the spray spargers. The subcooled ECC condenses the steam exiting the core and some liquid flows counter current through the upper tie plate (UTP) to cool the assembly from the top. In the peripheral region, where the fuel



assemblies are "tightly orificed" and the ECC is more subcooled, the condensation of steam exiting the UTP is sufficient to suppress steam updraft, and these fuel assemblies transition within about 10 seconds to a co-current downward flow to the lower plenum.

The flow regimes for the remaining fuel assemblies in the core transition to counter-current and co-current upward flow. The counter-current flow assemblies rapidly fill with ECC from the bypass region, while the co-current upward flow assemblies remove most of the steam from the lower plenum, while entraining the bypass leakage to cool the fuel.

As noted, the upper plenum mixture rapidly drains into the lower plenum through the low power assemblies until the lower plenum fills with a two-phase mixture and reflood begins. Reflood creates an upward flow of two-phase fluid that rapidly achieves sufficient magnitude to remove the decay power being generated. At this time, the LOCA temperature transient is terminated and the core begins to cool and eventually quenches.

## 2.2 ***Methodology Overview***

SPC's BWR LOCA methodology has evolved through four major model submittals and several intervening minor submittals.

- (1) The evolution began with the non-jet pump (NJP) BWR fuel heatup model documented in XN-235(A) (Reference 3) and approved for limited use.
- (2) The water reactor evaluation model (WREM)-based NJP-BWR ECCS evaluation model is documented in XN-75-55(A) and Supplements 1 and 2 (Reference 4). This model introduced the RELAP4 system model calculation and remains approved for NJP-BWR applications.
- (3) The EXEM/BWR LOCA ECCS evaluation model upgraded the NJP models for jet pump BWR applications. This model is documented in XN-NF-80-19(P)(A) Volumes 2, 2A, 2B, and 2C (Reference 5). The RELAP4 model was modified to become the RELAX code and the FLEX code was introduced in this submittal.
- (4) The revised EXEM/BWR model is documented in ANF-91-048(P)(A) (Reference 6), while ANF-91-048(P)(A) Supplements 1 and 2 (Reference 7) document a change to the RELAX jet pump model. This revised EXEM/BWR model is the currently approved evaluation model.

Minor BWR model submittals include a revised model to prevent return to nucleate boiling following calculation of CHF that is documented in XN-76-44(A) (Reference 8), incorporation of the NRC NUREG-0630 swelling and rupture model documented in XN-NF-82-07(P)(A) Revision

1 (Reference 9), replacement of the fuel rod response code GAPEX with RODEX2 in all SPC methodologies as documented in XN-NF-81-58(P)(A) Revision 2 and Supplements 1 and 2 (Reference 10). The EXEM BWR-2000 model retains features from these approved models and incorporates the changes documented in this report.

The EXEM BWR-2000 LOCA evaluation model consists of a series of computer codes linked together to perform loss-of-coolant accident analyses to demonstrate plant and fuel design conformance to 10 CFR 50.46 criteria (Reference 11) and 10 CFR 50 Appendix K (Reference 12) requirements. The EXEM BWR-2000 model computer codes and the information transfers are shown in Figure 2.1. Table 2.1 is a roadmap of the EXEM BWR-2000 methodology including codes, models, approved references, and references to sections of this report for each model change. Overall, the methodology analyzes the transient chronologically in phases consisting of (1) initialization, (2) blowdown, (3) refill or spray cooling, and (4) reflood. System calculations are performed for each phase of the transient. The results of these calculations are used to provide boundary conditions for fuel assembly heatup calculations that yield fuel rod temperatures and metal-water reaction results at the plane of interest for a single fuel assembly throughout the LOCA transient.

The initialization step includes developing initial plant and fuel data used as input for the RELAX system code and a heatup code. Core physics calculations are performed to provide reactor kinetics input, power distribution, and axial power shape. RODEX2 calculations are performed to determine exposure-dependent initial fuel rod conditions. Input for the swelling and rupture calculation is developed and entered into RELAX. XCOBRA calculations are made to provide steady-state thermal-hydraulic assembly pressure and flow conditions. Initial operating conditions are defined and entered into RELAX. Steady-state initialization calculations are performed with RELAX to determine that the code is calculating a correct steady state with regard to flow, pressure distributions, and loss coefficients. In addition, the initialization calculations confirm the steady-state energy balance for each core and fuel assembly node.

When the plant data input and initial steady-state conditions have been achieved, analysis of the system blowdown phase can begin. The system blowdown calculation is made using the RELAX code. A blowdown hot channel calculation also is made that provides boundary condition data for the hot assembly heatup calculation. This hot channel calculation models the single highest powered fuel assembly and can be embedded in the system blowdown

calculation or can be performed separately using upper and lower plenum boundary conditions from the system results. Once rated core spray is reached, the system refill calculation begins. With the EXEM BWR-2000 evaluation model, this calculation is made by extending the RELAX blowdown calculation through refill. RELAX calculates the ECC flow to the lower plenum using the same system and core model used in the blowdown calculation. This one-dimensional model ignores the multi-dimensional effects of ECC flow down the peripheral assemblies discussed in the event scenario. As a result, it predicts a conservatively delayed reflood time compared to expected behavior in a large BWR. The principal output of the RELAX calculation extended through refill or spray cooling is the calculated time of core reflood.

The fuel heatup is calculated using the HUXY computer code (Reference 13). HUXY models a plane of interest in the hot assembly. All rods at the plane of interest are modeled, including such internal structures as a water channel or water rods, and the external coolant channel. The code calculates rod-to-rod and rod-to-structure radiation heat transfer and convection heat transfer to the coolant flow. During the blowdown phase, convective cooling is calculated using the transient heat transfer coefficients and coolant temperatures calculated by the RELAX code. During the spray cooling phase, heat transfer is by radiation supplemented by spray cooling using the heat transfer coefficients given in Appendix K or determined from SPC tests of spray cooling for SPC fuel designs. At the calculated time of reflood, the spray heat transfer coefficients are increased to the approved reflood value, which is sufficient to terminate the temperature rise and cool the core.

### 2.3 *Blowdown Phase*

The blowdown portion of the BWR LOCA extends from accident initiation to the time at which rated low pressure core spray flow is established. This portion of the transient is calculated using the RELAX code. RELAX was developed from the PWR RELAP4-EM code (Reference 14), and is used to predict the interrelated effects of RCS thermal-hydraulics, core and system heat transfer, core neutronics, and reactor coolant pump interactions.

The RELAX code evolved from the RELAP4-EM code, which is part of the WREM developed by the NRC and documented in NUREG-75/056 (Reference 15). Many of the basic features of this code are retained in the RELAX code. SPC (then Exxon Nuclear Company) submitted the RELAP-4-EM code as part of the approved NJP BWR ECCS evaluation model. The Exxon Nuclear Company WREM-based NJP-BWR ECCS evaluation model and its conformance to 10

CFR Appendix K requirements are documented in report XN-75-55 (A) Revision 2 (Reference 4). To analyze jet pump BWRs, the RELAP4-EM code was modified to create the RELAX code, which was submitted and approved as part of the EXEM/BWR ECCS evaluation model. EXEM/BWR is documented in topical report XN-NF-80-19(P)(A) Volumes 2, 2A, 2B, 2C (Reference 5). Modifications to create RELAX included incorporating a drift flux slip flow model, a jet pump model, and three additional heat transfer regimes (natural convection, condensation, and pool film boiling).

Upgrades to the EXEM/BWR evaluation model were submitted and approved in topical report ANF-91-048(P)(A) (Reference 6). Upgrades to RELAX in that evaluation model include revising numerical methods to improve convergence and automatic time step control, replacing of the Dougall-Rohsenow correlation with a modified Dougall-Rohsenow correlation to eliminate the known nonconservatism, and improving the critical flow model, bubble mass integration model, drift flux model, pump model, and jet pump model. Supplements 1 and 2 (Reference 7) to ANF-91-048(P)(A) document an approved revision to the RELAX jet pump model.

The most recent revisions to RELAX, which are part of the EXEM BWR-2000 model and are documented in this report, include the following:

- [
- ]
- Implementation of the CE-EPR pump degradation model.
- Changes in nodalization and user-selected input.

The current EXEM BWR-2000 features and their conformance to Appendix K of 10 CFR 50 is presented in the following sections.

#### 2.3.1 Sources of Heat During the LOCA

Infinite operating time at 102% of licensed power is assumed, and a worst case power peaking distribution is input for both the blowdown and heatup calculations (Reference 4, Section 3.0).

#### 2.3.2 Initial Stored Energy in the Fuel

RODEX2 is the approved code for calculating initial stored energy. The stored energy calculated as a function of burnup and fuel rod conditions from RODEX2 are input to both HUXY

and RELAX. The initial fuel rod temperatures (stored energy) in both HUXY and RELAX are adjusted to be consistent with or higher than RODEX2 results (Reference 10).

### 2.3.3 Fission Heat

Fission heat is calculated using the point kinetics model in RELAX. Conservative reactivity feedback from moderator density (voids) and Doppler (fuel temperature) is input. A bounding scram reactivity curve is input (Reference 4, Section 3.3).

### 2.3.4 Decay of Actinides

Actinide decay equations from the NRC WREM model are used to calculate actinide decay heat. A conservatively high conversion ratio is input. No conservative multiplier is applied to the actinide decay calculations (Reference 15, Section 2.1; Reference 4, Sections 3.4 and 3.5; and Reference 6, Section 3.3).

### 2.3.5 Fission Product Decay

The 11 decay equation curve fit to the 1971 draft ANS standard for fission product decay heat from the WREM model is used to calculate fission product decay heat during blowdown. The draft ANS standard values are used for spray cooling and reflood. The required multiplier of 1.2 is applied to the fission product decay heat throughout the LOCA transient (Reference 15, Section 2.1 and Reference 4, Section 3.5).

### 2.3.6 Metal-Water Reaction Rate

The metal-water reaction rate is calculated using the Baker-Just equation, which is applied to the outer cladding surface as required. Once cladding rupture has been predicted, the reaction is initiated on the interior cladding surface as well. The effects of swelling and rupture also are included (Reference 14, Volume II, Section 4.4; Reference 4, Section 3.6; and Reference 9).

The Baker-Just metal-water reaction rate equation accommodates including a preaccident oxidation. The preaccident oxidation value, used to calculate the oxidation generated during a LOCA, is determined as stated on page D-22 of the safety evaluation report (SER) for the HUXY code (Reference 13) "...no larger than can be reasonably justified, including consideration of the effects of manufacturing processes, hot-functional testing and exposure." To determine the total oxidation required to ensure that the 10 CFR 50.46 maximum cladding oxidation limit (metal reacted  $\leq 0.17$  times the total thickness of the cladding before oxidation) is

not exceeded, SPC calculates the metal-water reaction oxidation that occurs during LOCA. Typically, SPC assumes no preaccident cladding oxidation thickness, although a small initial oxide is allowed if it can be justified.

### 2.3.7 Reactor Internals Heat Transfer

Heat transfer from significant nonnuclear sources is included in the calculations. These sources include the following components (Reference 4, Section 3.7):

- Reactor vessel
- Recirculation loop piping
- Lower plenum internals
- Steam dryers
- Shroud
- Shroud dome and separators.

### 2.3.8 Swelling and Rupture

The NUREG-0630 model is used to calculate swelling and rupture as documented in Reference 9.

### 2.3.9 Fuel Rod Thermal Parameters

SPC evaluation models use temperature-dependent thermal property data taken from the NRC WREM (Reference 15, Section 2.4). Initial gap conductance is equivalent to that calculated by RODEX2 for the conditions being analyzed (Reference 10). Thermal properties for gadolinia-bearing fuel rods are from Reference 16.

### 2.3.10 Break Spectrum

A spectrum of both large and small breaks for is evaluated. Double ended guillotine breaks with discharge coefficients ranging from 1.0 to 0.4 are calculated. Split breaks are calculated with break areas up to the cross-sectional area of the largest pipe (Reference 4, Sections 3.9 and 7.1).

### 2.3.11 Discharge Model

When saturated fluid conditions are calculated, choked flow is determined using the required Moody critical flow model. For subcooled liquid, the Henry-Fauske model is used (Reference

15, Section 3.2). A minor change was made to the critical flow model in RELAX (Reference 6, Section 3.1.4).

#### 2.3.12 Noding Near the Break and ECCS Injection Points

The system nodalization used in the vicinity of the break is defined in Reference 4, Section 3.11.

#### 2.3.13 Frictional Pressure Drops

Frictional pressure losses are calculated using the methods from the base RELAP4 code. The modified Baroczy correlation is used in the RELAX code to calculate two-phase friction multipliers. See the RELAP4 manual (Reference 17, Section 2.3).

#### 2.3.14 Momentum Equation

The momentum equation is taken from the basic WREM model (Reference 4, Section 3.13). This model has been shown to conform to Appendix K (Reference 18). A slip flow model based on drift flux was added to RELAX when EXEM/BWR was created (Reference 5, Section 2.2). The RELAX code also was upgraded in the revised EXEM/BWR submittal; the upgrade included changes to the numerical solution method, drift flux model, and the pump model (Reference 6, Section 3.1). A change to [ ] is documented in Section 3.1.1 of this report.

#### 2.3.15 Critical Heat Flux (CHF)

Earlier versions of RELAX calculated CHF using the [ ] as

documented later in Section 3.1.2 of this report.

#### 2.3.16 Post CHF Heat Transfer

The initial heat transfer correlations are identical to those documented in the WREM report (Reference 15, Section 3.4). The correlations were updated in the EXEM/BWR submittal by incorporating correlations for additional regimes, including natural convection, condensation, and pool film boiling (Reference 5, Volume 2A, Section 4.0). The EXEM/BWR model update

included replacing the Dougall-Rohsenow correlation with a modified Dougall-Rohsenow correlation to remove the known nonconservatism (Reference 6, Section 3.1.10).

#### 2.3.17 Pump Modeling

The EXEM BWR-2000 model uses the dynamic pump model taken from the RELAP4-EM code and the WREM. This model requires four-quadrant data to be input for the specific pump being modeled (Reference 17, Section 5.0, Reference 15, Section 3.1). A minor change to the pump model was documented in the EXEM/BWR revision (Reference 6, Section 3.1.8).

In EXEM BWR-2000, the two-phase pump degradation model based on Semiscale pump data has been replaced with a new degradation model based on much more prototypical data from the CE-EPRI tests. The new two-phase pump degradation model is documented in Section 3.1.3 of this report.

#### 2.3.18 Jet Pump Modeling

The jet pump model was included with the initial EXEM/BWR submittal (Reference 5, Volume 2A, Section 3.0). The jet pump model has been updated several times (Reference 6, Section 3.1.9; Reference 7). Modifications to jet pump noding and modeling also are included as part of this EXEM BWR-2000 upgrade; these modifications are described in Section 3.2.1.

#### 2.3.19 Single Failure

The worst single failure is assumed. This failure may be based on previous evaluations by the Nuclear Steam Supply System (NSSS) vendor or may be calculated by SPC (Reference 4, Section 3.17.1).

#### 2.3.20 Containment Pressure

For spray cooling, a conservative containment pressure is assumed (Reference 4, Section 3.17.2).

### 2.4 ***Refill or Spray Cooling Phase***

The refill or spray cooling period begins at the time rated core spray flow is achieved and ends at the time of core reflood. Calculations during this period consist of a system calculation to determine the flow of ECCS fluid into the reactor vessel lower plenum and a core heatup calculation. The system calculation is performed by extending the RELAX calculation through



refill and reflood. The principal results of the RELAX refill calculation are the time of reflood at the plane of interest and the time of reflood in the bypass region. These reflood times are input to the heatup calculation, which is performed using the HUXY code.

The HUXY code (References 13 and 19) computes rod temperatures and oxidation for the hot plane in the maximum power fuel assembly throughout the entire transient. As previously noted, during blowdown, heat removal is calculated by applying the RELAX calculated heat transfer coefficients and fluid temperatures as convection boundary conditions on the HUXY calculation. During the spray cooling period, HUXY calculates cooling by radiation among rods within the assembly, to the internal assembly structure such as water rods or internal channels, and to the assembly channel. Convection heat transfer also is calculated based on conservative spray cooling heat transfer coefficients applied to the rods in the assembly according to position. Spray cooling coefficients are based on a saturated sink temperature, and may vary among fuel designs. SPC often uses the conservative values specified in Appendix K, and confirms that the coefficients are appropriate by comparing HUXY calculations using the assumed spray cooling coefficients to measured spray cooling data for the specific fuel design. For some fuel designs, SPC has developed spray cooling coefficients directly from the measured spray cooling data. These coefficients have been reviewed and approved, and are applied for analysis of these specific fuel designs.

#### 2.4.1 Convective Heat Transfer Coefficients for Spray Cooling

After rated core spray flow from one low-pressure core spray system has been calculated, but before reflooding, spray cooling heat transfer coefficients are applied. The convective spray cooling heat transfer coefficients must be appropriate for the fuel design being analyzed. These coefficients may be conservative values (Appendix K) confirmed by analysis of experimental data.

#### 2.4.2 The Boiling Water Reactor Channel Box Under Spray Cooling

Before establishing rated spray flow, heat transfer from and wetting of the fuel channel is treated the same way as for the fuel rods in the hot channel, except that [

] After rated spray flow, but before wetting of the channel, a coefficient of 5 Btu/hr-ft<sup>2</sup>-°F is applied to both sides of the channel. Channel wetting is assumed to occur

60 seconds after the time determined using the Yamanouchi analysis for the elevation under consideration (Reference 4, Section 3.19).

For the core bypass side of the canister after the time of bypass reflood, the heat transfer coefficient beneath the bypass mixture level is set to a conservative value, 25 Btu/hr-ft<sup>2</sup>-°F (Reference 6, Section 2 and Correspondence Page 43).

## 2.5 ***Reflood Phase***

The reflood phase begins at the time of reflood for the plane of interest. The RELAX calculation has been modified to predict the time at which reflood entrained cooling has reached the plane of interest. The RELAX code is not required to calculate system behavior beyond the initial reflood, and the system calculation can be terminated after the time of hot plane reflood. The HUXY calculation continues through reflood by applying the Appendix K reflood heat transfer coefficient, 25 Btu/hr-ft<sup>2</sup>-°F. This level of cooling is sufficient to terminate any temperature rise and to eventually cool the core.

### Reflood Heat Transfer

Once the two-phase reflooding fluid is calculated to reach the plane of interest, the coefficient of 25 Btu/hr-ft<sup>2</sup>-°F is applied (Reference 4, Section 3.18).

Table 2.1 LOCA Model References

Model	Reference	This Report
<b>Core Physics Input</b>	Ref. 21; Ref. 20	Sect. 2.2
Delayed Neutron Fraction per Mean Lifetime	Ref. 21; Ref. 20	
Moderator Density Reactivity Table	Ref. 21; Ref. 20	
Doppler (Fuel Temperature) Reactivity Table	Ref. 21; Ref. 20	
U-238 Capture Coefficient	Ref. 21; Ref. 20	
Gamma Smearing	Ref. 4	
Axial Power Distribution	Ref. 21; Ref. 20	
Rod Bow Considerations	Ref. 22	
Power Spike Considerations	Ref. 14, Vol. 1, Sect. 12.3	
Radiation Model Radial Pin Power Distribution	Ref. 21; Ref. 20	
Gadolinia Rod treatment	Ref. 21; Ref. 20	
RODEX2 Power Histories	Ref. 10	
<b>Fuel Rod Models</b>		
RODEX2 Thermal Mechanical Models	Ref. 10	Sect. 2.2
RELAX Models	Ref. 7; Ref. 6; Ref. 5; Ref. 4; Ref. 15; Ref. 15; Ref. 17	Sect. 2.3; 3.1, 3.2
FLEX Models	Ref. 6; Ref. 5	Sect. 2.2
HUXY Models	Ref. 6; Ref. 5; Ref. 4; Ref. 3; Ref. 13; Ref. 19	Sect. 2.2; 2.4; 2.5
Cladding Swelling and Rupture	Ref. 9	Sect. 2.3.8
<b>Containment Models</b>	Ref. 4, Sect. 3.17.2	Sect. 2.3.20
<b>RELAX Blowdown</b>	Refs. 14, 15, 4, 5, 6, & 7	Sect. 2.3
Fluid Equations	Refs. 15, 4, & 5	Sect. 2.3
Numerical Solutions	Ref. 6	Sect. 2.3
Momentum Equations	Ref. 4, Sect. 3.13; Ref. 5, Sect. 2.2	Sect. 2.3.14
Heat Transfer Correlations	Ref. 15, Sect. 3.4; Ref. 5 Vol. 2A, Sect. 4; Ref. 6, Sect. 3.10	Sect. 2.3.16
Pump Model	Ref. 17, Sect. 5; Ref. 15, Sect. 3.1; Ref. 6, Sect. 3.1.8	Sect. 2.3.17; 3.1.3

Table 2.1 LOCA Model References (Cont.)

Model	Reference	This Report
<b>RELAX Blowdown (Continued)</b>		
Jet Pump Model	Ref. 5, Vol. 2A, Sect. 3.0; Ref. 6, Sect. 3.1.9; Ref. 7	Sect. 2.3.18; 3.2.1
Discharge Model	Ref. 15, Sect. 3.2; Ref. 6, Sect. 3.1.4	Sect. 2.3.11
Reactor Internals Heat Transfer	Ref. 4, Sect. 3.7	Sect. 2.3.7
CHF Correlation		Sect. 2.3.15; 3.1.2
CHF Lockout	Ref. 4; Ref. 8	
Fission Heat	Ref. 4, Sect. 3.3	Sect. 2.3.3
Fission Product Decay Heat	Ref. 14, Sect. 2.1; Ref. 4, Sect. 3.5	Sect. 2.3.5
Actinide Decay Heat	Ref. 15, Sect. 2.1; Ref. 4, Sect. 3.4; Ref. 6, Sect. 3.3	Sect. 2.3.4
Material Properties	Ref. 15, Sect. 2.4; Ref. 10	Sect. 2.3.9
Frictional Pressure Drop	Ref. 17, Sect. 2.3	Sect. 2.3.13
Phase Separation	Ref. 5; Ref. 6	Sect. 2.3; 3.1.1
Initial Oxide Thickness	Ref. 13, Appendix D	
Nodalization	Ref. 4, Sect. 3.11	Sect. 2.3.12; 3.2.1; 3.2.3; 3.2.4
<b>RELAX Refill Model</b>	Ref. 5, Vol. 2B	Sect. 2.2
Bypass Region Model	Ref. 5, Vol. 2B, Sect. 4.0	Sect. 3.2.2
Phase Separation Models	Ref. 5, Vol. 2B, Sect. 5.1	Sect. 3.1.1; 3.2.2
<b>HUXY Heatup Model</b>	Ref. 3	Sect. 2.2
General Fuel Model	Ref. 13, Sect. 2.1.2	
Radiation Model	Ref. 13, Sect. 2.1.3	
Convection Model	Ref. 13, Sect. 2.1.4	
Material Properties	Ref. 13, Sect. 3	
Blowdown Cooling Model	Ref. 5, Sect. 2.0	Sect. 2.3
Spray Cooling Model	Ref. 4, Sect. 3.18; Ref. 2	Sect. 2.4
Reflood Cooling Model	Ref. 4, Sect. 3.19	Sect. 2.5
Metal-Water Reaction Model	Ref. 13, Sect. 2.5	Sect. 2.3.6
Swelling and Rupture Model	Ref. 9	Sect. 2.3.8

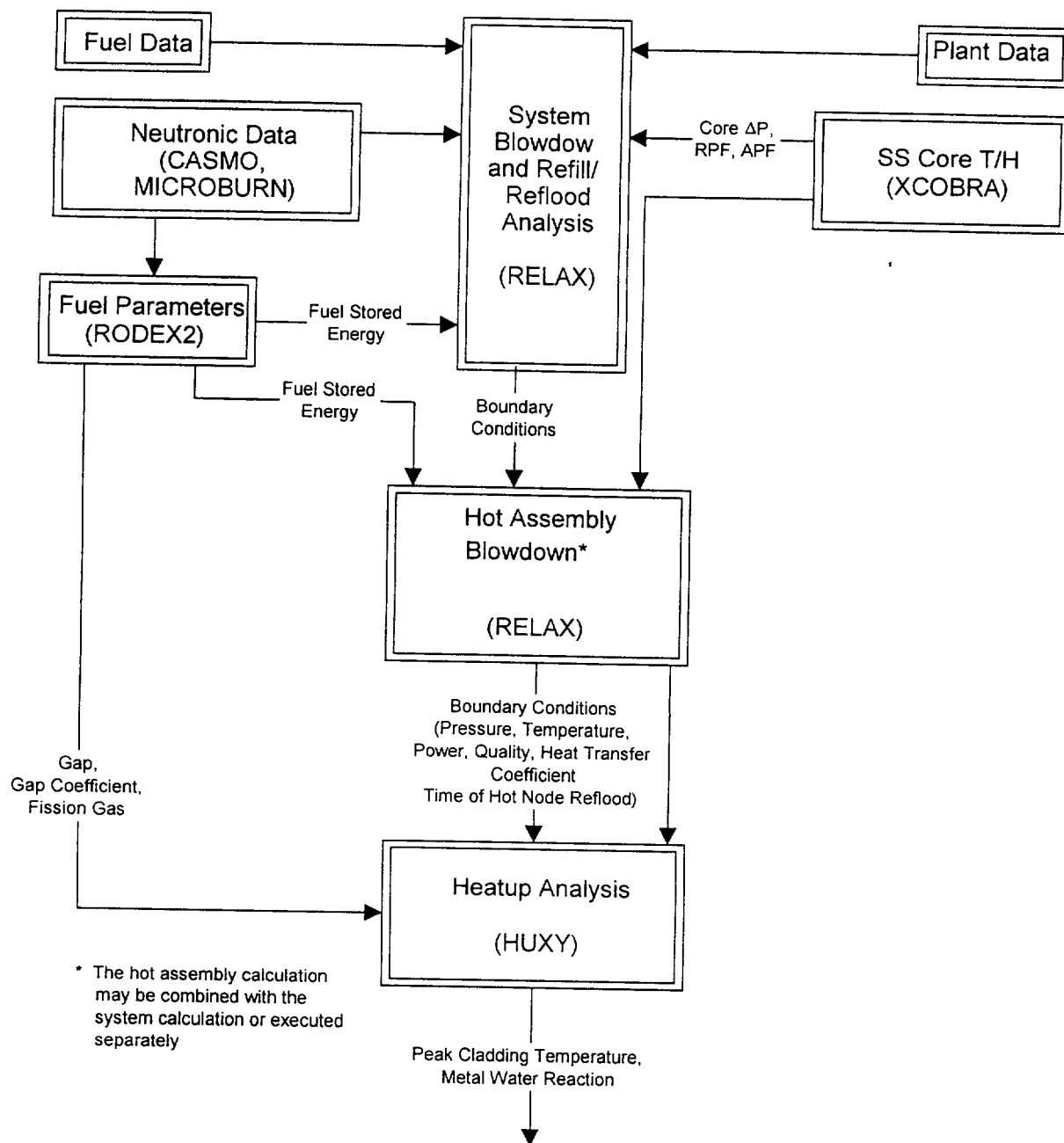


Figure 2.1 EXEM BWR-2000 Methodology

### 3.0 Model Changes

The currently approved EXEM/BWR evaluation model requires the use of plant and fuel data, core physics calculation results from CASMO and MICROBURN and steady-state thermal-hydraulic results from XCOBRA. The EXEM/BWR evaluation model codes consist of the RODEX2 code, which provides burnup-dependent fuel parameters; the RELAX code, which calculates the system and hot channel blowdown transient; the FLEX code, which calculates the system response during refill to the time of core reflood; and the HUXY code, which takes input from the system calculation results and computes the fuel heatup of the maximum power assembly at the plane of interest over the entire LOCA transient.

Changes were made to EXEM/BWR to correct deficiencies in the methodology and to address issues raised during the 1997 NRC inspection of SPC's LOCA methodologies. The EXEM BWR-2000 revisions described in this document represent minor revisions to the EXEM/BWR methodology. Only two codes, FLEX and RELAX, are affected by the changes. The RODEX2 and the HUXY codes do not change, nor do any of the codes providing input to the methodology, neither does the way these codes are applied. The principal methodology change was to run the RELAX code from the end of blowdown through the time of core reflood to replace the FLEX calculation with an extended RELAX calculation. This change eliminates the FLEX code from the methodology. Therefore, the code changes described in the following sections apply only to the RELAX code.

#### 3.1 *Replacement of FLEX with RELAX*

Replacing FLEX with RELAX improves the methodology by eliminating the need to transfer the system calculation from the RELAX code to a second code, FLEX. The FLEX code was originally introduced to simplify the refill calculation when EXEM/BWR was created. With the computers available at that time, running RELAP4-based codes was very expensive, and the results tended to become unstable during periods of cold water injection. These problems were avoided by using the separate simplified FLEX model, and the overall calculations were demonstrated to be conservative. Since that time, the numerics of the RELAX code have been significantly upgraded and computer running time and costs no longer are limiting. SPC has determined that RELAX, with the changes described in the following sections, adequately calculates the phenomena that determine the flow of liquid to the lower plenum and can be used for the refill phase. The RELAX calculation is now extended beyond the time of rated core

spray flow and continues until the lower plenum has filled with a steam/water mixture and liquid has entered the core, resulting in sufficient entrainment at the plane of interest to cool the core. As in the previous EXEM/BWR model, the calculated heat transfer coefficients from the refill analysis are not used in the heatup analysis during the spray cooling period; RELAX does calculate heat transfer during spray cooling, but this heat transfer is not input to HUXY. The RELAX refill calculation provides only the calculated times of core and bypass reflood.

### 3.2 **RELAX Code Changes**

RELAX was changed for two reasons. The first was to extend the applicability of the RELAX code through refill until the time of reflood. The second was to resolve minor bugs and improve the methodology by eliminating potential problems. Sections 3.2.1 through 3.2.6 describe the changes to RELAX.

#### 3.2.1 Extension of Ohkawa-Lahey Drift Flux Model

One of the original changes to create the RELAX code for the EXEM/BWR evaluation model incorporated a drift flux model to provide phase separation in the core. The EXEM/BWR drift flux model is described in Section 2.0 of XN-NF-80-19(P)(A), Volume 2A, Revision 1 (Reference 5). In this model, the drift flux is calculated as a function of void fraction using a flow-regime-dependent drift flux formulation, as shown in Figure 2.1 of Reference 5. Drift flux correlations developed by Ishii and Ohkawa-Lahey were incorporated as part of this drift flux modeling.

Subsequently, the Ishii formulation has been found to have a singularity and could yield nonphysical results for some conditions. When the EXEM/BWR model was revised, the NRC reviewer questioned the use of the Ishii drift flux formulation (Reference 6). At that time, SPC defended use of the model because no significant problems had been observed as a result of using this formulation. However, the potential for obtaining nonphysical results still exists and SPC has now elected to eliminate this potential problem.

[

]

[

]

The effect of this change is to remove the nonphysical discontinuity without greatly changing the calculated drift flux phenomena. Figure 3.1 shows the effect of this change on the calculated void fraction distribution during steady-state operation in a hot fuel assembly. The calculated effect on void fraction is quite small.



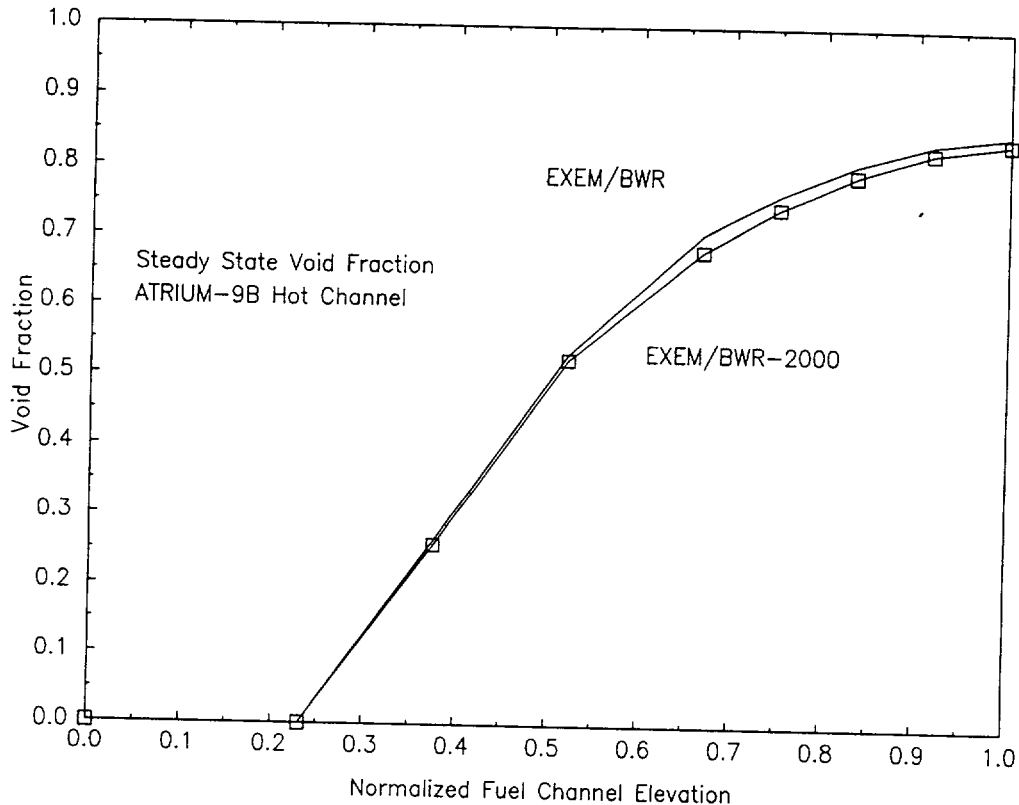


**Figure 3.1 Effect of Drift Flux Models on Hot Channel Void Distribution**

### 3.2.2 CHF Correlations

Another feature added to the RELAX code to improve the EXEM BWR-2000 methodology and eliminate a potential problem area is the [

] Extensive testing is performed to demonstrate and correlate the CHF performance over a wide range of possible conditions. This results in a CHF correlation that applies to a specific SPC fuel design(s). These correlations are reviewed and approved by the NRC. SPC fuel and core designs are developed based on results of the design-specific CHF correlation; however, [

]

[

]

As an example of using a design-specific CHF correlation, the ANFB CHF correlation (Reference 24) has been added to RELAX. This addition provides an initial steady-state CHF margin consistent with fuel design calculations and RELAX initialization parameters. The ANFB critical power correlation is an empirical representation of planar average thermal-hydraulic fluid conditions at which boiling transition has been experimentally determined. The minimum heat flux required to produce boiling transition is predicted from fluid conditions of pressure, mass velocity, and enthalpy averaged over the plane of interest. The correlation contains correction factors for the effects on boiling transition caused by a nonuniform axial heat flux profile and the grouping of the relatively high-powered rods (Reference 24).

The formulation of the ANFB correlation is as follows:

The ANFB correlation was introduced into the code by constructing a bridge between RELAX and the ANFB subroutines used in the steady-state calculations used to initialize many of the RELAX core parameters. [

] The enthalpies required by ANFB also are the enthalpies calculated in the drift flux junctions. Because CHF is calculated based on node centers, the flow-weighted enthalpies calculated at the volume junctions are averaged. Boundaries of applicability include pressure in the range of 500 psia to 1500 psia, enthalpy as described in Figure 3.2, core inlet subcooling using mixture enthalpies in the range of 1.0 to 250.0 Btu/lb<sub>m</sub>, and mass flow of 0.1 to 1.5 M lb<sub>m</sub> / hr ft<sup>2</sup>. Outside the applicability range of the ANFB correlation, the RELAX code uses the existing approved correlations. At the boundaries of the ANFB correlation, an interpolation to the existing correlation is implemented to smooth the transition. The value of the width of the interpolation band for the enthalpy vs. mass flux boundary is described in Table 3.1. The interpolation band around the mass flow and pressure limits is 5% of the boundary values. For the enthalpy vs. mass flux boundary, the interpolation is performed conservatively outside of the correlation applicability range. For the boundaries of pressure and mass flux, the interpolation is performed within the range of applicable values. The subcooling boundary is not used for transient calculations but can be activated by the user for steady-state calculations.

An interpolation scheme similar to the one presented here also will be used with the implementation of other SPC CHF correlations approved by the NRC.

**Table 3.1 Value of Width of the Interpolation Band  
for the Enthalpy vs. Mass Flux Boundary**



**Figure 3.2 Boundaries of ANFB Applicability**

### 3.2.3 CE-EPRI Pump Degradation Model

SPC's EXEM/BWR evaluation model currently uses a two-phase degradation model based on early Semiscale pump data. Since the original WREM model was approved, two-phase testing has been performed on centrifugal pumps that are much more representative of reactor coolant pumps than the small-scale pumps used in the Semiscale program. The NRC questioned the applicability of the Semiscale pump degradation data during its 1997 inspection (Reference 25). Along with the pump model for SPC's ECCS Evaluation Model for PWR LBLOCA (EMF-2087(P)(A) - Reference 26), the RELAX pump model has been modified to incorporate a new two-phase pump performance degradation model based on data from the CE-EPRI pump two-phase performance program (Reference 27). The CE-EPRI pump data are more representative of PWR and BWR reactor coolant pumps than the Semiscale pump data traditionally used for this purpose.

RELAX treats two-phase pump head degradation by first calculating the single-phase pump head, then subtracting a degradation correction term:

$$H = H_{1\phi} - M_H (H_{1\phi} - H_{2\phi}) \quad (3.2)$$

where

$H_{1\phi}$  = single-phase pump head  
 $H_{2\phi}$  = two-phase, fully degraded pump head  
 $M_H$  = head difference multiplier

This equation uses either user supplied single-phase homologous head curves and two-phase head difference curves or default curves built into RELAX. Default single-phase homologous curves are available for either Westinghouse or Bingham reactor coolant pumps. The built-in difference curves supplied by RELAX are based on Semiscale two-phase degradation data. In the previous RELAX formulation, the head difference multiplier,  $M_H$ , is solely a function of pump void fraction and must be supplied by the user.

The CE-EPRI pump two-phase degradation test results are based on pumps more representative of PWR and BWR reactor coolant pumps (RCP) than the Semiscale pumps, and make possible a more realistic analysis of two-phase degradation effects. The CE-EPRI test pump is more closely scaled to a BWR RCP than the Semiscale pump in three key areas:

pump size, pump type (radial vs. mixed flow), and pump specific speed. Specific speed is a characteristic number providing a measure of geometric equivalence among pumps. Figure 3.3, based on Reference 28, shows the relative specific speeds of the Semiscale and CE/EPRI pumps and of representative primary coolant pumps for BWRs and PWRs. The new degradation model based on CE-EPRI data can be implemented in RELAX by using the existing formulation except for the head difference multiplier,  $M_H$ , which includes a pump speed/flow and inlet pressure dependency.

The revised RELAX code calculates  $M_H$  by using a formula based on the CE-EPRI data. The formula incorporates dependencies for pump speed, flow, and inlet pressure. This formula is designed to optimize the accuracy of the two-phase degradation calculation in the AN and VN octants of the pump performance plane. These octants are the most critical for BWR LOCA analysis and are defined as

AN - positive flow rate and rotation speed,  $v/a \leq 1.0$

VN - positive flow rate and rotation speed,  $a/v < 1.0$

where the pump speed ratio is given by

$a = \text{actual rotational speed} / \text{rated rotational speed}$

and the pump flow ratio is given by

$v = \text{actual volumetric flow rate} / \text{rated volumetric flow rate}.$

Head difference multipliers generally approach 0.0 at void fractions of 0.0 and 1.0. In these two limiting cases we have single-phase flow, either liquid or vapor. For intermediate void fractions, head difference multipliers rise to a maximum of 1.0 in the range of void fractions for which maximum degradation occurs. The commonly used Semiscale formulation predicts maximum degradation over a wide range of void fractions (0.2 to 0.9), while the model based on CE-EPRI data indicate that maximum degradation occurs in a much narrower range of void fractions (0.6 to 0.9).

#### Two-Phase Head Difference Multiplier in AN Region

In the AN octant, head difference multipliers derived from the CE-EPRI data are seen to depend primarily on pump void fraction, hence an analytical expression in terms of void fraction,  $x$ , has

been derived that accurately reproduces the EPRI data at a v/a ratio of 1.0. In RELAX, the following curve fit for  $M_H$  is used throughout the AN octant, independent of the v/a ratio:



#### Head Difference Multiplier in VN Region

The CE-EPRI data indicate that, in the VN octant, the void fraction for maximum degradation is a function of the ratio a/v, moving toward lower void fractions as a/v decreases. A curve fit to the EPRI data allows the void fraction for maximum degradation to be expressed as



Using Equation 3.7 for  $\alpha_{MAX}$ , the head difference multiplier in the VN octant may be approximated analytically by the following quadratic functions:



To smoothly merge the multiplier formulations used in the AN and VN octants, Equations 3.3 - 3.9 are used in the VN octant for  $a/v$  values between 0.0 and 0.9.

Between  $a/v = 0.9$  and 1.0, both AN and VN region multipliers are calculated, and a linear interpolation (based on  $a/v$ ) between these two values is used to obtain the actual multiplier to be used.

#### Pressure Dependence of Pump Head Degradation

The CE-EPRI data show that the magnitude of two-phase degradation effects depends on pump inlet pressure. Two-phase degradation effects tend to become more significant at lower pressures, presumably because of the greater difference in phase densities at lower pressures. Kastner and Seeberger (Reference 28) indicate the range of pump pressures and void fractions that might be encountered in hypothetical LOCA analyses. Pressures significantly below 850 psia are encountered only at void fractions above 0.8, where degradation effects become insignificant. The CE-EPRI data show very little difference between 1000 psia and 850 psia head degradation in the AN region near rated operating conditions. At off-rated conditions, Kastner and Seeberger show a significant difference (approximately 33%) between low-flow AN region head degradation at 1000 psia and 850 psia. CE-EPRI results reveal an approximate 33% difference between 1000 psia and 850 psia head degradation in the high-flow VN region.

The head difference multiplier formulations are based on CE-EPRI data at 1000 psia. In RELAX, these equations are used for all pressures above 1000 psia. At pressures between 1000 psia and 850 psia, an adjustment factor increasing linearly from 1.0 to 1.33 is applied to the two-phase head multiplier. This pressure correction factor is given by



where  $P_{inlet}$  is the pump inlet pressure (psia).

#### Implementation of CE-EPRI-Based Two-Phase Degradation Model

The CE-EPRI-based two-phase degradation model specifies only the pump two-phase head difference multiplier formulation. This multiplier is intended for use with head difference curves derived from the CE-EPRI data. Table 3.2 shows the appropriate head difference curves. The head difference  $dh$  used in Table 3.2 is defined as

$$dh = h_{1\phi} - h_{2\phi} \quad \text{where} \quad h = \frac{H_{actual}}{H_{rated}} \quad \text{and } H \text{ is pump head.} \quad (3.13)$$

#### Pump Two-Phase Torque Degradation Model

RELAX treats two-phase pump torque degradation in the same way that it treats head degradation, by first calculating the single-phase pump torque, then subtracting from it a degradation correction term as

$$B = B_{1\phi} - M_B (B_{1\phi} - B_{2\phi}) \quad (3.14)$$

where

$B_{1\phi}$  = single-phase pump torque  
 $B_{2\phi}$  = two-phase, fully degraded pump torque  
 $M_B$  = torque difference multiplier.

The CE-EPRI data also include torque degradation data and present a more realistic means for treating two-phase torque degradation in BWR reactor coolant pumps than the Semiscale torque degradation data. This methodology adequately represents the CE-EPRI torque degradation data, and these data can be implemented in a RELAX model simply through input deck modifications, i.e., replacing Semiscale-based data with CE-EPRI-based data.

Table 3.3 shows torque difference homologous curves based on CE-EPRI data; Table 3.4 shows a torque difference multiplier curve derived from the CE-EPRI data and intended for use with the data in Table 3.3. The torque difference,  $db$ , used in Table 3.4 is defined as

$$db = b_{1\varphi} - b_{2\varphi} \quad (3.15)$$

where  $b = \frac{B_{\text{actual}}}{B_{\text{rated}}}$  and  $B$  is pump torque.

**Table 3.2 Head Difference Homologous Curves Based on CE-EPRI Data**

**Table 3.3 Torque Difference Homologous Curves Based on CE-EPRI Data**

**Table 3.4 Torque Difference Multiplier Table Based on CE-EPRI Data**

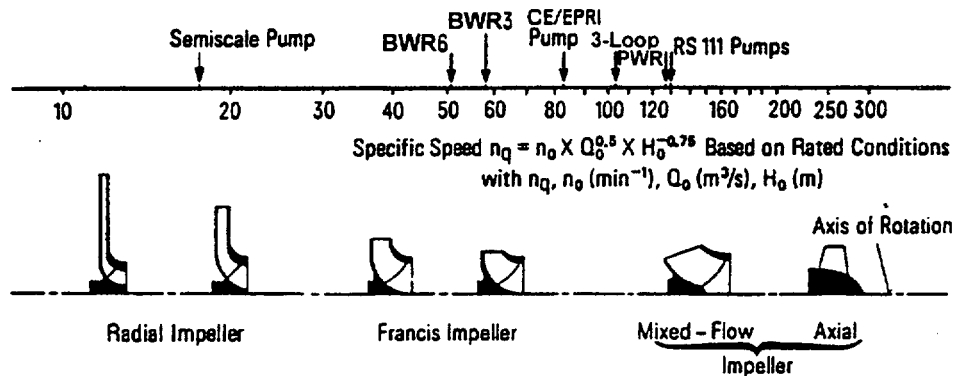


**Figure 3.3 Pump Types and Specific Speeds**

### 3.2.4 RELAX Reflood Criteria

The reflood time is calculated by RELAX without the use of other codes. The reflood criteria are defined based on the results of SPC's fuel cooling test facilities (FCTF) tests that show a level of entrained liquid mass flux sufficient to cool the fuel. There are three reflood time criteria:

[

[

]

### 3.2.5 Enthalpy Injection Model

RELAX predicts an unrealistic over-condensation effect when large quantities of subcooled water are injected into a volume containing a two-phase mixture. This effect is observed in LOCA simulations where the core spray systems inject subcooled water into the plenum above the core during blowdown. In this event, the upper plenum is predicted to undergo a large unrealistic depressurization that draws steam and liquid into the upper plenum and suppresses the flow of liquid down through the core and bypass volumes. This result is caused by the homogenous equilibrium nature of the RELAX code.

Condensation effects of this type are not new to one-dimensional homogenous codes such as RELAP4 and RELAX. The current EXEM/BWR methodology compensates for this effect with the FLEX code, which discards safety injection water as soon as the collapsed liquid level exceeds the sparger elevation in the upper plenum.

To better model safety injection condensation and CCFL effects with RELAX, the Sector Steam Test Facility (SSTF) tests (Reference 1; Pages 6.5-12 through 6.5-15) were reviewed to gain insight as to how a BWR system behaves during the refill/reflood portion of a LOCA transient. It was noted that an attempt to limit the penetration of liquid down through the core was made in the SSTF tests. These tests showed that CCFL could not occur at the top of the bypass and liquid was always able to penetrate downward between the fuel channels. These test results contradicted one-dimensional, homogeneous calculations of CCFL for this geometry.

SSTF tests also were performed to study the mixing behavior in the upper plenum. These tests show that the two-phase mixture level in the upper plenum reaches the spray header elevation where a localized condensation region builds up. When this occurs, the cooler-localized mixture

partially collapses the fluid and the CCFL condition in the peripheral bundles breaks down. The downward flow through the peripheral bundles suppresses the level of the two-phase mixture in the upper head. This continues until the upper plenum inventory uncovers the sparger and the system returns to its previous behavior with the CCFL condition in the peripheral bundles re-established. The two-phase mixture swells up into the upper head and the process starts over. It also should be noted that these particular tests were performed with the bypass filled with water. Otherwise, the holdup of liquid in the upper head could not have been sustained as explained in the previous paragraph.

Thus, based on SSTF results, the unrealistic condensation effect predicted by RELAX in the unusual situation where the levels in the upper plenum reach the sparger was concluded to introduce a false one-dimensional CCFL condition at the core and bypass exits. To resolve this issue, SPC introduced a method into RELAX to manage this condensation. The method changes the temperature of the injection liquid to be closer to the upper plenum saturation conditions. The following rules determine the new fill system parameters.

[

]

If the percentage of collapsed liquid volume in the upper plenum drops below the activation percentage minus 1%, the original fill system fluid conditions are reestablished and maintained until the upper plenum collapsed liquid level achieves or exceeds the activation percentage again (i.e., if the user specifies the activation percentage to be 30%, the method will reset to the original parameters at 29% until the activation percentage is again achieved). This process continues until core reflood is predicted.

The selection of the sparger elevation used for the calculation of the activation percentage has been chosen based on the SSTF test results. The selection of resetting the fill system parameters after a reduction of collapsed liquid inventory by 1% reasonably represents the

elevation change to uncover the sparger ring and produces results that emulate those observed in the SSTF tests.

### 3.2.6 Other Changes

A small discontinuity exists in RELAX for volumes using the Wilson Bubble rise model. When the quality within the volume approaches 0.0, small changes in quality introduce large changes in level swell at low pressures. A model change was needed to allow smooth transition to a liquid solid volume.

For volumes that have qualities between 0.0 and 0.00005, a linear interpolation is performed for bubble velocity calculated on quality to 100 ft/s. This approach stabilizes the level swell for volumes that are nearly 100% liquid full.

### 3.3 ***Applications Changes***

The EXEM BWR-2000 evaluation model described in Section 3.0 replaces the FLEX code with the RELAX code for analysis of the refill/reflood phases of a LOCA. RELAX is used in the current EXEM/BWR methodology to predict LOCA blowdown phenomena and its calculation is stopped at the end of blowdown (EOB). EOB usually is the time when rated low-pressure core spray (LPCS) flow is reached. In EXEM BWR-2000, the RELAX calculation is extended to provide analysis of the refill/reflood phases of a LOCA.

The RELAX reactor system nodalization describes the geometry of a BWR reactor coolant system including the fluid volumes, fluid flow paths, and heat conductor volumes and surface areas (Reference 31). The current standard RELAX nodalization is optimized for blowdown analysis. Several changes to the current RELAX BWR reactor coolant system nodalization have been made to improve the analysis of the refill phase of a LOCA without affecting the conservative prediction of blowdown phenomena. These applications changes are part of the EXEM BWR-2000 methodology. The changes are as follows:

[

]

[

]

Figure 3.4 shows the RELAX nodalization to be used in BWR LOCA analyses with the EXEM BWR-2000 methodology.

The EXEM BWR-2000 methodology uses the RELAX code to calculate from the initiation of the LOCA pipe break to the time of core hot node reflood. Section 4.0 describes applications of the revised methodology to a BWR plant. Section 5.0 provides validation for the revised methodology.



**Figure 3.4 Typical RELAX BWR System Model  
(Recirculation Discharge Line Break)**

### 3.3.1 Increased Jet Pump Noding and Modified Jet Pump Exit Description

The nodalization used with RELAX in the current EXEM/BWR model represents the BWR jet pump array as two jet pumps; one representing the jet pumps connected to the recirculation pump piping where the break is assumed to occur (broken loop), and the other representing the jet pumps connected to the unaffected piping loop (intact loop). RELAX has a mechanistic jet pump model that calculates pressure and flow behavior in jet pump mixing regions.

In the currently approved EXEM/BWR model, each jet pump is modeled with a single RELAX volume. An average diameter and area is input to describe the jet pumps with this one-node modeling. In a BWR plant, each jet pump is vertically distributed over a large elevation change. For example, in a BWR/3 reactor, the jet pump is 16.1 feet high. During a LOCA, a vertical fluid density distribution in the jet pumps will occur because of the large elevation change. Also, the geometry of the fluid region in the jet pumps changes over the vertical height. The diameter of the mixer section at the top of the jet pumps is much smaller than the exit diameter at the bottom where the jet pumps discharge to the lower plenum. [

Figure 3.5 RELAX Jet Pump Model

### 3.3.2 Phase-Separation Model in the Bypass

In the revised EXEM BWR-2000 methodology, the bypass region (node 11 in Figure 3.4) is changed from a homogenous volume to a phase-separated volume using the [

] RELAX volume nodes are specified as either homogeneous nodes or phase-separated nodes. Fluid density and enthalpy are calculated as functions of vertical elevation in the phase-separated RELAX volumes when two-phase fluid conditions exist. The Wilson Model provides a calculation of the velocity of the bubbles in the two-phase mixture region of the phase-separated volumes. [

] The phase separation model is used to track the mixture level in the downcomer, which is the most important function of the model for blowdown analysis. In a BWR, the height of the mixture level in the downcomer is monitored. If the mixture level is lower than the normal operating range, signals are activated to start the ECCS. With phase separation selected, RELAX calculates the level of the mixture and predicts the occurrence of the ECCS initiating signals.

[

]

This application change provides a method for extending the RELAX analysis through the refill phase without affecting the blowdown results. With this modification, RELAX will track the liquid mass change in the guide tubes, the bypass, and the lower plenum during refill. During the blowdown period of a LBLOCA the RELAX calculation predicts essentially homogeneous behavior in the bypass region, even though the phase-separated model is selected. This occurs

because the rapid depressurization results in continuous flashing in the bypass and prevents the formation of a mixture level. [

]

### 3.3.3 Core Nodalization for LOCA Analysis

[

]



**Figure 3.6 RELAX Average Core Model, Top Peaked**

Figure 3.7 RELAX Hot Channel Model, Top Peaked

#### 3.3.4 Upper Plenum Nodalization

[

]



## 4.0 Model Application and Sensitivities

Section 4.0 presents application examples and sensitivity analysis for the EXEM BWR-2000 methodology. Section 4.1 presents the application of the methodology to break spectrum LOCA analyses of a BWR/3. Section 4.2 presents time-step and RELAX model nodalization sensitivity studies and [

]

### 4.1 BWR LOCA/ECCS Analysis Example Problems

A set of example problems was selected based on previous EXEM/BWR results from a BWR/3 break spectrum analysis. The sample problems were analyzed with the EXEM BWR-2000 evaluation model, including the input changes described in Section 3.0, to demonstrate the effects of applying the new methodology.

#### 4.1.1 Break Spectrum Example Problems

The plant parameters, ECCS parameters, and break characteristics evaluated for a break spectrum analysis results in a large number of LOCA break calculations. For the example problems, a group of eight representative calculations were selected from the break spectrum cases.

For the plant analyzed, the single failure that results in the maximum loss of ECCS capacity is failure of the LPCI valve. Assuming LPCI valve failure (SF-LPCI), two LPCS pumps remain available. All the highest PCT cases resulted from the assumed SF-LPCI condition, so six of the eight example problems presented include this failure. The other ECCS single failures analyzed in the example problems are as follows:

- 1) A diesel generator failure (SF-DG) that leaves two LPCI pumps and one LPCS pump available.
- 2) An HPCI system failure that leaves four LPCI pumps and two LPCS pumps available.

The PCTs for the top-peaked axial power profile calculations generally are higher than the equivalent center-peaked axial calculation, so all the example analyses assumed a top-peaked axial power profile.

Table 4.1 lists the eight selected example problems.

The RELAX system nodalization used for the model confirmatory analyses is shown in Figure 4.1. Figure 4.2 shows the RELAX hot channel nodalization. In Figure 3.4, the steamline junction (J32) is between volumes 27 and 6. In modeling some BWRs with SPC's current evaluation model, this junction has also been modeled between volumes 27 and 5, as is the case for the results presented in Section 4.0. The predicted blowdown response of a system is not affected by the different junction location as the junction is modeled at the proper elevation in both cases. Also volumes 5 and 6 are rather large and closely coupled, and the main steam isolation valve closes quickly (approximately 3 seconds) after the initiation of a LOCA event.

Table 4.2 summarizes the key results for break spectrum calculations with the EXEM BWR-2000 methodology. The LOCA analysis parameters included in Table 4.2 are calculated time of rated spray (end of blowdown), length of refill or heatup period, calculated time of reflood, the maximum temperature at end of blowdown (time of rated spray flow), and PCT.

**Figure 4.1 RELAX BWR System Model  
(Recirculation Suction Line Break)**



**Figure 4.2 RELAX Hot Channel Model, Top Peaked**

**Table 4.1 EXEM BWR-2000 LOCA Methodology Demonstration  
Calculations**

<b>Discharge Coefficient or Break Size</b>	<b>Break Type</b>	<b>Break Location</b>	<b>ECCS Single Failure</b>	<b>Abbreviation</b>
1.0	Double-ended guillotine	Recirculation pump suction line	Low Pressure Coolant Injection (LPCI) Valve	1.0 DEG/PS SF-LPCI
0.8	Double-ended guillotine	Recirculation pump suction line	Low Pressure Coolant Injection (LPCI) Valve	0.8 DEG/PS SF-LPCI
1.0	Double-ended guillotine	Recirculation pump discharge line	Low Pressure Coolant Injection (LPCI) Valve	1.0 DEG/PD SF-LPCI
2.78 ft <sup>2</sup>	Split	Recirculation pump discharge line	Low Pressure Coolant Injection (LPCI) Valve	2.78 ft <sup>2</sup> /PD SF-LPCI
1.0 ft <sup>2</sup>	Split	Recirculation pump discharge line	Low Pressure Coolant Injection (LPCI) Valve	1.0 ft <sup>2</sup> /PD SF-LPCI
0.5 ft <sup>2</sup>	Split	Recirculation pump discharge line	Low Pressure Coolant Injection (LPCI) Valve	0.5 ft <sup>2</sup> /PD SF-LPCI
1.0	Double-ended Guillotine	Recirculation pump suction line	Diesel Generator Failure (Loss of 1 LPCI Pump and 1 LPCS Pump)	1.0 DEG/PS SF-DG
1.0 ft <sup>2</sup>	Split	Recirculation pump discharge line	High Pressure Coolant Injection (HPCI) System Failure	1.0 ft <sup>2</sup> /PD SF-HPCI

**Table 4.2 EXEM BWR-2000 Methodology LOCA Result Summary**

#### 4.1.2 Large-Break LOCA Example Problem

[

] EXEM BWR-2000 will produce PCT results that are lower than EXEM/BWR for most LOCA cases. EXEM BWR-2000 analyses of pump discharge line LOCAs and SBLOCAs generally show the most PCT reduction compared to the EXEM/BWR results. The EXEM/BWR features that added unnecessary conservatism to pump discharge line break and SBLOCA analyses include [

]

The effect of the methodology changes on PCT is not as significant for the pump suction line LBLOCA cases. This is especially true for pump suction breaks with degraded ECCS performance. The 1.0 DEG/PS SF-LPCI and the 0.8 DEG/PS SF-LPCI cases in Table 4.2 are in this category.

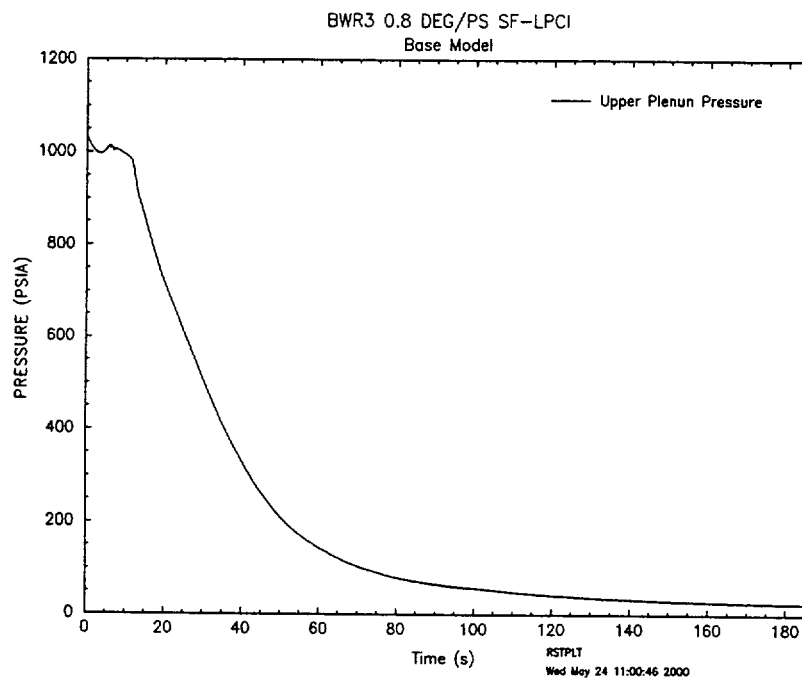
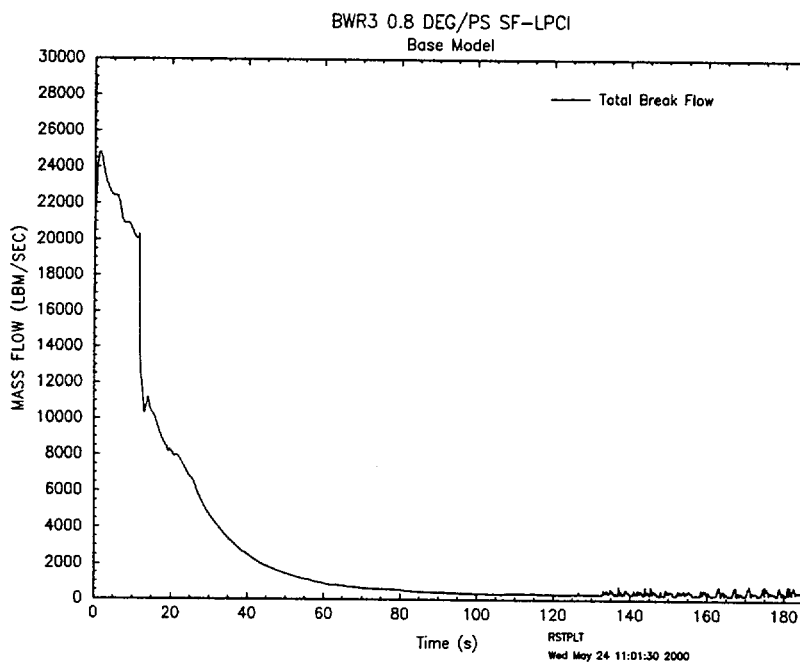
Table 4.3 lists the major event times for the 0.8 DEG/PS SF-LPCI case. Figures 4.3 through 4.19 are graphs of the important thermal-hydraulic parameters calculated by RELAX for the limiting LOCA. The key parameters from the hot channel analysis are shown in Figures 4.20 through 4.24. The PCT is calculated by the HUXY code (Reference 13). Figure 4.25 shows the HUXY results for the PCT rod.

**Table 4.3 Event Times for the  
BWR/3 0.8 DEG/PS SF-LPCI (LOCA)**

<b>Event</b>	<b>Time (sec)</b>
Initiate break	0.0 (0.0)
Initiate scram	0.6 (0.6)
MSIV fully closed	5.0 (5.0)
Low-low water mixture level trip	5.5 (5.7)
Jet pump uncovers	7.8 (8.7)
Recirculation suction uncovers	11.3 (11.7)
Lower plenum flashes	12.9 (13.3)
LPCS valve starts to open	41.0 (42.1)
LPCS pump at rated speed	29.0 (29.0)
LPCS flow starts	41.0 (42.1)
End of blowdown	87.6 (87.2)
ADS valve opens	125.4 (125.7)
Time of hot node reflood	184.3 (159.1)
PCT	184.3 (159.1)

( ) – Values using currently approved EXEM/BWR methodology



**Figure 4.3 Upper Plenum Pressure****Figure 4.4 Total Break Flow**

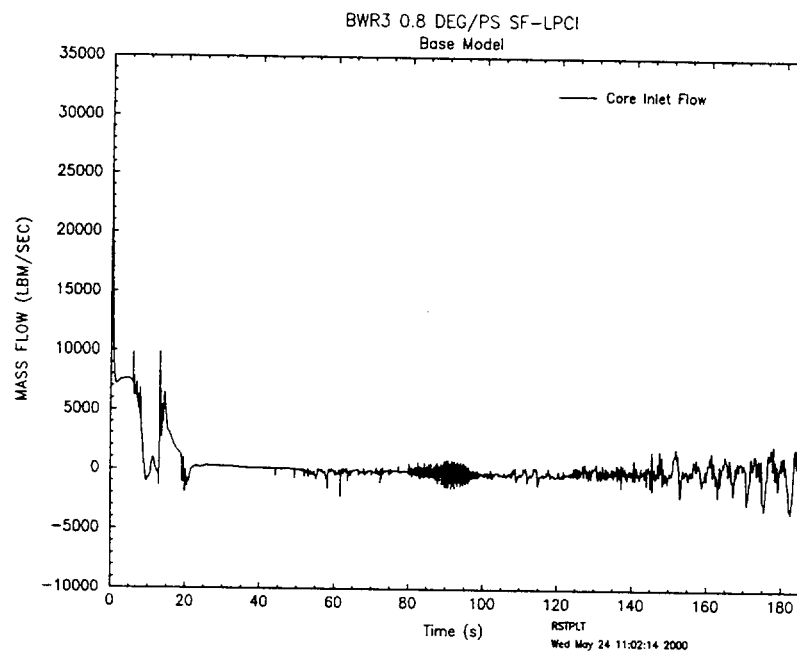


Figure 4.5 Core Inlet Flow

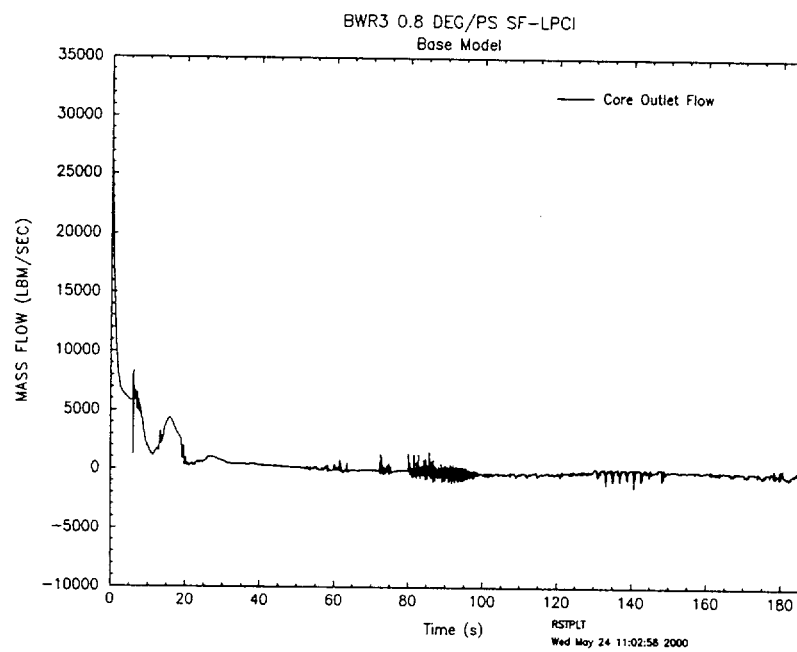
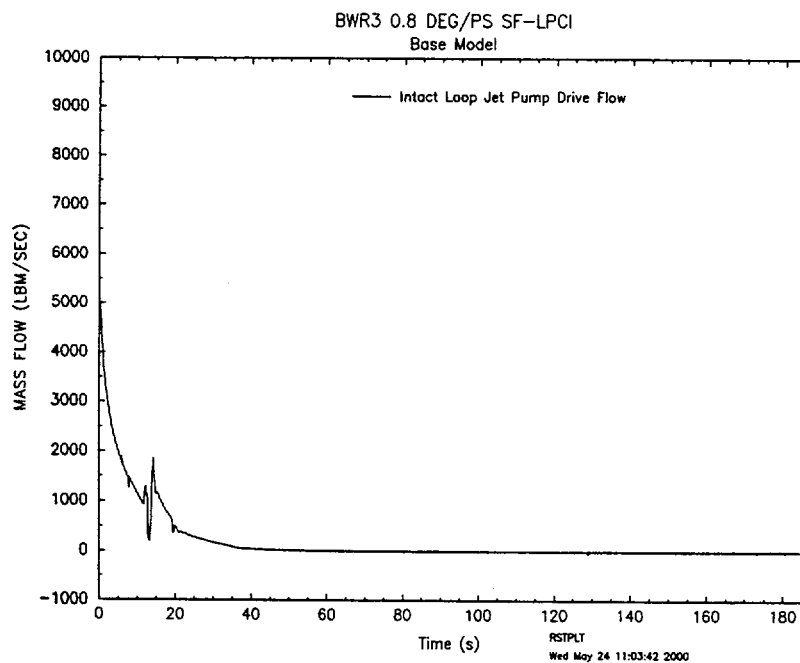
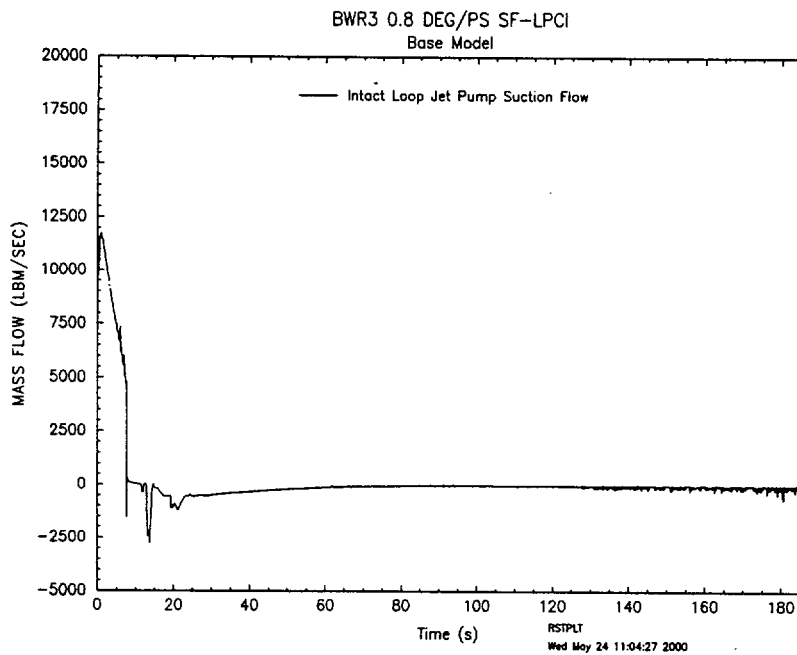


Figure 4.6 Core Outlet Flow

**Figure 4.7 Intact Loop Jet Pump Drive Flow****Figure 4.8 Intact Loop Jet Pump Suction Flow**

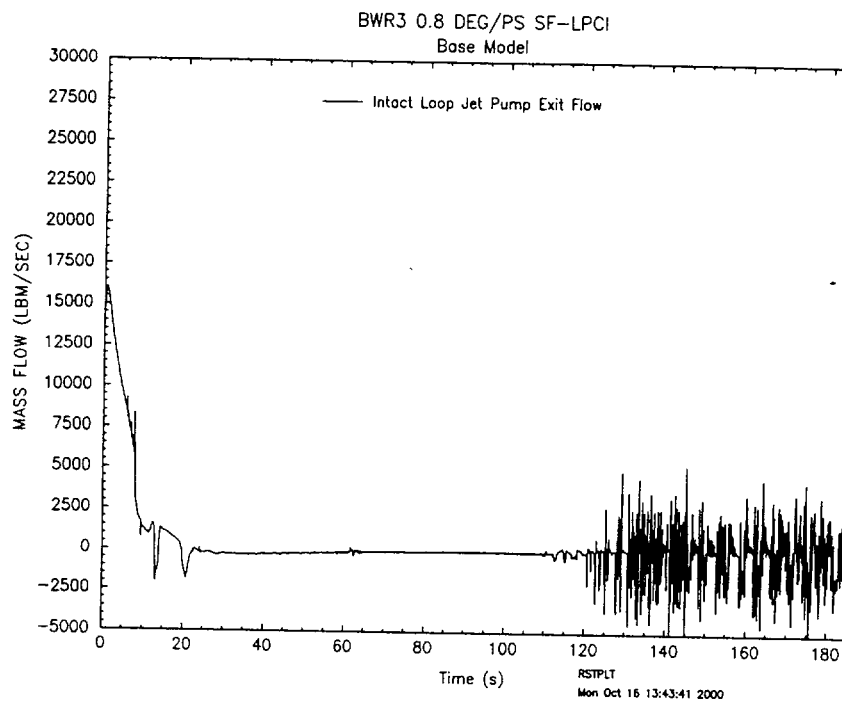


Figure 4.9 Intact Loop Jet Pump Exit Flow

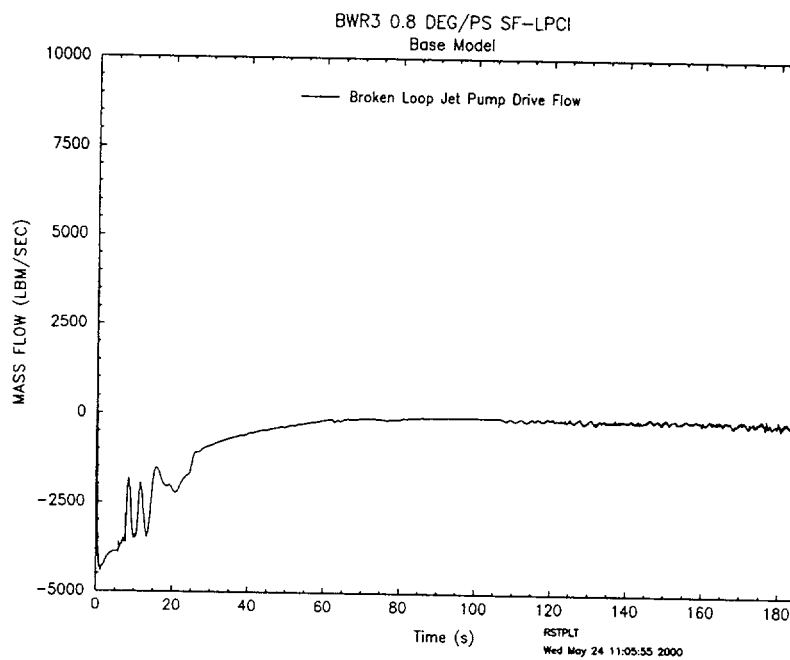
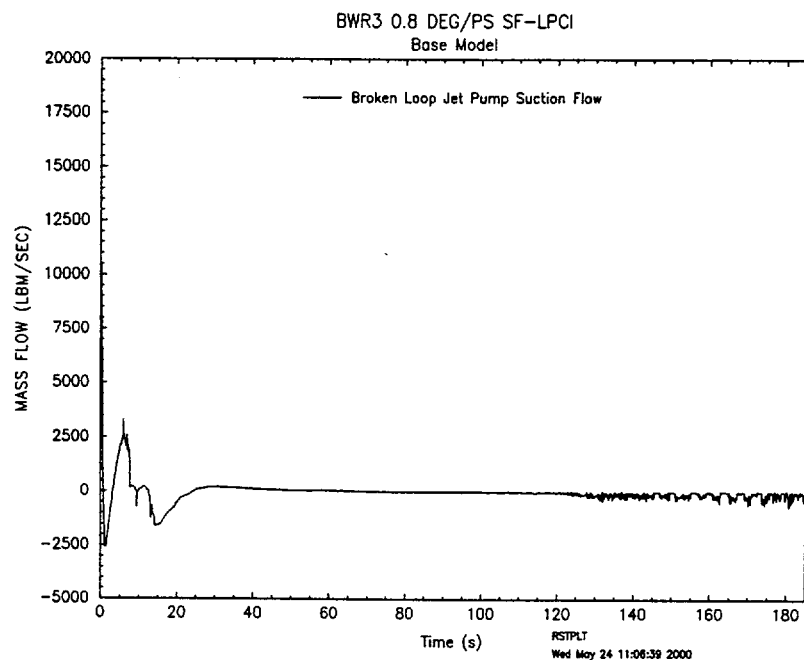
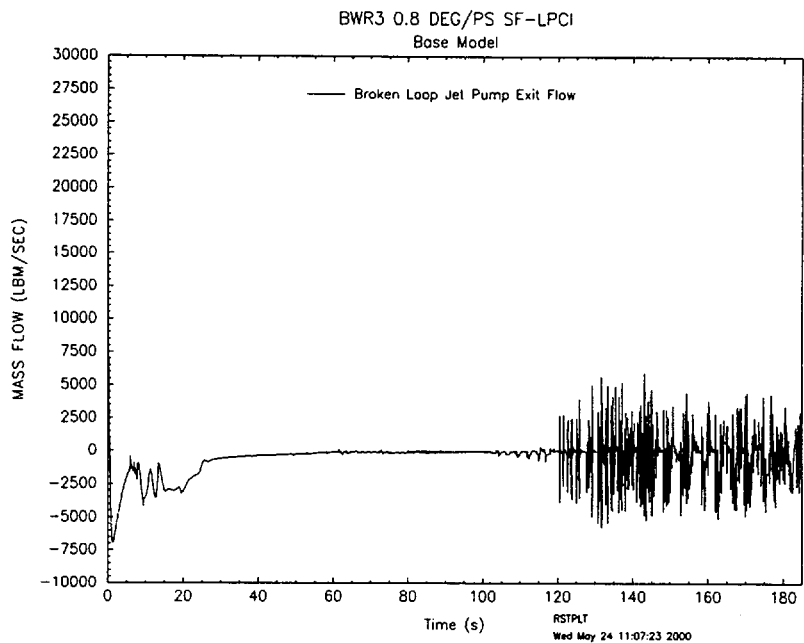


Figure 4.10 Broken Loop Jet Pump Drive Flow

**Figure 4.11 Broken Loop Jet Pump Suction Flow****Figure 4.12 Broken Loop Jet Pump Exit Flow**

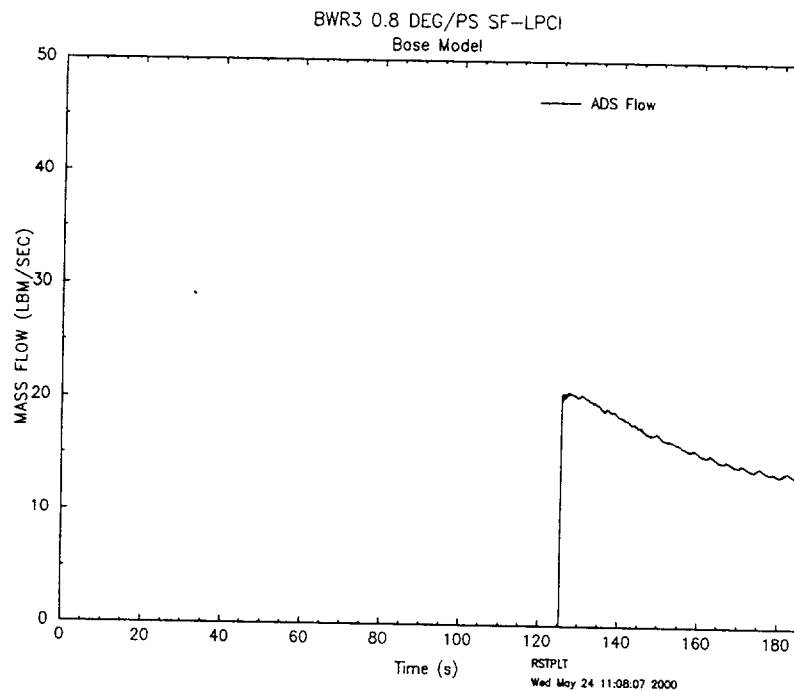


Figure 4.13 ADS Flow

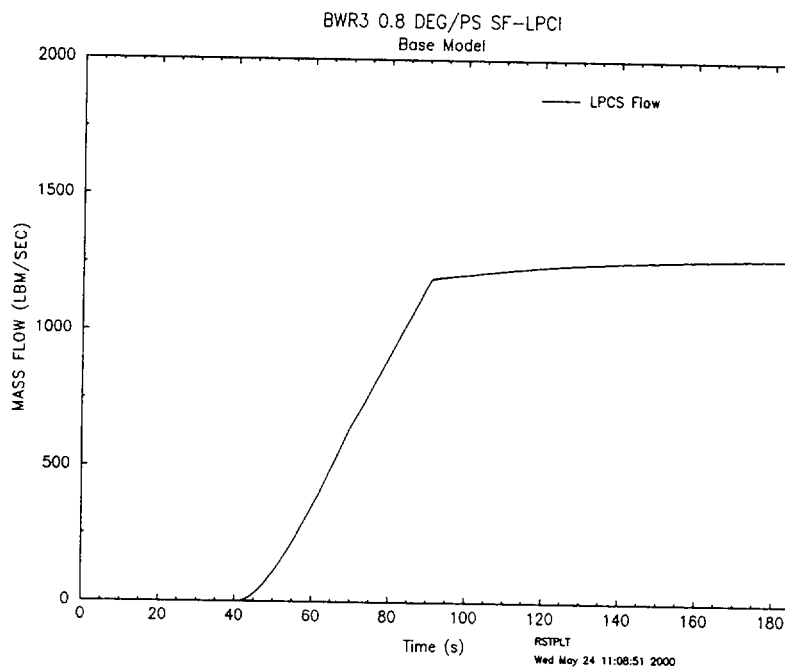


Figure 4.14 LPCS Flow

EXEM BWR-2000 ECCS Evaluation Model

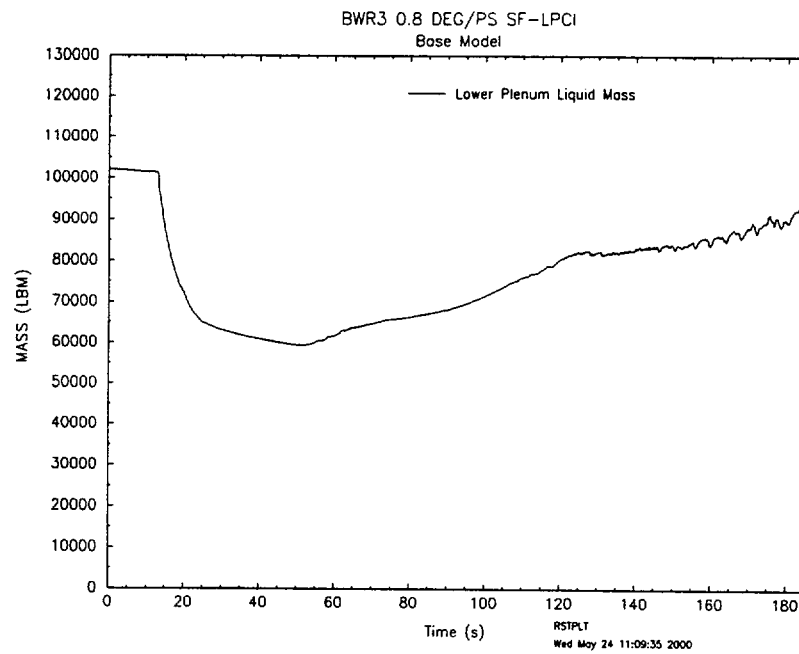


Figure 4.15 Lower Plenum Liquid Mass

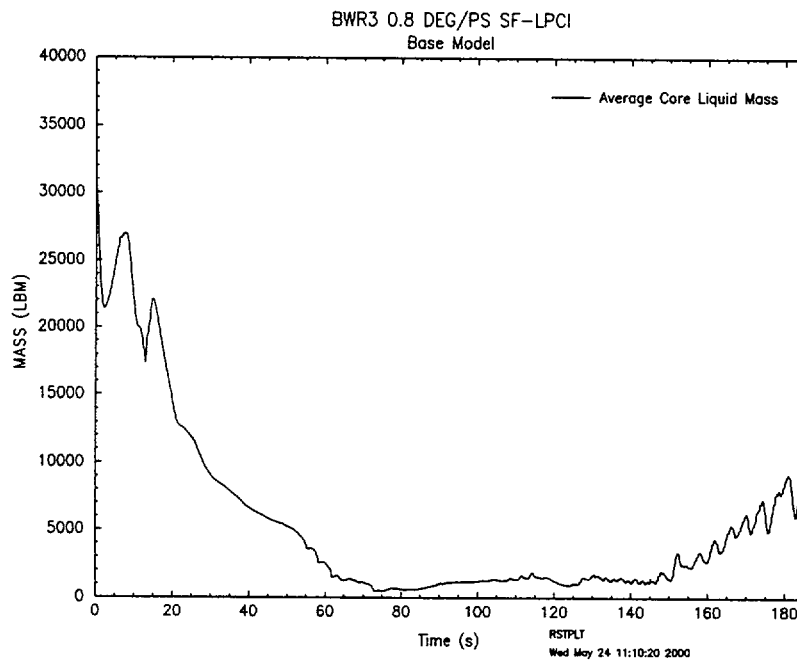
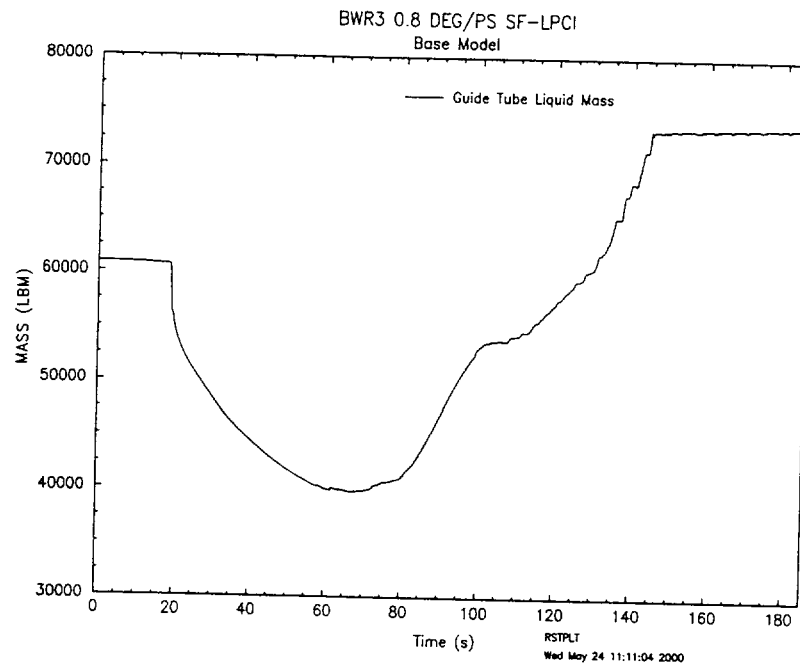
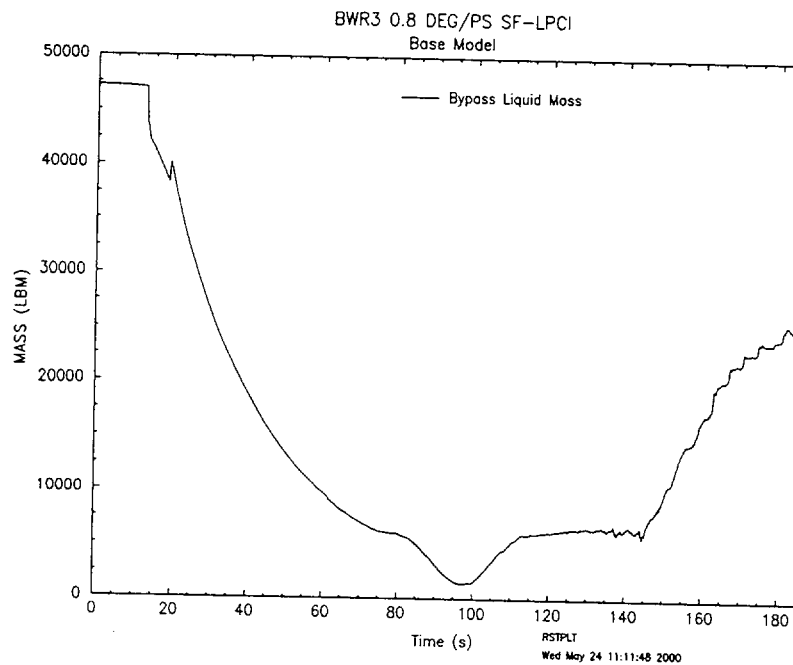
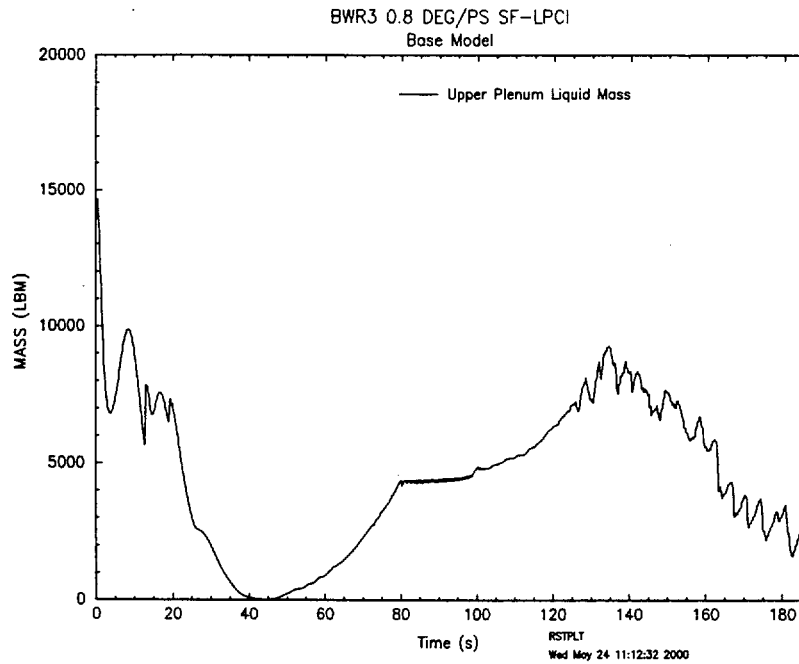
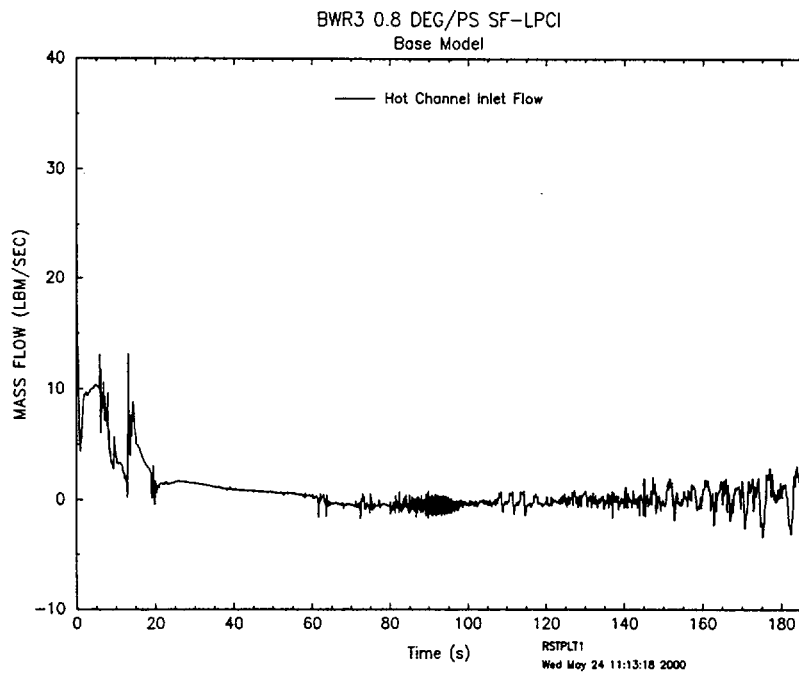


Figure 4.16 Average Core Liquid Mass

**Figure 4.17 Guide Tube Liquid Mass****Figure 4.18 Bypass Liquid Mass**



**Figure 4.19 Upper Plenum Liquid Mass****Figure 4.20 Hot Channel Inlet Flow**

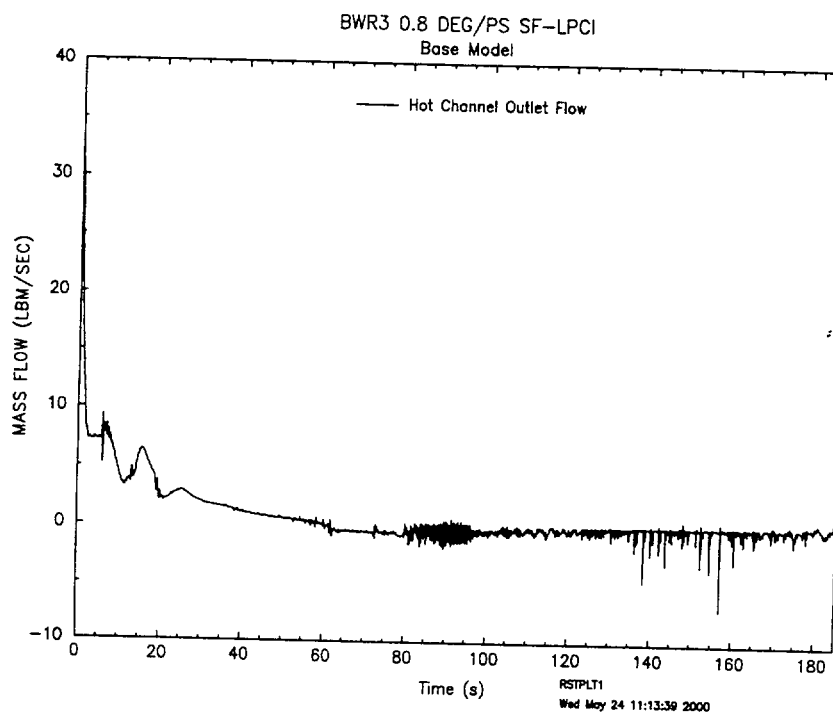
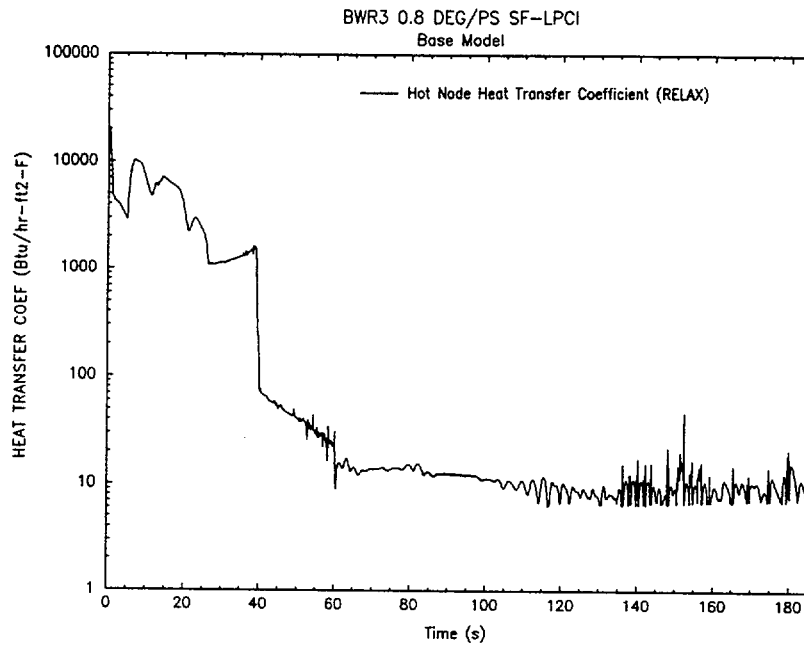
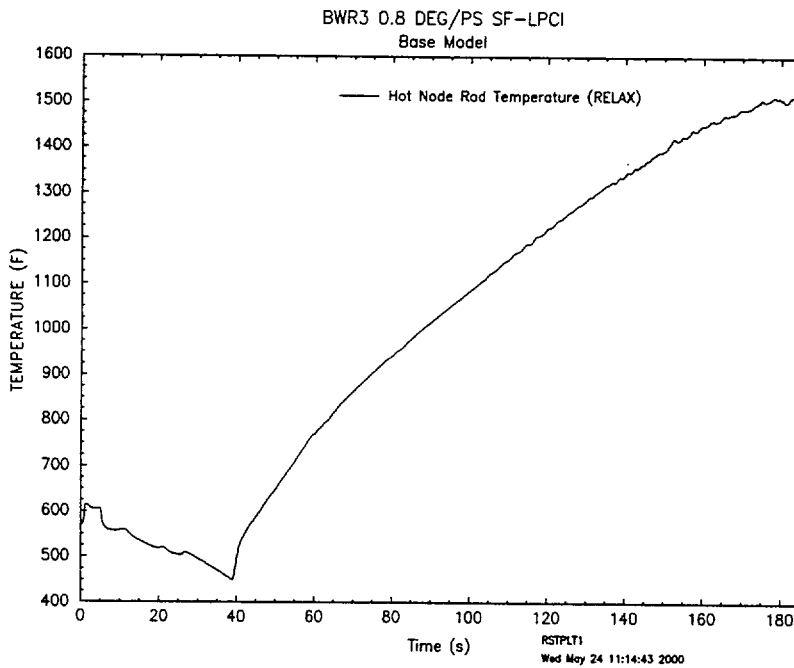


Figure 4.21 Hot Channel Outlet Flow

Figure 4.22 Hot Node Entrainment Flow

**Figure 4.23 Hot Node Heat Transfer Coefficient (RELAX)****Figure 4.24 Hot Node Rod Temperature (RELAX)**

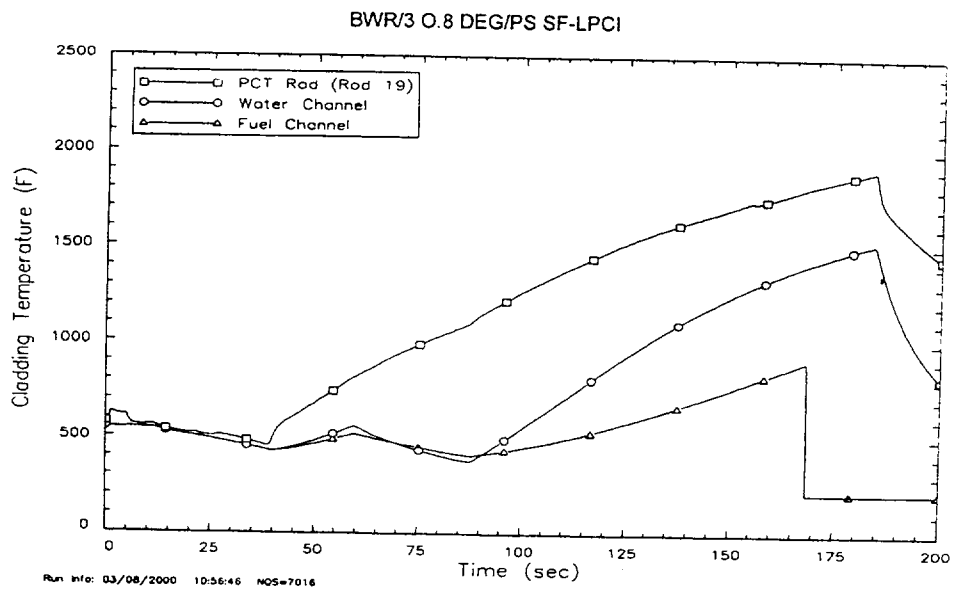


Figure 4.25 HUXY Analysis

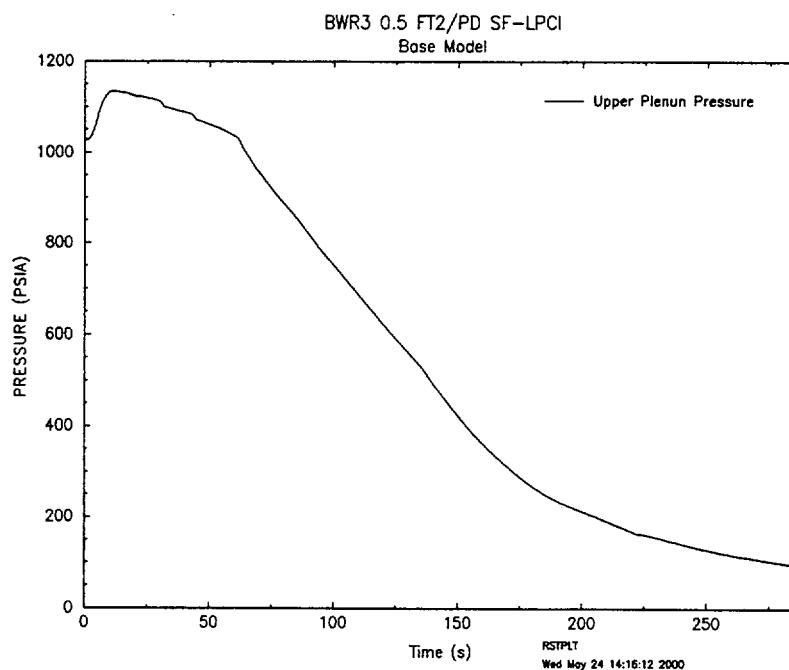
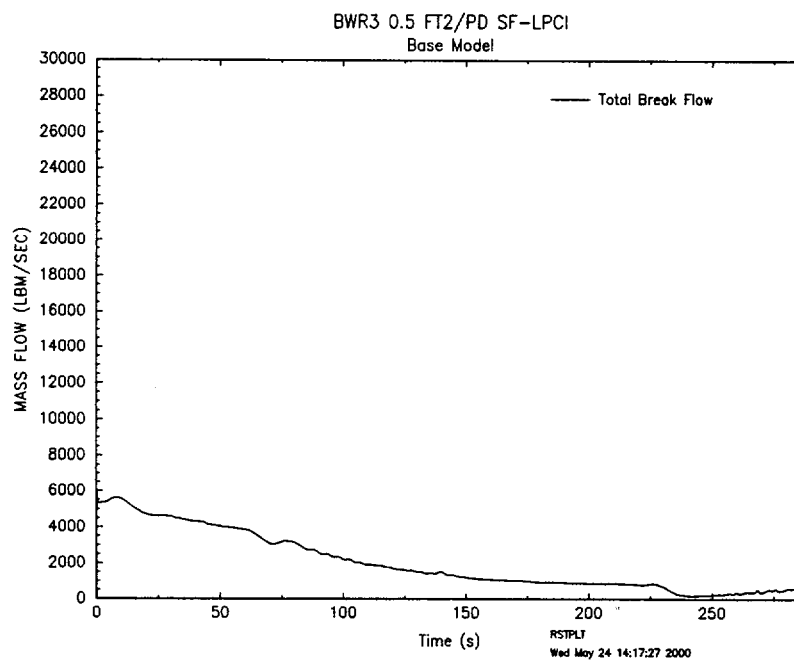
#### 4.1.3 Small-Break LOCA Example Problem

BWR SBLOCA phenomena will differ from LBLOCA behavior because automatic depressurization system (ADS) operation is needed to reduce the reactor system pressure and achieve maximum ECCS delivery. Also, the time interval between the initiation of ECCS flow and the time rated ECCS flow is reached will be long. Therefore, it is appropriate to include the details from one of the SBLOCA example problems. Table 4.4 lists the event times for the 0.5 ft<sup>2</sup>/PD SF-LPCI analysis with the revised methodology. Figures 4.26 through 4.43 show the RELAX system parameters for this SBLOCA case. Figures 4.44 through 4.48 show the hot channel results. Figure 4.49 shows the HUXY PCT rod results.

**Table 4.4 Event Times for the  
BWR/3 0.5 Ft<sup>2</sup>/PD SF-LPCI (LOCA)**

<b>Event</b>	<b>Time (sec)</b>
Initiate break	0.0 (0.0)
Initiate scram	0.5 (0.6)
MSIV fully closed	5.0 (5.0)
Low-low water mixture level trip	15.7 (15.5)
Jet pump uncovers	37.2 (38.0)
Recirculation suction uncovers	59.0 (59.2)
Lower plenum flashes	63.9 (59.6)
HPCI valve starts to open	15.7 (15.5)
HPCI pump at rated speed	40.7 (40.5)
HPCI flow starts	61.5 (59.5)
LPCS valve starts to open	169.3 (169.5)
LPCS pump at rated speed	30.7 (30.5)
LPCS flow starts	169.3 (169.5)
End of Blowdown	272.0 (264.4)
ADS valve opens	135.7 (135.5)
Time of hot node reflood	286.3 (303.5)
PCT	286.3 (303.4)

( ) – Values using currently approved EXEM/BWR methodology

**Figure 4.26 Upper Plenum Pressure****Figure 4.27 Total Break Flow**

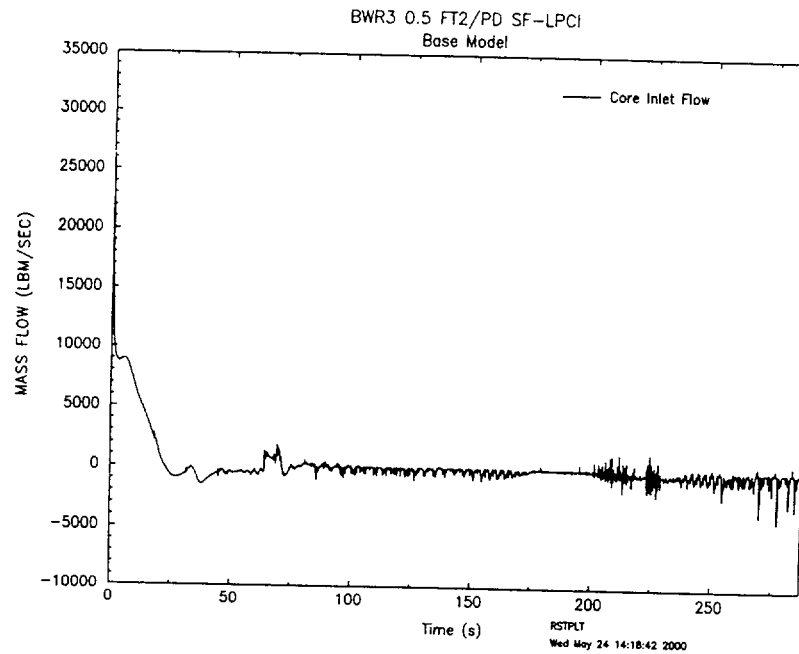


Figure 4.28 Core Inlet Flow

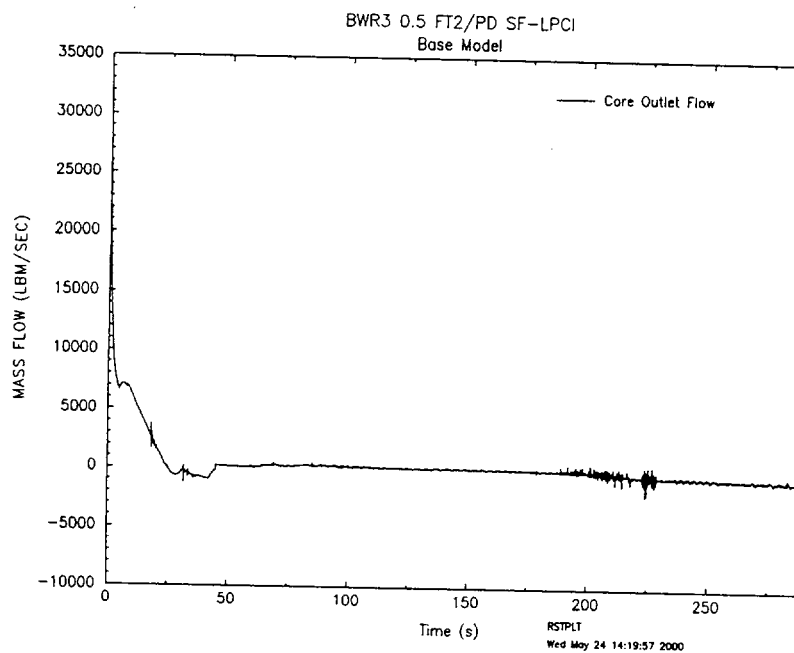
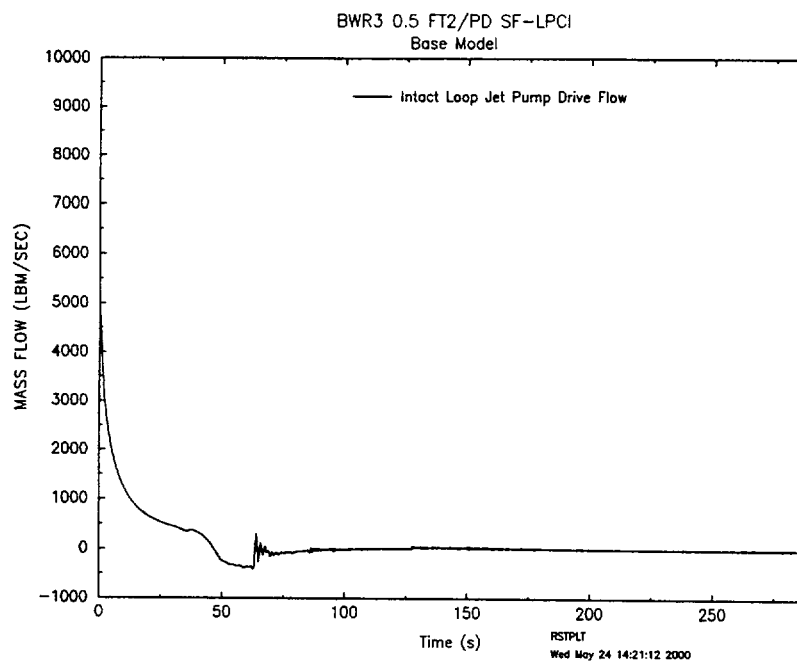
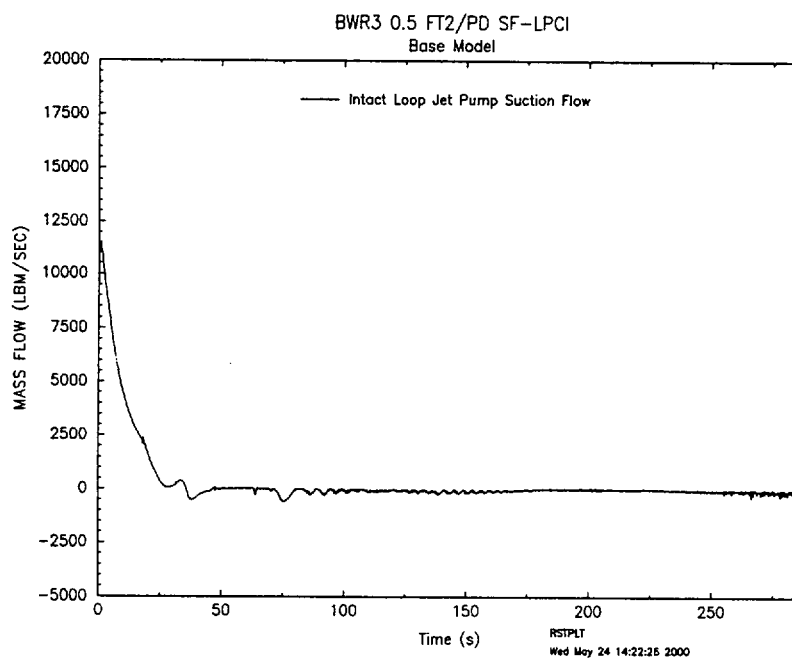
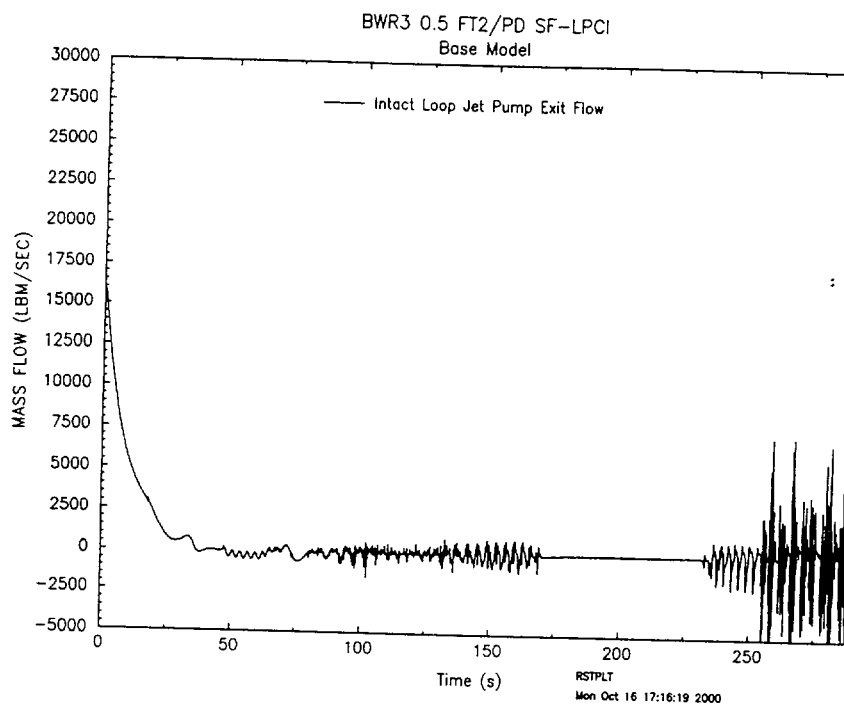
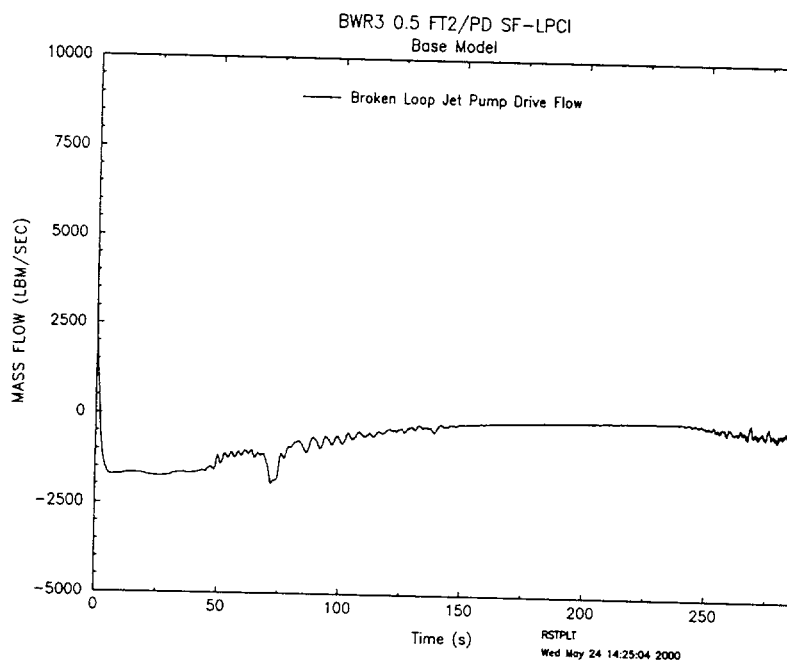
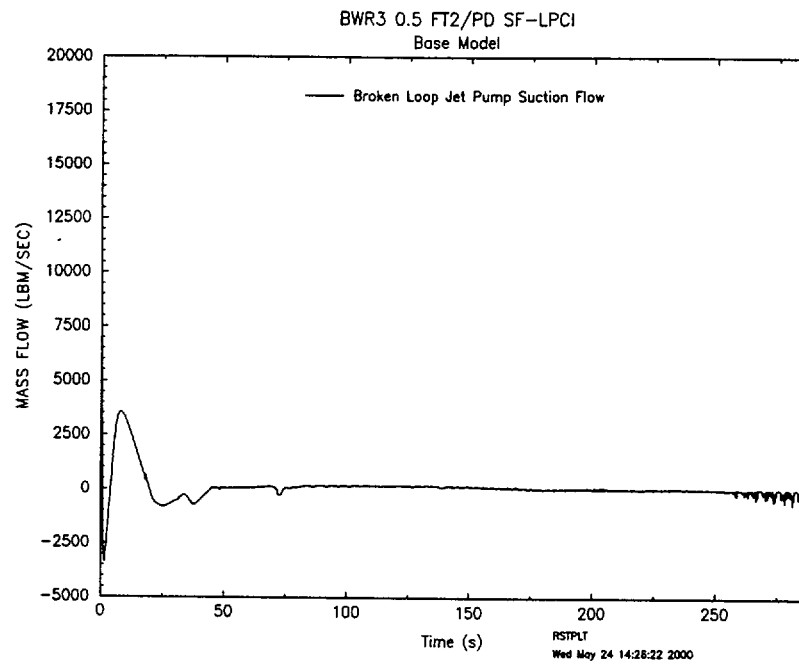
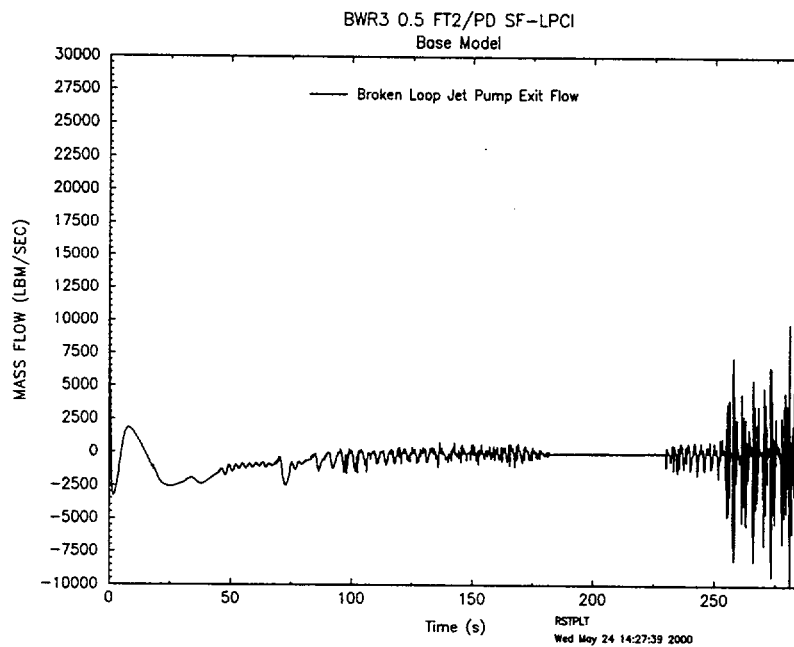


Figure 4.29 Core Outlet Flow



**Figure 4.30 Intact Loop Jet Pump Drive Flow****Figure 4.31 Intact Loop Jet Pump Suction Flow**

**Figure 4.32 Intact Loop Jet Pump Exit Flow****Figure 4.33 Broken Loop Jet Pump Drive Flow**

**Figure 4.34 Broken Loop Jet Pump Suction Flow****Figure 4.35 Broken Loop Jet Pump Exit Flow**

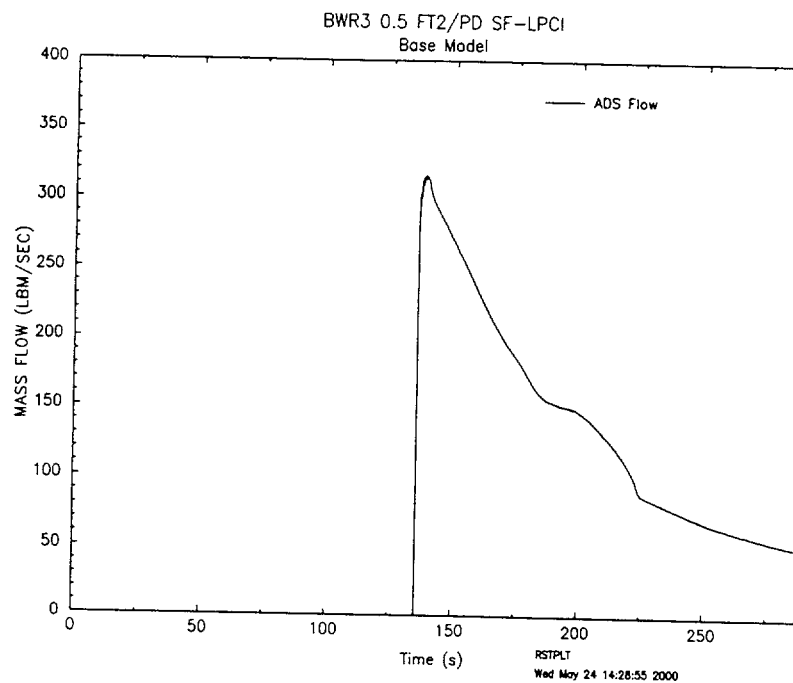


Figure 4.36 ADS Flow

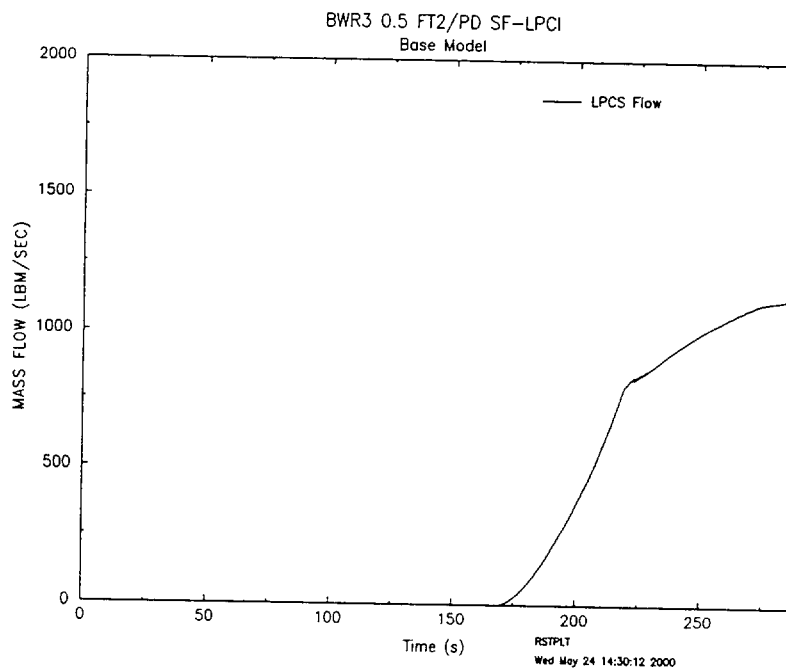


Figure 4.37 LPCS Flow

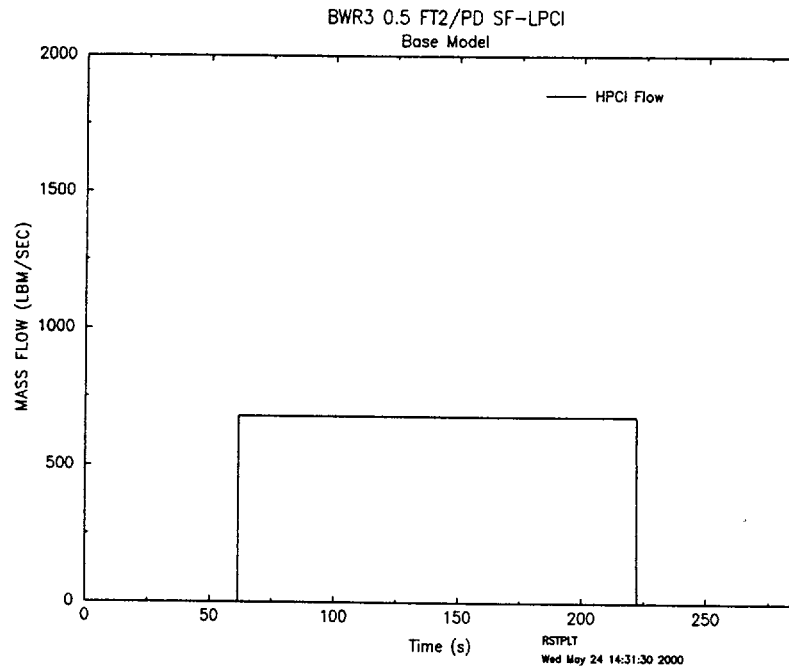


Figure 4.38 HPCI Flow

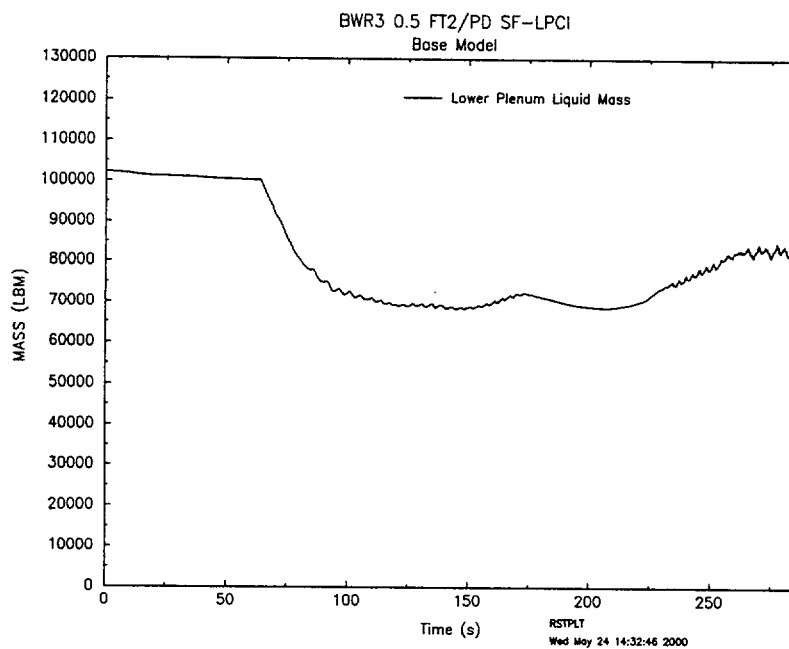


Figure 4.39 Lower Plenum Liquid Mass

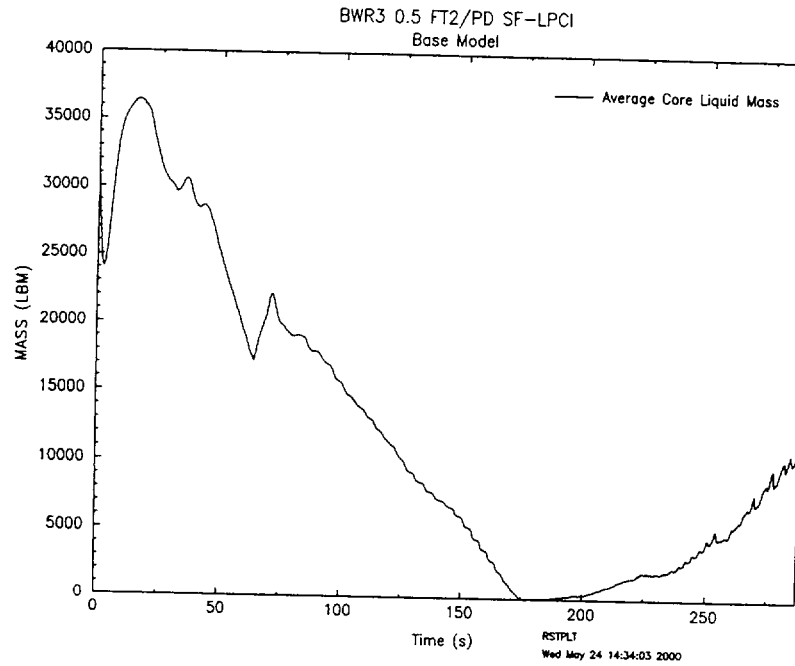


Figure 4.40 Average Core Liquid Mass

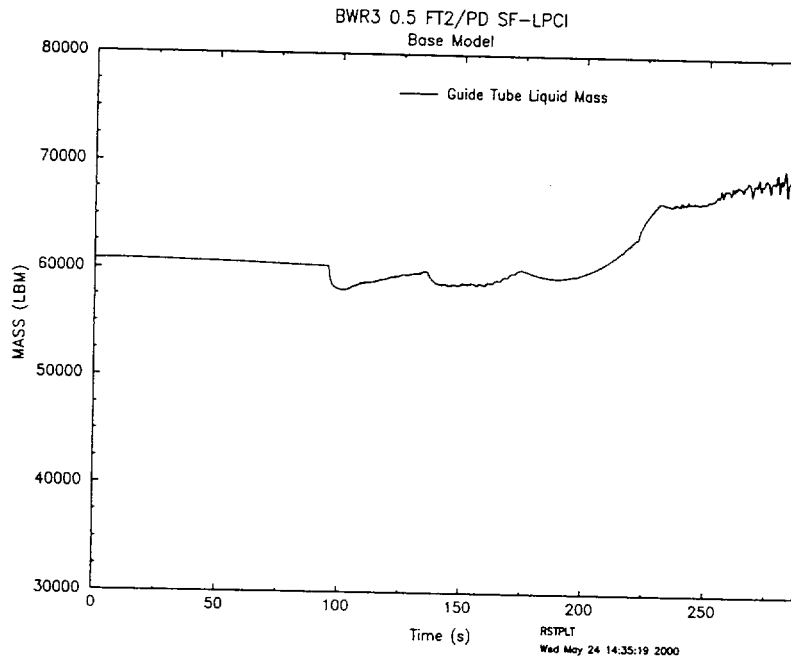


Figure 4.41 Guide Tube Liquid Mass

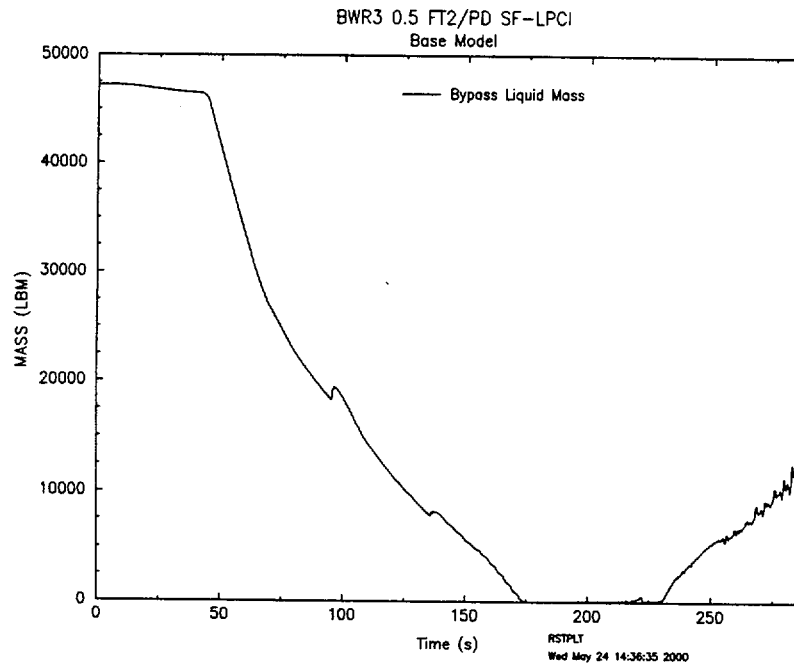


Figure 4.42 Bypass Liquid Mass

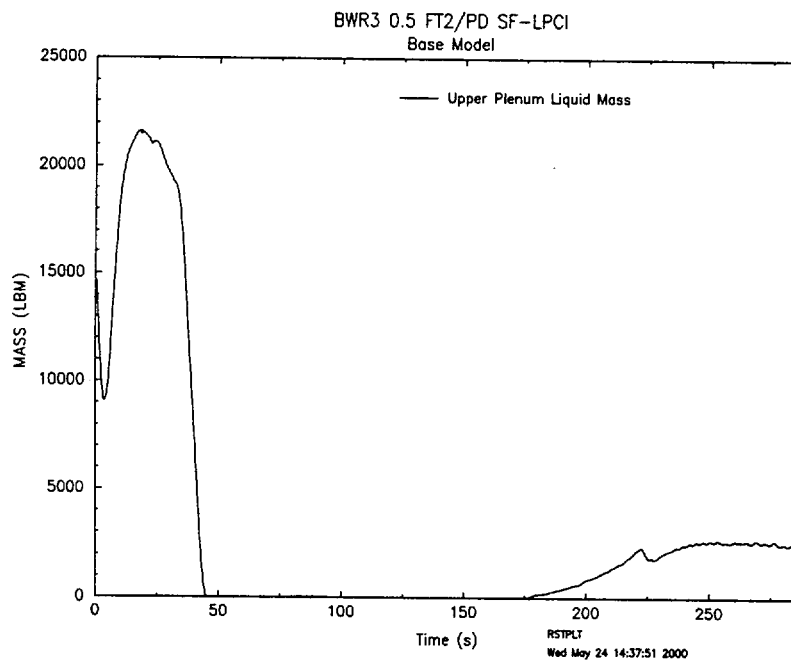


Figure 4.43 Upper Plenum Liquid Mass

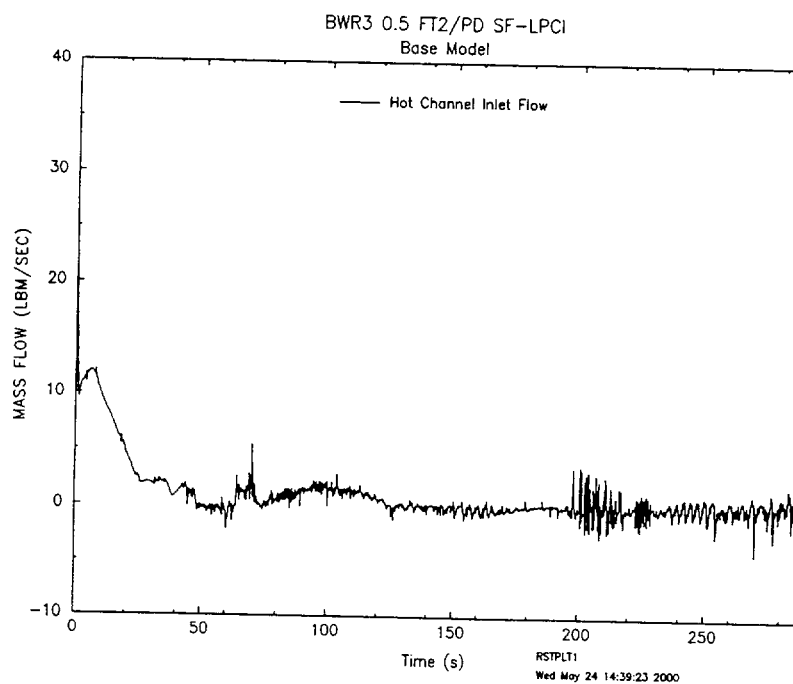


Figure 4.44 Hot Channel Inlet Flow

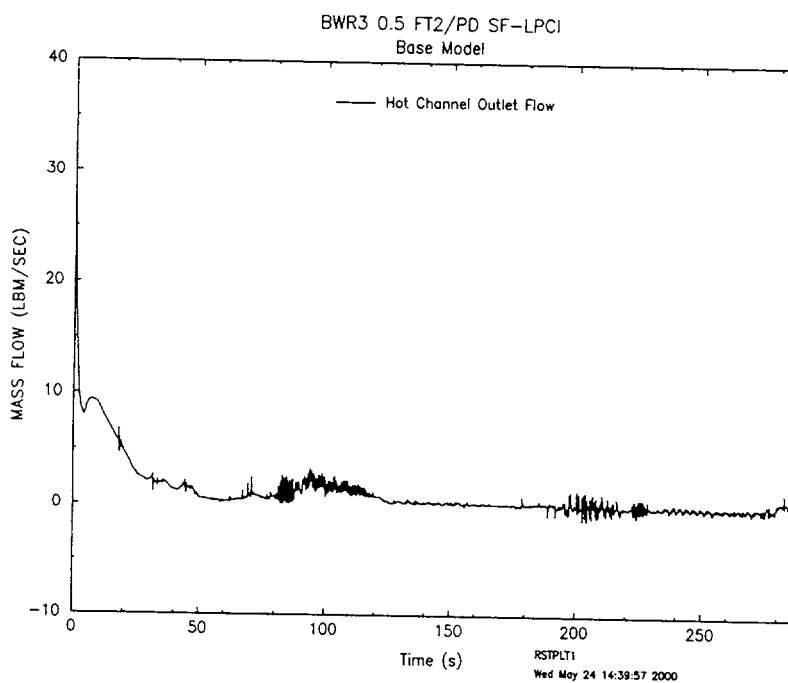
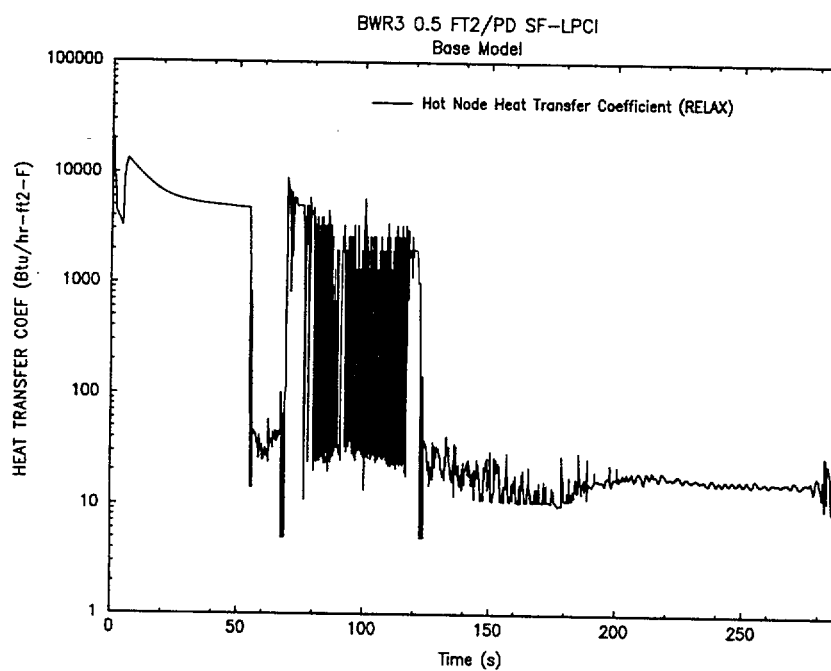


Figure 4.45 Hot Channel Outlet Flow



**Figure 4.46 Hot Node Entrainment Flow****Figure 4.47 Hot Node Heat Transfer Coefficient (RELAX)**

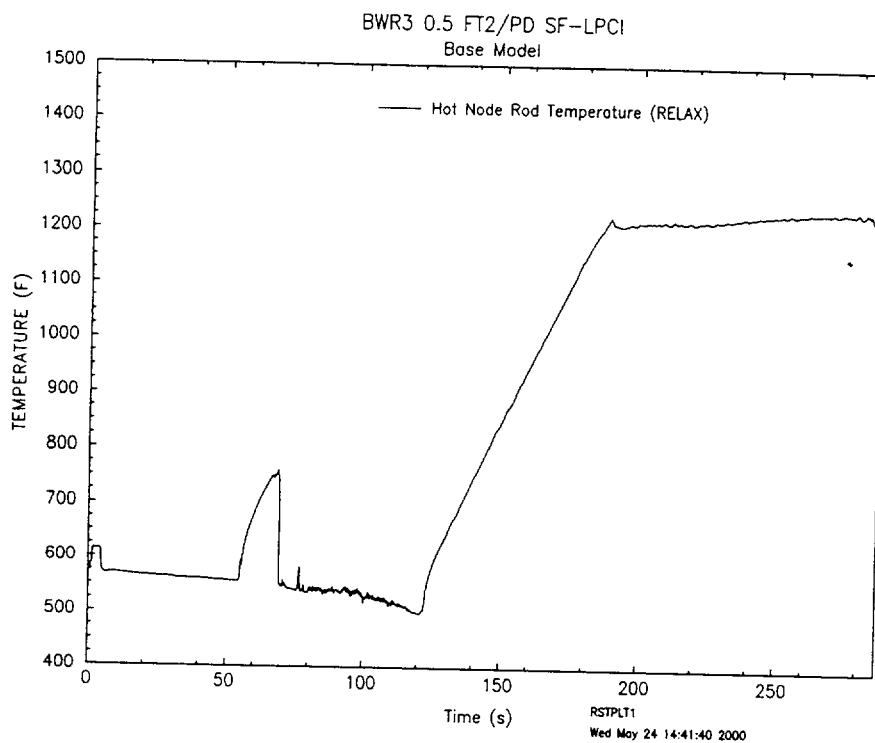


Figure 4.48 Hot Node Rod Temperature (RELAX)

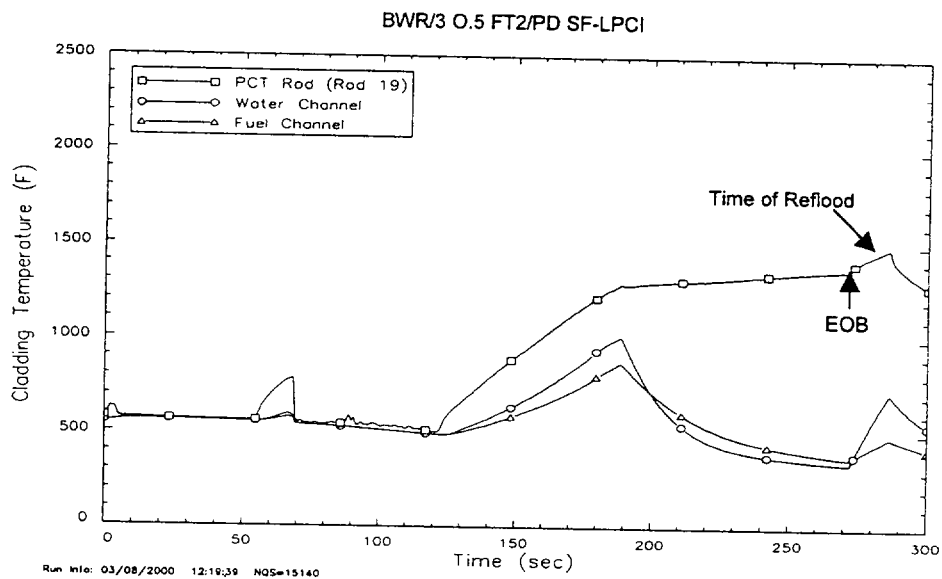


Figure 4.49 HUXY Analysis

## 4.2 ***EXEM BWR-2000 Methodology Sensitivity Studies***

This section presents the results from several sensitivity studies. In a sensitivity analysis, a specific modification is made to the proposed RELAX BWR LOCA/ECCS model described in Section 3.0. A LOCA calculation is then completed using the modified model and the results are compared to the base calculation. These studies are performed to confirm that the results are not excessively sensitive to RELAX nodalization or RELAX inputs.

### 4.2.1 RELAX Nodalization Sensitivity Studies

This section covers three nodalization sensitivity studies.

- Average core nodalization
- Upper plenum nodalization
- Hot channel nodalization.

The limiting 0.8 DEG/PS SF-LPCI LOCA case is used as the base calculation for the sensitivity studies.

#### RELAX Average Core Nodalization Sensitivity Study

[

] Figure 4.50

shows the three-node average core RELAX model used for the core nodalization sensitivity study. Table 4.5 summarizes of the key results from the sensitivity study compared to the base analysis.

From Table 4.5, the key LOCA parameters for the two cases are very similar. The time of core reflood is 4.8 seconds earlier in the sensitivity study than the base case, and the sensitivity study PCT is lower because of the earlier reflood.

Figure 4.51 compares the total core mass for the two 0.8 DEG/PS SF-LPCI cases. The initial (time zero) mass is higher for the eight-node core model because finer nodalization provides a more accurate calculation of steady-state core fluid quality. After the beginning of the LOCA,

the two calculations show very similar results. Figure 4.52 shows the high-power, hot-channel, and node-fuel-rod-surface temperature. Again, the trends are very similar for the two analyses. However, the base-case temperature results are higher than the sensitivity study results, therefore the model is conservative.

**Table 4.5 Core Nodalization Sensitivity Study  
Summary of Results**

**Figure 4.50 RELAX 3 Node Average Core Model**

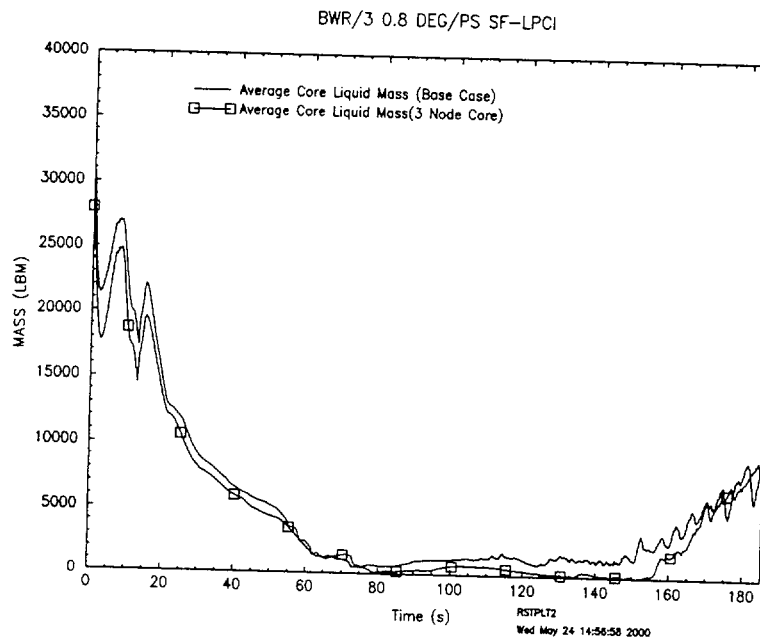


Figure 4.51 Average Core Liquid Mass – Core Nodalization Sensitivity Study

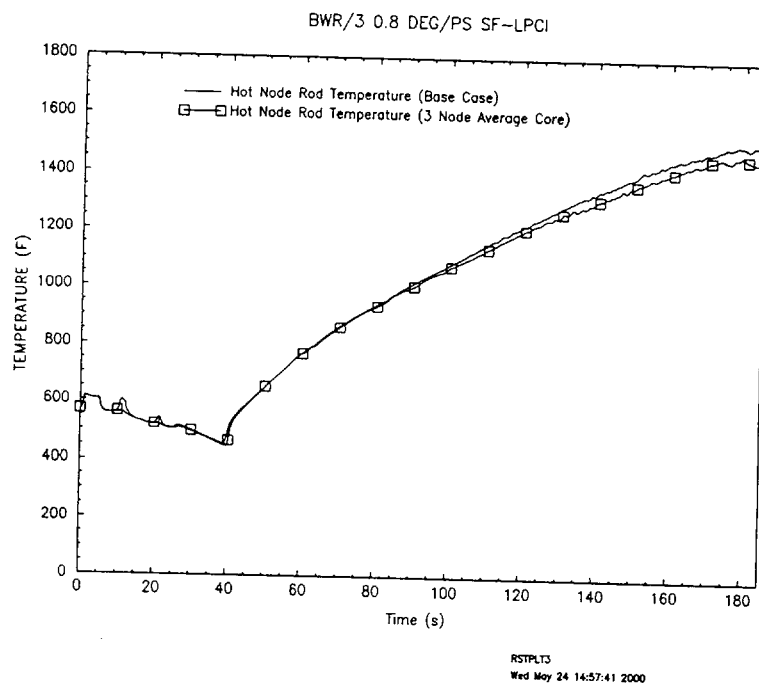


Figure 4.52 RELAX Hot Node Surface Temperature - Core Nodalization Sensitivity Study

RELAX Upper Plenum Nodalization Sensitivity Study

The upper plenum modeling methods for the EXEM BWR-2000 are explained in Section 3.3.4. In this section the results of an upper plenum nodalization sensitivity analysis are presented to assess the impact of upper plenum modeling. [

]

Table 4.6 summarizes the key results for the upper plenum nodalization sensitivity calculation for the limiting 0.8 DEG/PS SF-LPCI LOCA.

The results of the key parameters from the alternative upper plenum model analysis are very similar to the base case results. Figure 4.53 compares the liquid mass in the lower plenum region for the two calculations. The lower plenum mass calculation for the sensitivity analysis matches the trend observed in the base case. This indicates that the RELAX calculation of ECCS flow from the upper plenum through the core and the bypass to the lower plenum is not sensitive to upper plenum nodalization. Therefore, upper plenum nodalization will not affect RELAX calculation of the refill/reflood phase of a LOCA.

Figure 4.54 shows the RELAX calculated high-power, hot-channel, node-fuel-rod-surface temperature calculation for the two cases. The results from the calculation with the alternative upper plenum model are nearly identical to those for the base-case surface temperature calculation.

**Table 4.6 Upper Plenum Nodalization Sensitivity Study  
Summary of Results**

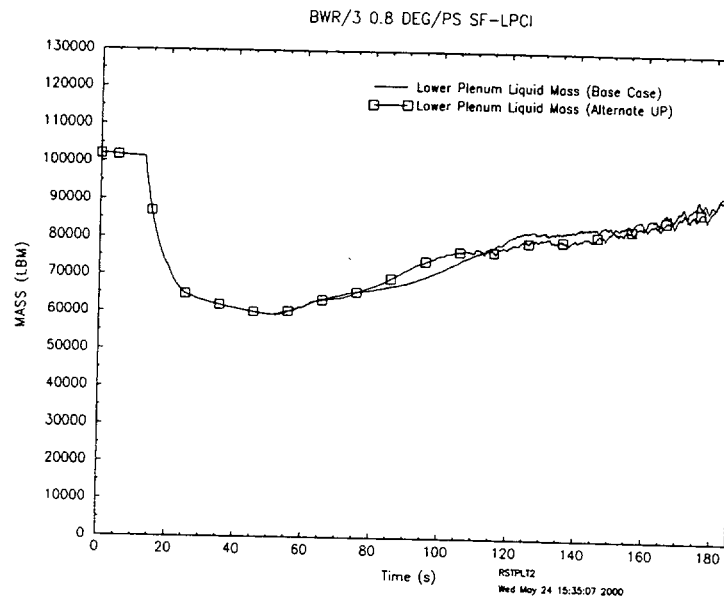


Figure 4.53 Lower Plenum Liquid Mass - Upper Plenum Nodalization Sensitivity Study

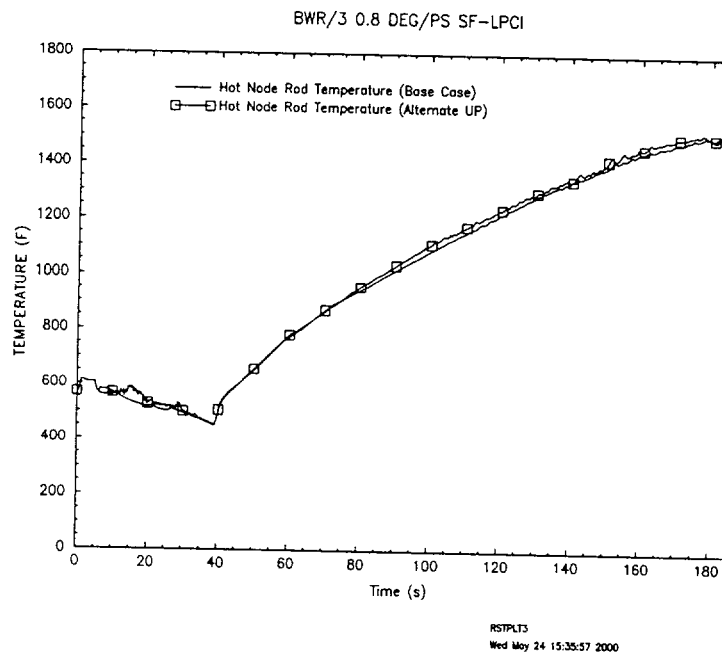


Figure 4.54 RELAX Hot Node Surface Temperature - Upper Plenum Nodalization Sensitivity Study (RELAX)



### RELAX Hot Channel Model Nodalization Sensitivity Study

The eight-node hot channel model used in EXEM BWR-2000 is shown in Figure 4.2. Figure 4.55 shows the 16-node hot channel model used for the sensitivity study. In the Figure 4.55 model, the hot channel nodes are of equal length. The impact of hot-channel nodalization on the calculation of CHF using ANFB (Reference 24) is assessed in this sensitivity study.

The 16-node model was analyzed using the lower and upper plenum boundary conditions from the 0.8 DEG/PS SF-LPCI break spectrum calculation. Nodes 1 and 18 are the time dependent volumes in the 16-node model. During the initial seconds of a LBLOCA, the critical power ratio will decrease in the hot channel and CHF may be approached in the hot node. [

]

The 16-node model RELAX calculation of high-power, hot-channel, node-fuel-rod-surface temperature is compared with the eight-node model calculation in Figure 4.57. The eight-node model temperature calculation is higher and, therefore, slightly more conservative than the 16-node analysis.

**Figure 4.55 RELAX 16-Node Hot Channel Model**

**Figure 4.56 Heat Flux and CHF - Hot Channel Nodalization Sensitivity Study**

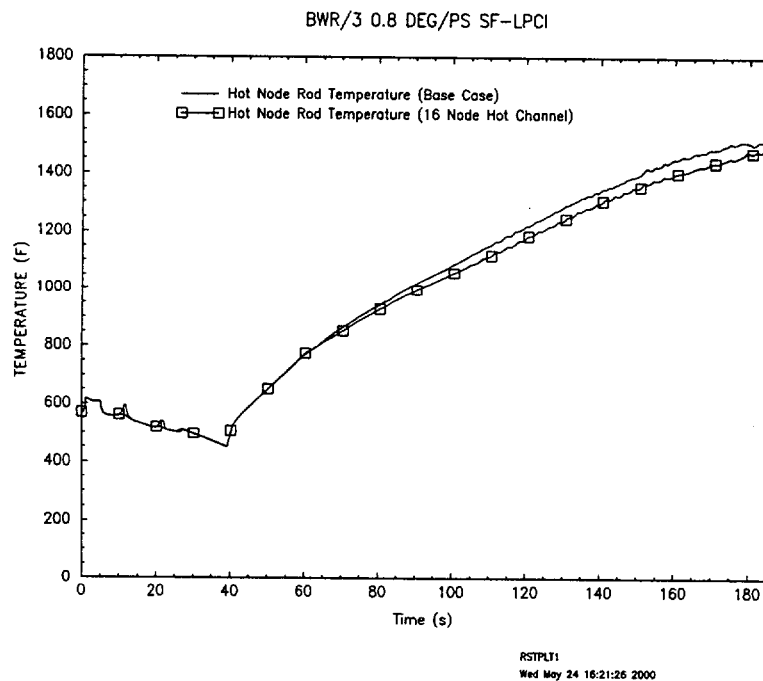
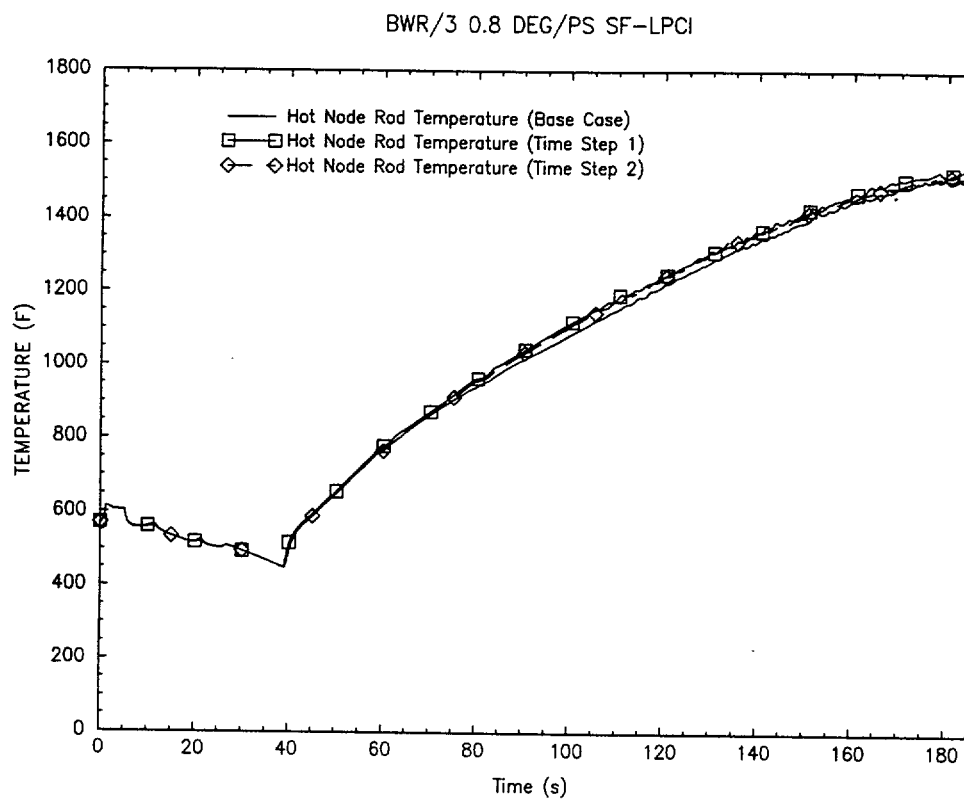


**Figure 4.57 RELAX Hot Node Surface Temperature - Hot Channel Nodalization Sensitivity Study**

#### 4.2.2 Time Step Convergence

The RELAX iterative numerical solution method is documented in Section 3 of ANF-91-048(P)(A) (Reference 6). This solution method selects the correct time interval required to obtain a converged solution for each time-step advancement. A measure of the errors in the linearized energy equation and the linearized pressure equation for each RELAX volume is used to define convergence. This measure is called the "convergence criterion." For BWR LOCA applications, a convergence criterion is used that is more rigorous than the code default value. This is accomplished by applying a 0.5 multiplier to the criterion. A RELAX LOCA analysis performed with the more rigorous criterion will generally advance with smaller average time-step intervals than the equivalent analysis with the default criterion. The 0.5 multiplier was used in the base-case analysis.

Two sensitivity calculations were completed to demonstrate time-step convergence for EXEM BWR-2000. These calculations analyzed the limiting 0.8 DEG/PS SF-LPCI case. The first sensitivity calculation was performed with a 0.3 convergence criterion multiplier applied to both the system and the hot channel calculations. The second calculation used a 0.2 multiplier. Figure 4.58 shows the RELAX-calculated fuel-rod-surface temperature of the highest power RELAX hot channel heat conductor. The temperature calculation results from the base case are very similar to the results from the two sensitivity analyses. These results confirm that EXEM BWR-2000 achieves numerical convergence.



RSTPLT2  
Wed May 24 16:50:46 2000

**Figure 4.58 RELAX Hot Node Surface Temperature - Time Step Convergence Sensitivity Study**

## 5.0 Model Validation

The model validation for EXEM BWR-2000 serves two purposes: To validate the applicability of the new evaluation model and to respond to the 1997 NRC inspection concern of inadequate validation for the RELAX code. Validation of the EXEM BWR-2000 ECCS evaluation model was accomplished by benchmark comparisons against FIST (References 35 and 36) and TLTA (Reference 38) experimental results. A good representation of a BWR is the FIST facility (Reference 35). FIST provides a 1:624 scale (power-to-volume), full-height model of a 218-inch diameter BWR/6 vessel and recirculation system. The heated assembly is a full-scale 8x8 array with 2 water rods. FIST includes those components normally modeled in LOCA analyses, i.e., heated assembly, jet pumps, steam separator, steam dome, steam line with isolation and relief valves, upper and lower plenums, bypass region, and two recirculation loops, one of which contains the "break". The break is scaled on a break area-to-system volume basis.

The EXEM BWR-2000 methodology conservatively simulates the core as a single average assembly during refill and reflood. The FIST facility and TLTA simulation also model a single fuel assembly and the time scale, fluid mass, energy distributions, velocities, accelerations, and lengths are essentially the same in the test facility as in the prototype plant. Thus, the FIST data are appropriate to validate the EXEM BWR-2000 methodology.

Scale effects have been observed in the refill-reflood period of a BWR LOCA (Reference 1). With power-to-volume scaling, component length is preserved, but component diameters are significantly reduced. As a result, multi-dimensional effects, which could occur in the reactor vessel plenum regions of a large BWR, may not be observed in small-scale tests. For example, the flow of ECC fluid from the upper plenum to the lower plenum in the test is via leakage paths and countercurrent flow in the heated bundle. Large tests with multiple parallel channels of varying power have shown that the lower power peripheral assemblies provide a relatively direct and easy flow path for the ECC to flow from the upper plenum to the lower plenum. Because the EXEM BWR-2000 methodology and single assembly tests neglect this flow path, both will yield conservative reflood results relative to behavior in an actual BWR. Thus the conservatism caused by this effect is excluded from the FIST and TLTA benchmark comparisons.

In the EXEM BWR-2000 methodology, the RELAX code is used to calculate the thermal hydraulic response of the reactor and recirculation system during the blowdown and refill

periods. The HUXY code is used for evaluating the heat-up of a fuel assembly during these periods.

### 5.1 *FIST Benchmarks*

Figure 5.1 provides the RELAX nodal representation of the FIST facility. This diagram is very similar to that used in normal plant licensing analyses, differing only where the unique FIST geometry may have an undue influence on the calculation. For instance, in licensing calculations, the jet pump inlet mixing (throat), diffuser and tailpipe sections are modeled as separate regions. The FIST jet pump throat and diffuser sections are rather small compared to the tailpipe section. Therefore, the throat and diffuser sections are combined into a single region and the tailpipe is divided into two equal volume regions. The heated region (simulated core) is modeled by 7 axial regions with a 1.4 peak/average chopped cosine power distribution and a total heated length of 150 inches.

The heater rods are the "direct" type, i.e., the energy is generated in the cladding region of the simulated fuel rods. The internal region of the rods is filled with ceramic cement. The data sheet for the ceramic cement provides the range of thermal conductivity, but no information is available for the specific heat. Also, significant differences occur between the thermal expansion of the Inconel heater tubes and the ceramic cement filler. The cement is in paste form when placed in the tubes, so voids may exist and/or cracks may form when the tubes expand. [

]

The model has two upper plenum regions. The lower region (Upper Plenum 1) represents the region from the end-of-heated length (EHL) to the beginning of the shroud spherical head. In the actual plant, this region includes the HPCS and LPCS spargers. The upper region (Upper

Plenum 2) represents the region within the shroud spherical head, the steam separator standpipes, and the steam separator itself.

The Upper Downcomer region represents the area outside the steam separators from the steam dryers down to the flange on the shroud head. During normal steady operation, water level is maintained within this region. The Level 2 trip is located in this region and activates the ECCS with appropriate delays.

The Middle Downcomer region runs from the flange on the shroud head to the top of the jet pump rams head and contains the Level 1 trip. The Level 1 trip causes the main steam isolation valve(s) (MSIV) to close and starts the ADS valve timer.

The Lower Downcomer is the annular region between the vessel wall and the core shroud and contains the two jet pumps. This region is common to the suction of both recirculation loops.

The recirculation pumps themselves are isolated during the tests and, by adjusting the pump inertia, the pump speed decay is matched for each transient modeled; the recirculation system dynamics are included. The pump isolation valves are located so that the fluid volume contained between the vessel and isolation valves corresponds to the scaled (1:624) recirculation loop volume.

The jet pumps contain a nozzle and inlet mixer section, a diffuser section, and a tailpipe section. The FIST jet pumps were designed to provide a full-height jet pump section, scaled core flow, BWR reverse flow characteristics, and to include the interaction between the jet pumps as in the actual BWR.

The model has two lower plenum regions. The Lower Lower Plenum represents the lower plenum region below the exit of the jet pumps. The Upper Lower Plenum represents the lower plenum region above the jet pump exit and includes the fuel support (orifice region) and lower tie plate. Normal BWR leakage paths provide flow to the bypass region via the upper lower plenum and guide tube.

The guide tube region represents a scaled guide tube and includes the volumes within the guide tube but outside the fuel support up to the beginning-of-heated-length (BHL). An orificed flow path simulates the leakage paths between the lower plenum and the guide tube/bypass region, including the lower tie plate flow holes and the channel to the lower tie plate seal.



The bypass region extends from the BHL elevation to the top guide. In the actual test facility, the flow between the bypass and upper plenum is controlled by eight 1-inch-diameter holes.

The RELAX modeling of the emergency core cooling system (HPCS, LPCS, and LPCI) head/flow characteristics are derived from the test data, i.e., the flows are entered in table format as a function of the dome pressure. At the same dome pressure, the test and RELAX calculation have the same ECC flow. The HPCS system is initiated when the downcomer water level reaches Level 2 with a 20-second delay. Normally the LPCS and LPCI are initiated at the time of the break, but do not immediately begin injection because the system pressure is above their shut-off heads. The recirculation pumps have little impact on the dynamics of the event because they are both isolated early into the event, but the inertia of the recirculation pumps has been adjusted to achieve a speed decay characteristic consistent with the test data. The ADS is tripped at Level 1 with a 120-second delay (105 seconds for BWR/4 simulation). Before isolation, the valve representing the MSIV is used as a pressure control valve. For long transients such as for small breaks, the MSIV flow area is adjusted as a function of time to yield a calculated pressure comparable with the test pressure.

The FIST data (Reference 36 and 37) include three tests that produced significant temperature responses (although less than 1000°F). The tests, 6DB1B, 4DBA1, and 6SB2C, model BWR/6 large-break, BWR/4 large-break, and BWR/6 small-break loss-of-coolant events. Boundary input taken from the test data include the following:

1. Initial conditions such as power, flow, inlet temperature, dome pressure and lower plenum pressure at the side entry orifice.
2. Transient power (as a function of time)
3. MSIV closure rate
4. Pump speed decay
5. Time of recirculation drive and suction line isolation
6. ECCS pressure/flow characteristics.



**Figure 5.1 RELAX Nodal Model for FIST**

### 5.1.1 Large-Break Test 6DB1B

Test 6DB1B is a BWR/6 DBA simulation, with HPCS, LPCS and LPCI available and scaled 1.878 ft<sup>2</sup> suction line (Junction 32) and 0.348 ft<sup>2</sup> drive line breaks (Junction 33). An average central orifice region bundle is modeled with a power of 5.045 MW.

The transient begins with a coincident double-ended recirculation line break and power trip. The flow through the broken jet pump loop (Jet Pump 2) decreases rapidly and then reverses. The flow through the intact jet pump decays exponentially and settles out slightly negative. Figures 5.2 and 5.3 compare the measured and predicted flows at the jet pump exits. The flow response is well predicted throughout the event.

The FIST MSIV, doubling as a pressure control valve and an isolation valve, begins closing immediately to control the system pressure. Pressure is maintained until the mixture level in the lower downcomer region reaches the elevation of the recirculation loop suction nozzles (at about 8 seconds) and the break becomes uncovered resulting in increased volumetric flow out of the break. The measured and predicted system pressure responses are compared in Figure 5.4. Because the RELAX model does not contain a pressure control system, the MSIV flow area was input as a boundary condition, assuming the valve flow area is proportional to the valve stem position as measured in the test. RELAX calculates a higher depressurization rate than that observed in the test, particularly after about 20 seconds. This is attributed to three factors. First, although this RELAX calculation is regarded as "best estimate," the Moody critical flow model is used once the conditions become saturated at the break. The Moody critical flow model is known to be conservative (over estimates the flow), particularly during low quality conditions, resulting in too large a depressurization rate. Second, the RELAX upper plenum regions are modeled as homogeneous regions. The steam condensation is overestimated in these regions once HPCS and LPCS injection begins (22 seconds and 46 seconds, respectively). By using two upper plenum regions and the enthalpy injection model described in Section 3.2.5, the impact of this phenomenon is minimized. Lastly, the test data suggests that at between 20 and 25 seconds the middle downcomer flow increases noticeably. It is surmised that liquid has carried over from the upper plenum regions and limits the depressurization rate when it reaches the break. Thus the measured depressurization rate is seen to decrease in the 20- to 25-second period of the transient.

As shown in Figure 5.5, the downcomer mass decreases because of inventory loss through the break. RELAX and the test data agree quite closely. Note the increase in the FIST lower downcomer mass in the 22- to 26-second period of the transient. This confirms the observation that the measured downcomer liquid flow rate increased during this period and caused the change in the depressurization rate.

The RELAX calculated mass and the mass from the test data may differ at event initiation and during the first few seconds of the transient. The test data uses differential pressure measurements to determine the mass between points. Until the dynamic hydraulic losses become significantly less than elevation head losses, the "measured" mass may be overly influenced by the hydraulic losses. Also, the definition of the RELAX regions does not always correspond exactly with that of the test data regions.

Figures 5.6 through 5.12 compare the calculated and measured mass inventory for other regions of interest. RELAX predicts the trends and, for the most part, conservatively under predicts the mass distribution.

Figure 5.8 compares the calculated and measured mass inventory in the combined upper plenum regions. The calculated times of injection for the HPCS, LPCS, and LPCI are 22, 46, and 51 seconds, respectively. At about 50 seconds, the mass in the upper plenums begins increasing. At approximately 125 seconds, the upper plenum mass increases to the point where a "significant" quantity of liquid flows down into the bypass region resulting in a sudden increase in the bypass region mass (Figure 5.9). The liquid from the bypass drains to Region 16 (Figure 5.10) via Region 17 (Figure 5.11). Figure 5.12 compares the calculated and measured mass inventory in the bundle. Also shown in Figure 5.12 is the hot node mass flow rate along with the reflood criterion and calculated time of reflood.

Figures 5.13 through 5.20 compare the calculated (RELAX and HUXY) rod temperature response at the 75-inch and 87-inch elevations with the more responsive thermocouple measurements from the test. The temperatures remain essentially at saturation until mid-plane dryout occurs at about 40 seconds. Note that this dryout condition corresponds to the nearly depleted bundle mass condition shown in Figure 5.12. The calculated temperature response at the 75-inch elevation does not show rewetting until 174 seconds (Figure 5.14, for example).

Table 5.1 compares the calculated and measured key events. These results demonstrate that RELAX conservatively modeled the blowdown and refill periods of this test.

**Table 5.1 Comparison of Events**

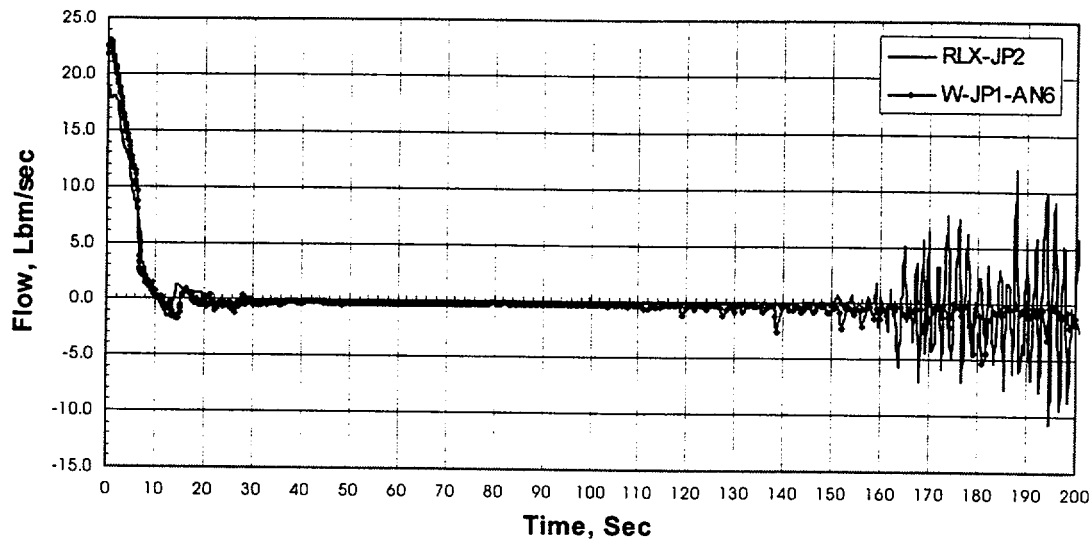


Figure 5.2 FIST BWR/6-DB1-B Jet Pump 1 Flow

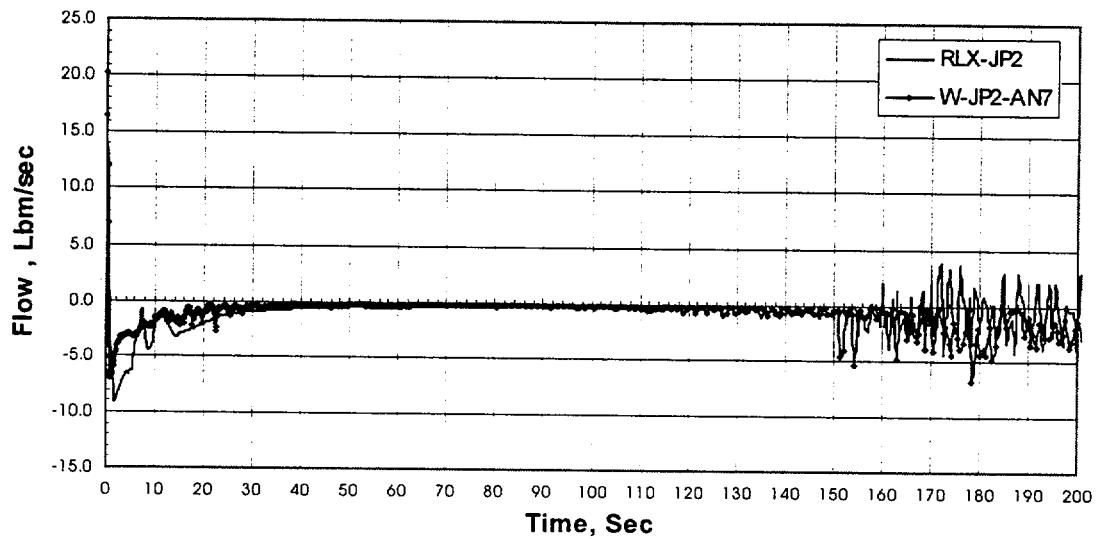


Figure 5.3 FIST BWR/6-DB1-B Jet Pump 2 Flow

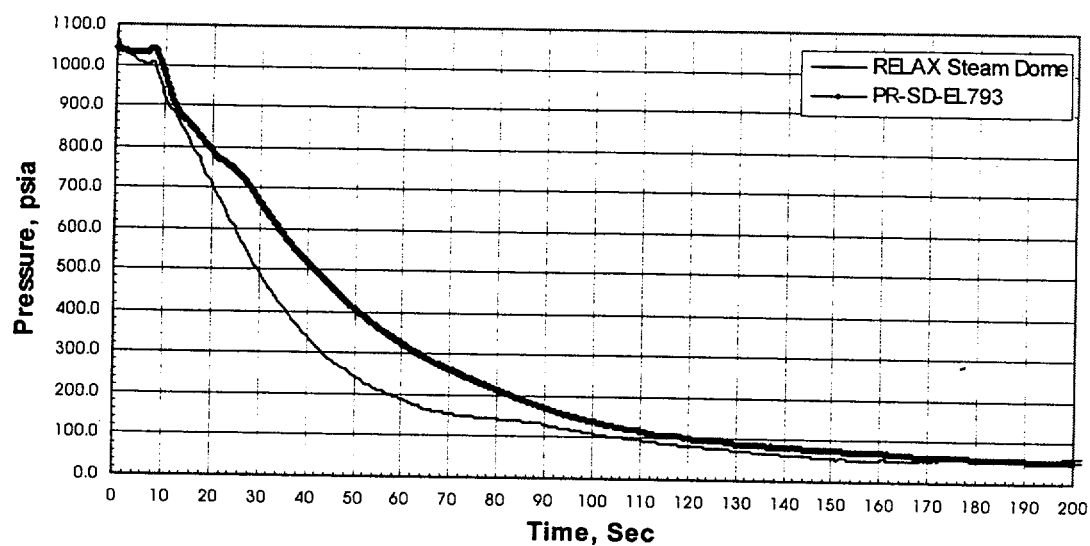


Figure 5.4 FIST BWR/6-DB1-B Pressure Response

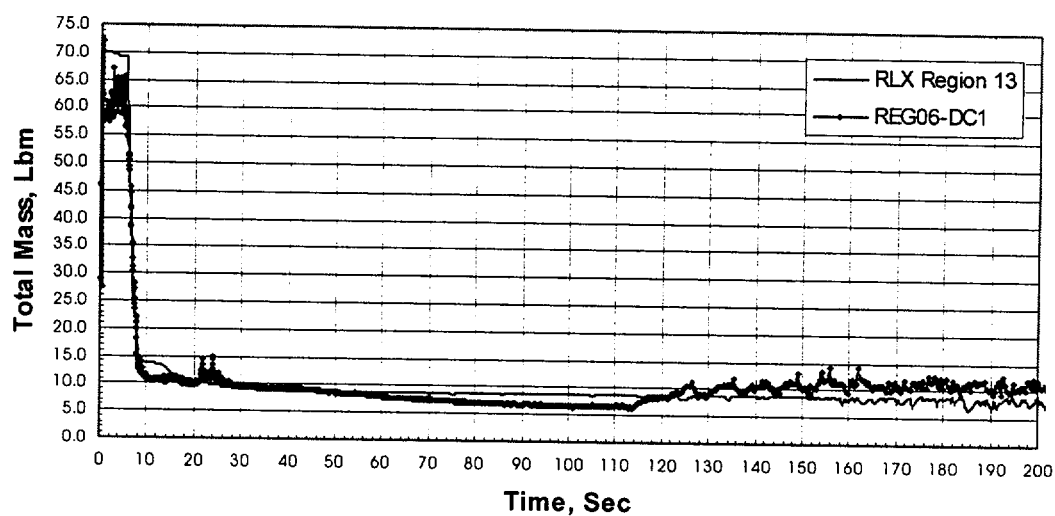


Figure 5.5 FIST BWR/6-DB1-B Lower Downcomer Mass Inventory

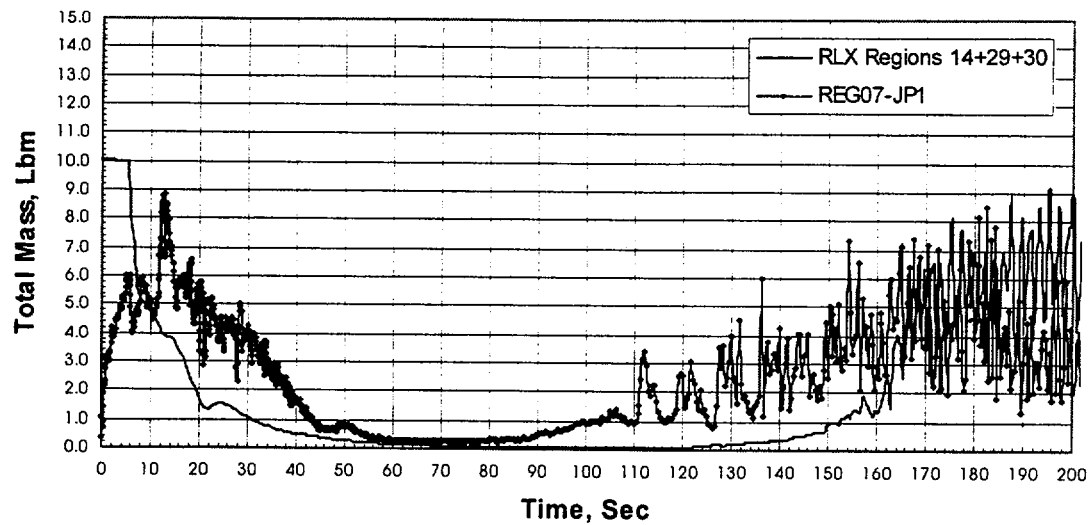


Figure 5.6 FIST BWR/6-DB1-B Jet Pump 1 Mass Inventory

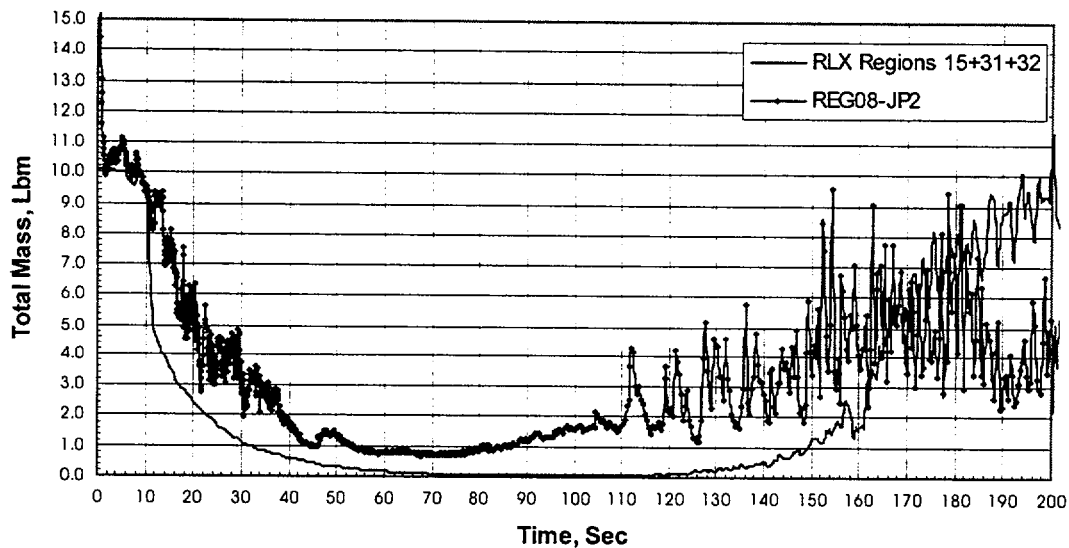


Figure 5.7 FIST BWR/6-DB1-B Jet Pump 2 Mass Inventory



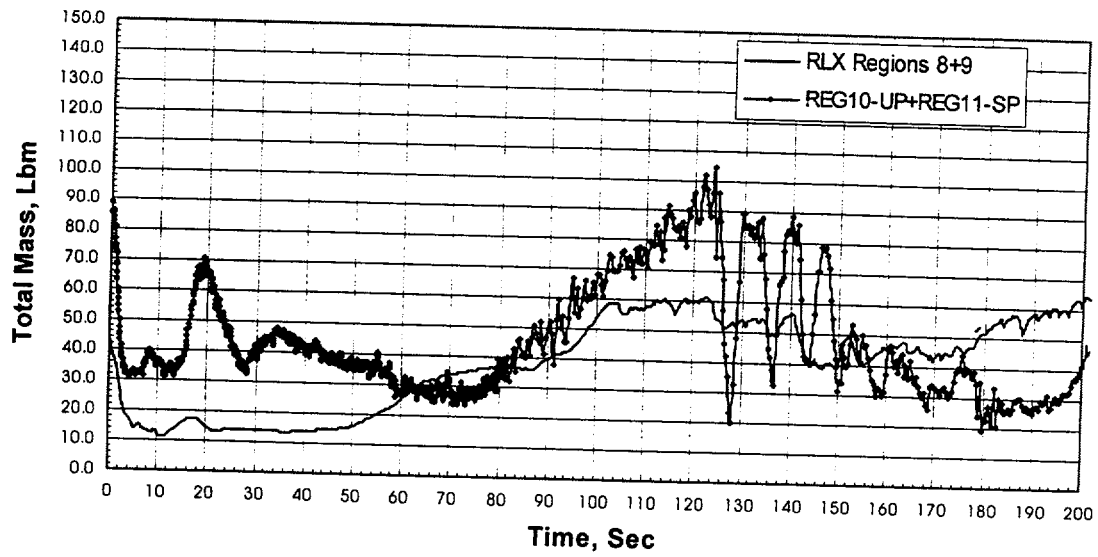


Figure 5.8 FIST BWR/6-DB1-B Upper Plenum Mass Inventory

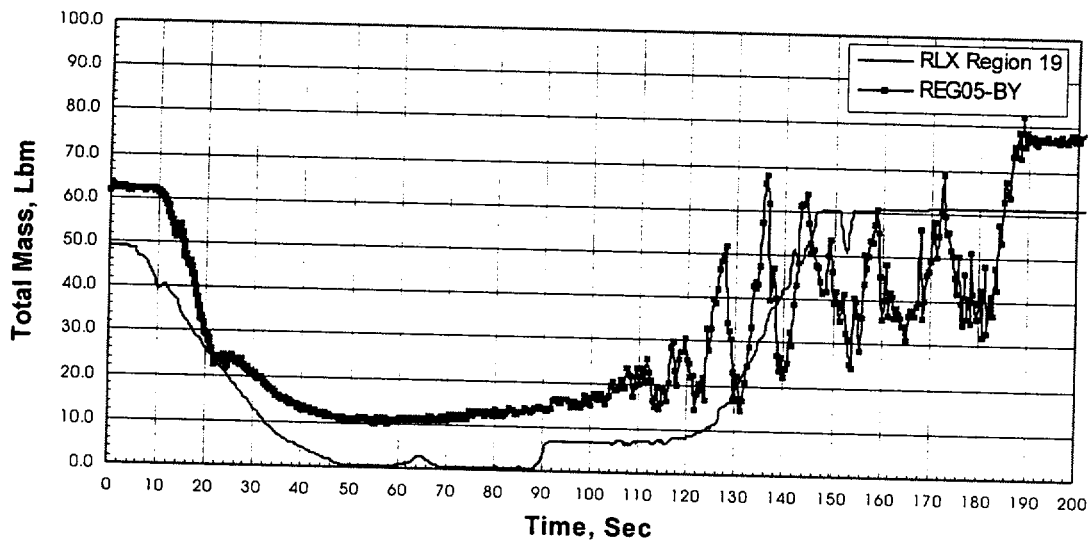


Figure 5.9 FIST BWR/6-DB1-B Bypass Region Mass Inventory

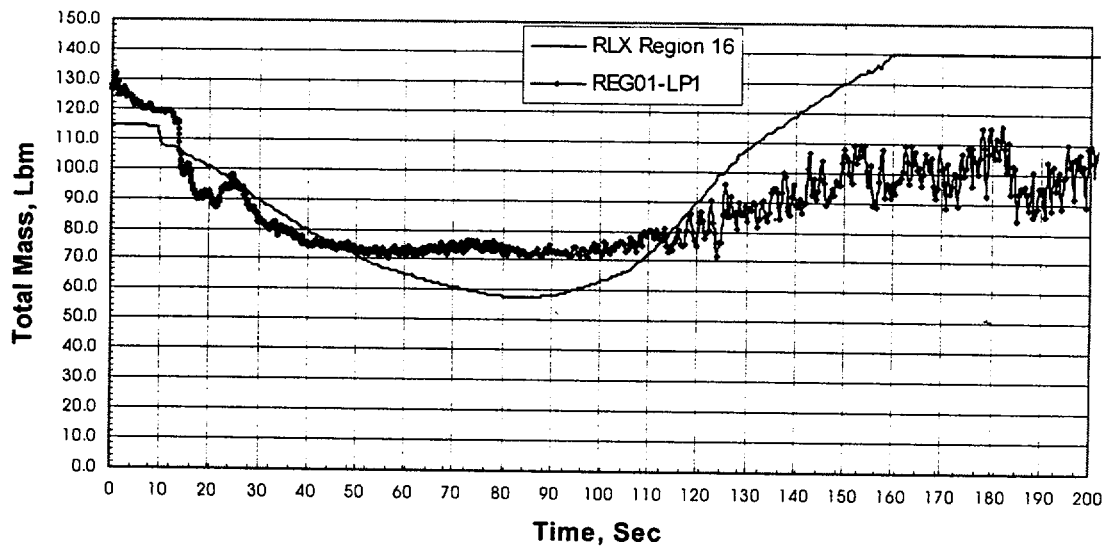


Figure 5.10 FIST BWR/6-DB1-B Lower Lower Plenum Mass Inventory

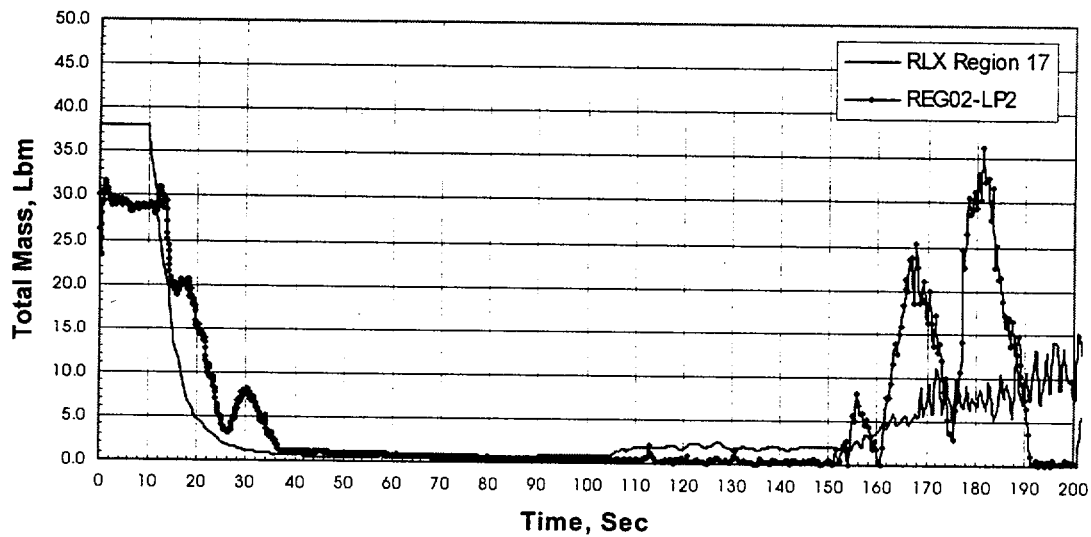


Figure 5.11 FIST BWR/6-DB1-B Upper Lower Plenum Mass Inventory

**Figure 5.12 FIST BWR/6-DB1-B Bundle Mass Inventory**

**Figure 5.13 FIST BWR/6-DB1-B Temperature Response 75-Inch  
Elevation (1 of 4)**

**Figure 5.14 FIST BWR/6-DB1-B Temperature Response 75-Inch  
Elevation (2 of 4)**

**Figure 5.15 FIST BWR/6-DB1-B Temperature Response 75-Inch  
Elevation (3 of 4)**

**Figure 5.16 FIST BWR/6-DB1-B Temperature Response 75-Inch  
Elevation (4 of 4)**

**Figure 5.17 FIST BWR/6-DB1-B Temperature Response 87-Inch  
Elevation (1 of 4)**

**Figure 5.18 FIST BWR/6-DB1-B Temperature Response 87-Inch  
Elevation (2 of 4)**

**Figure 5.19 FIST BWR/6-DB1-B Temperature Response 87-Inch  
Elevation (3 of 4)**



**Figure 5.20 FIST BWR/6-DB1-B Temperature Response 87-Inch  
Elevation (4 of 4)**

### 5.1.2 Large-Break Test 4DBA1

Test 4DBA1 is a BWR/4 design basis accident (DBA) simulation with a 1.065 in<sup>2</sup> (scaled from 4.14 ft<sup>2</sup>) suction line and 0.1645 in<sup>2</sup> (scaled from 0.064 ft<sup>2</sup>) drive line breaks. In this test, the break sizes are scaled 1:560. The test simulates a failure of a single diesel generator, resulting in the loss of one LPCI pump. One HPCI, one LPCS, and two LPCI are assumed available. The HPCI is connected to the upper plenum and the LPCIs are connected to the intact drive line. In an actual BWR/4 plant, the HPCI injects through the feedwater line. Because the upper plenum is a homogeneous volume in RELAX, SPC methodology connects the feedwater line to the middle downcomer and the HPCI to the upper downcomer. The FIST ECCS pumps all are tripped on at 30 seconds, as opposed to the BWR/6 DBA tests where Level 2 trips with a delay are used. Also, the HPCI is tripped off at a pressure of 115 psia, consistent with an actual BWR/4 (turbine-driven pumps). No other physical changes were made to the system. The initial power of 6.08 Mw simulates a peak power bundle.

Because of the large break size (relative to BWR/6), the large-break causes a very rapid depressurization. FIST attempts to maintain the system pressure through positioning the MSIV. Figure 5.21 compares the calculated and measured dome pressure responses. In this simulation, the RELAX MSIV valve flow area is constant as a function of time until the Level 1 trip, instead of applying the valve flow area as a boundary condition. The pressure decreases immediately from the time of the break. The FIST Level 1 trip occurs at 1.7 seconds and the MSIV is fully closed at 3.4 seconds. In the RELAX calculation, the Level 1 trip occurs at 2.74 seconds and the MSIV is closed at 4.74 seconds.

Figures 5.22 and 5.23 compare the measured and calculated flow from the jet pumps. These figures show excellent agreement between the measured and calculated results. Figures 5.24, 5.25, and 5.26 compare the ECCS flow. Because the ECCS pumps are tripped on at 30 seconds (boundary condition) and the RELAX depressurization rate is greater than that of the test, the flows reach rated conditions almost immediately. The HPCI flow is only momentary because the RELAX pressure is below 150 psia (HPCI shutoff pressure) at 30 seconds.

Figures 5.27 through 5.34 compare the calculated and measured mass inventory. RELAX follows the trend of the test results and, in general, produces conservative predictions. As shown in Figure 5.28, Jet Pump 1 begins refilling at about 37 seconds. This is from the LPCI that must first refill the drive line (Region 23) before flow begins into the jet pump and lower



downcomer. Coincident with this, the lower lower plenum begins to refill (Figure 5.30), which in turn causes the upper lower plenum to begin refilling at 80 seconds (Figure 5.31). The bundle mass begins increasing at 85 seconds (Figure 5.32) and rewetting of the bundle mid-plane is calculated at 94.8 seconds (see Table 5.2). Figure 5.32 also shows the hot node mass flow rate along with the reflood criterion and the calculated time of reflood.

Figures 5.35, 5.36, and 5.37 compare heater rod temperature responses at various elevations within the heated assembly. The thermocouple measurements plotted are the most responsive reported in the database. The test data demonstrated that the timing of the rewet depends on the elevation within the heated assembly, with the lower elevations rewetting first. Both the HUXY and the RELAX calculated peak temperatures bound that measured in the test, even though the calculated time PCT is sooner than that observed in the test. In this test reflooding was observed from the bottom up. This is primarily because of the LPCI injection into the intact jet pump recirculation loop.

Table 5.2 compares calculated and measured event timing. Because of the more rapid RELAX depressurization rate, several events are calculated to occur sooner than observed in the test. Overall, this results in a conservative PCT calculated as the conservative HUXY spray cooling heat transfer coefficients are applied. It is concluded that RELAX/HUXY conservatively modeled the 4DBA1B FIST test.

**Table 5.2 Comparison of Events**

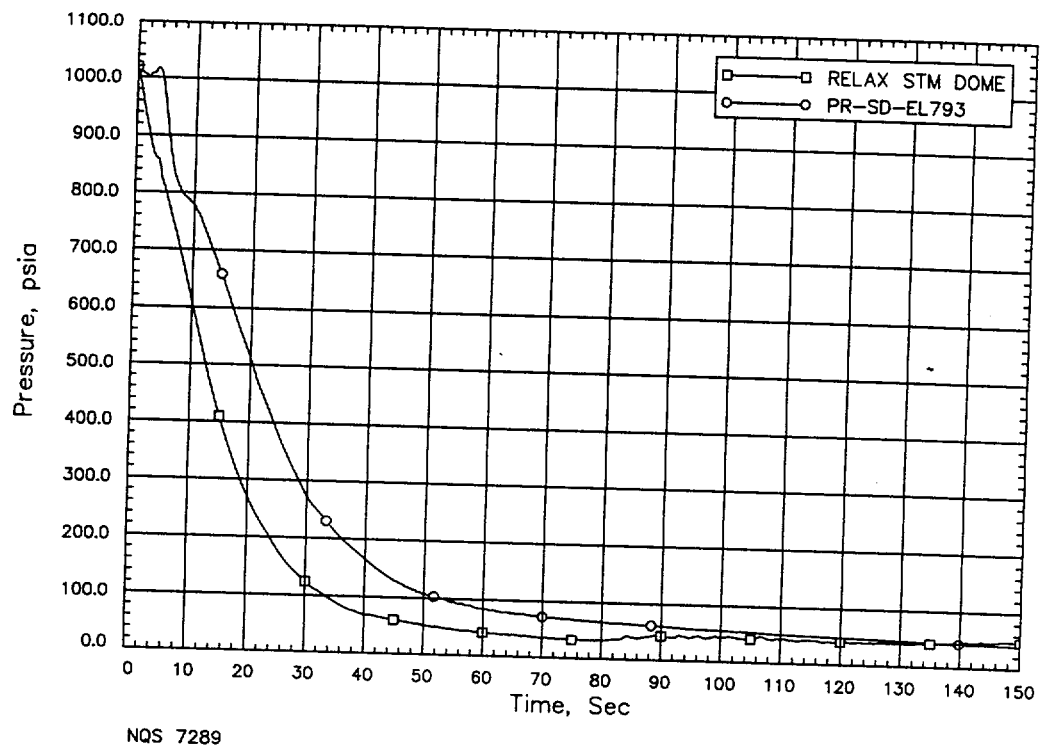


Figure 5.21 FIST BWR/4-DBA-1 Dome Pressure Response

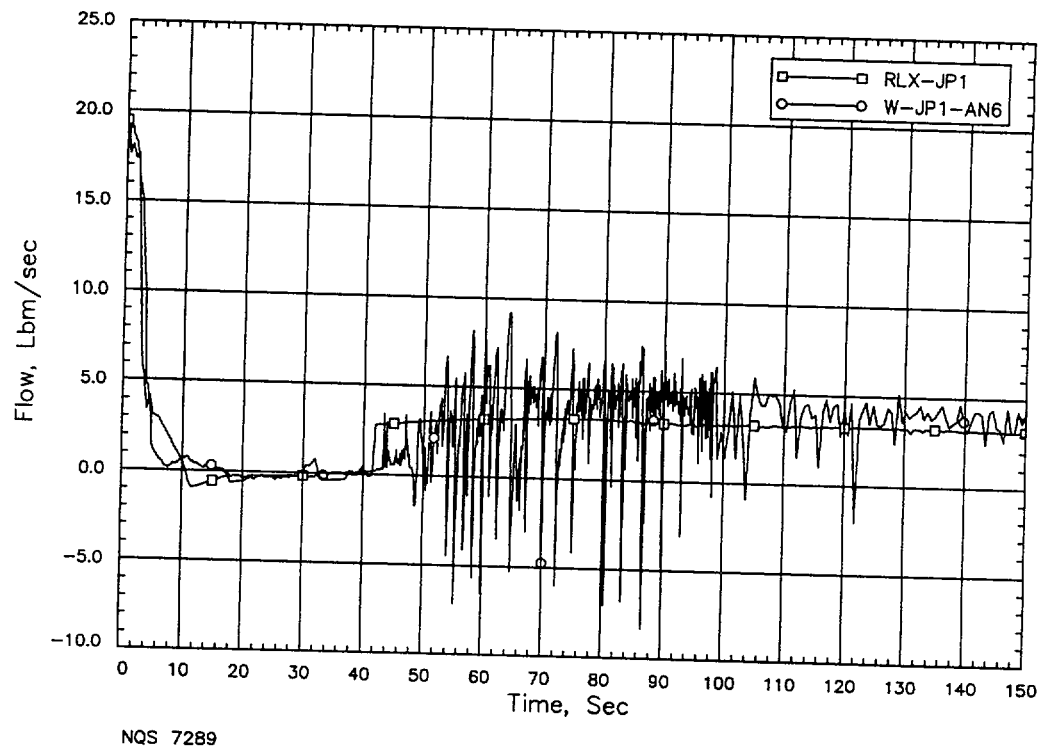


Figure 5.22 FIST BWR/4-DBA-1 Jet Pump 1 Flow Comparison

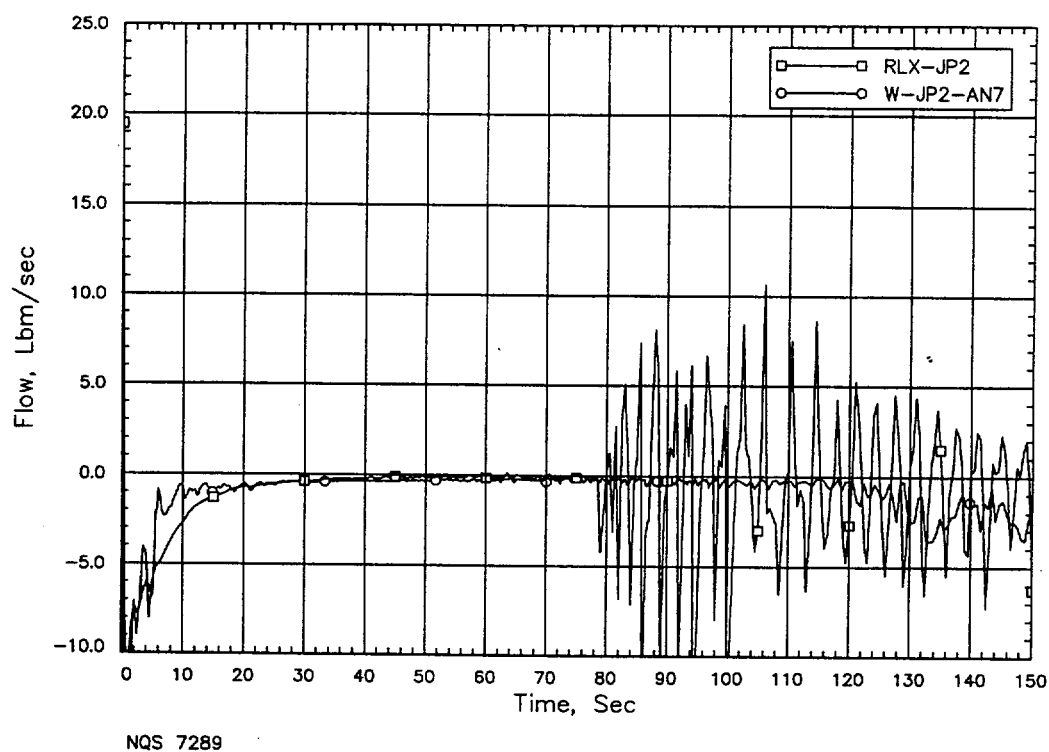


Figure 5.23 FIST BWR/4-DBA-1 Jet Pump 2 Flow Comparison

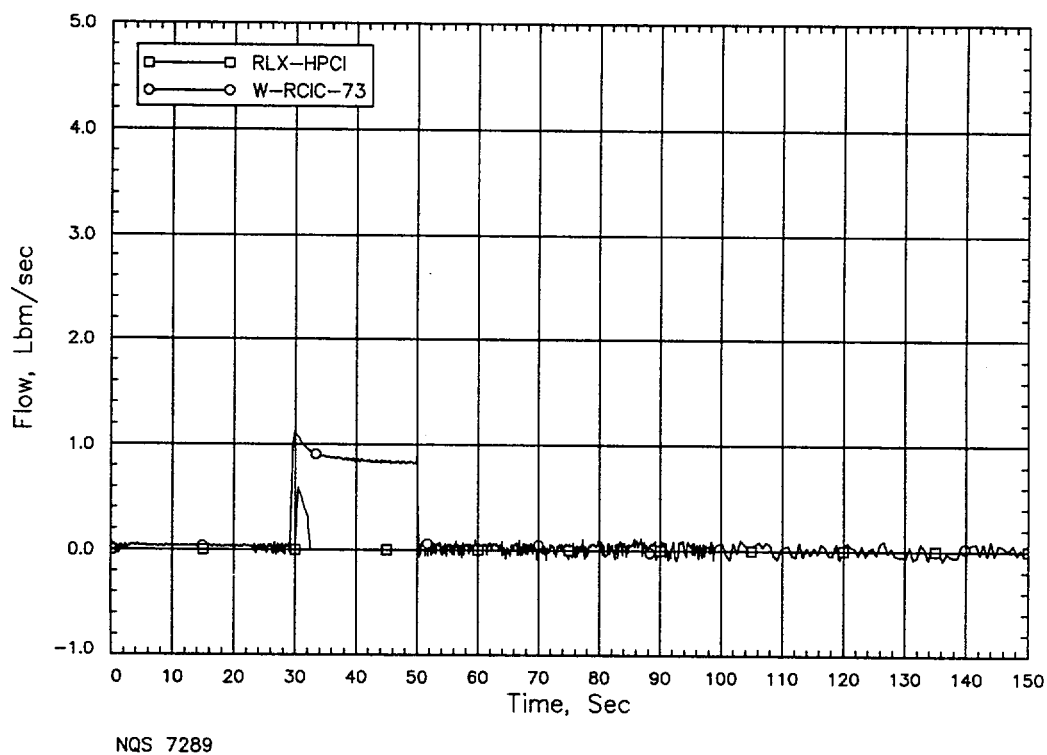


Figure 5.24 FIST BWR/4-DBA-1 HPCI Flow Comparison

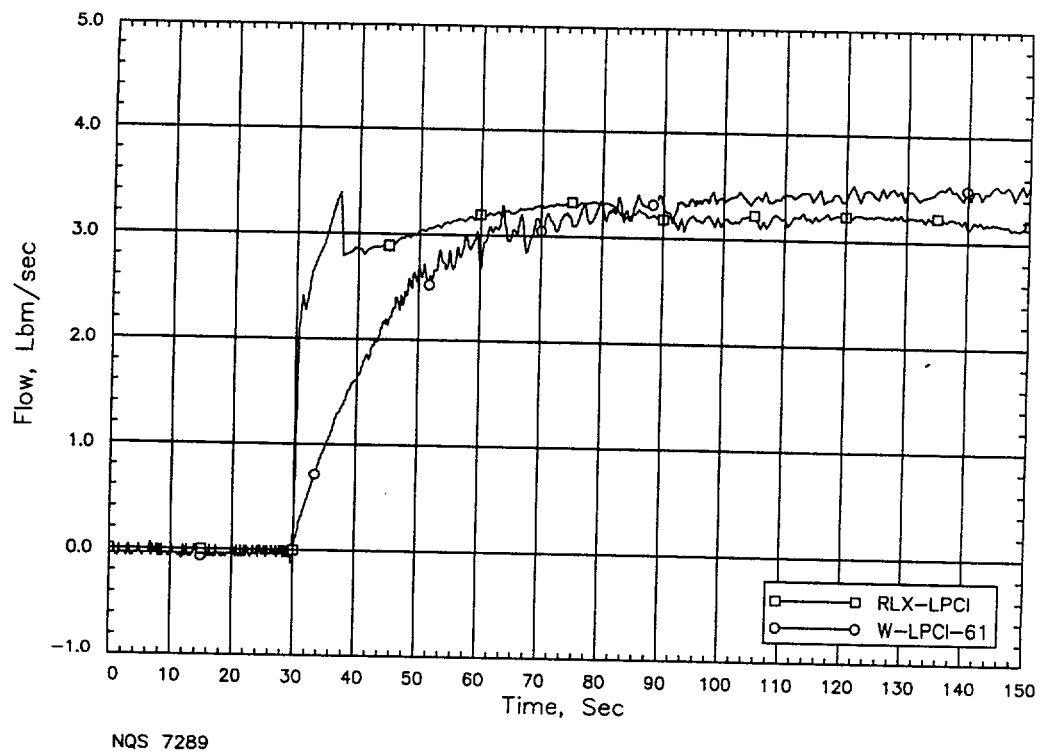


Figure 5.25 FIST BWR/4-DBA-1 LPCI Flow Comparison

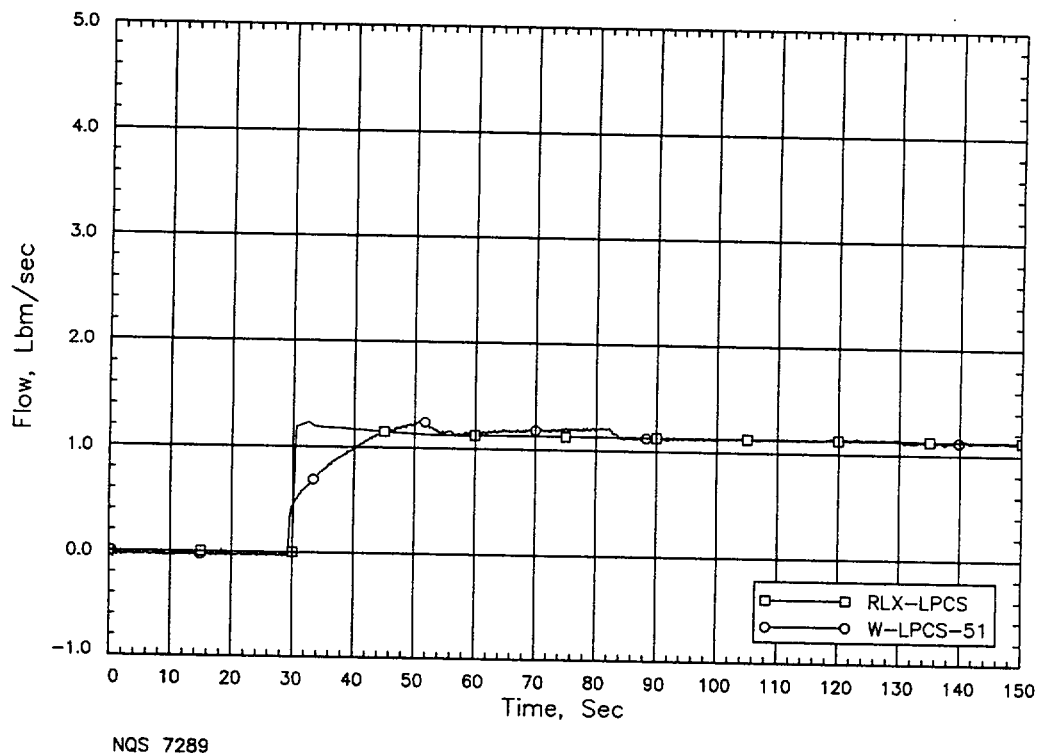
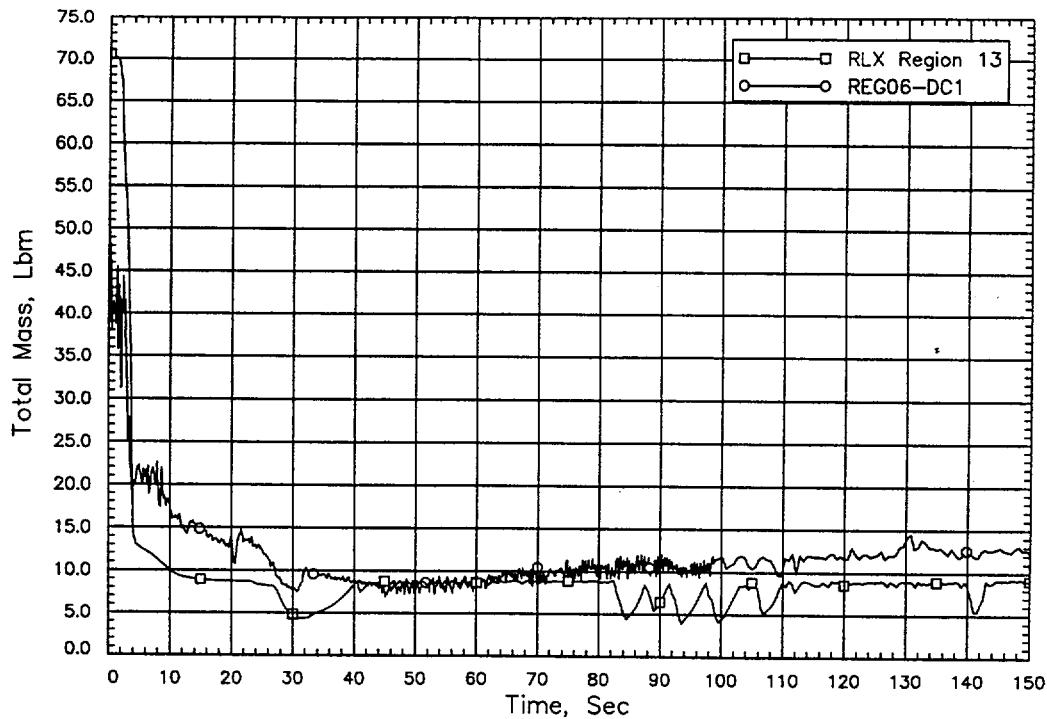
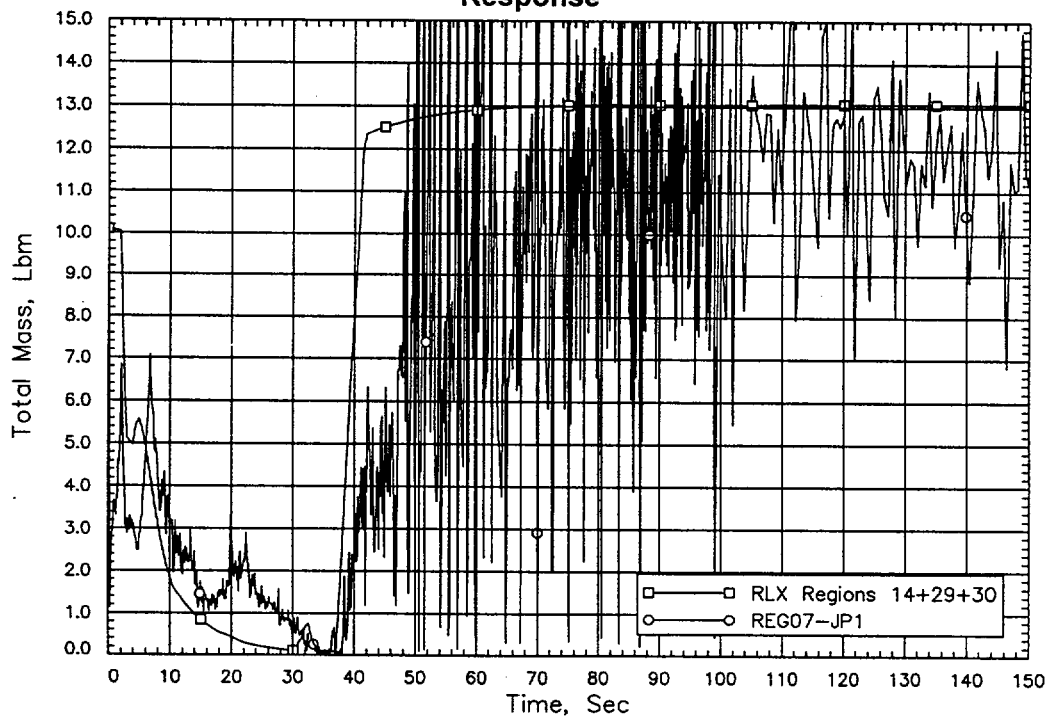


Figure 5.26 FIST BWR/4-DBA-1 LPCS Flow Comparison



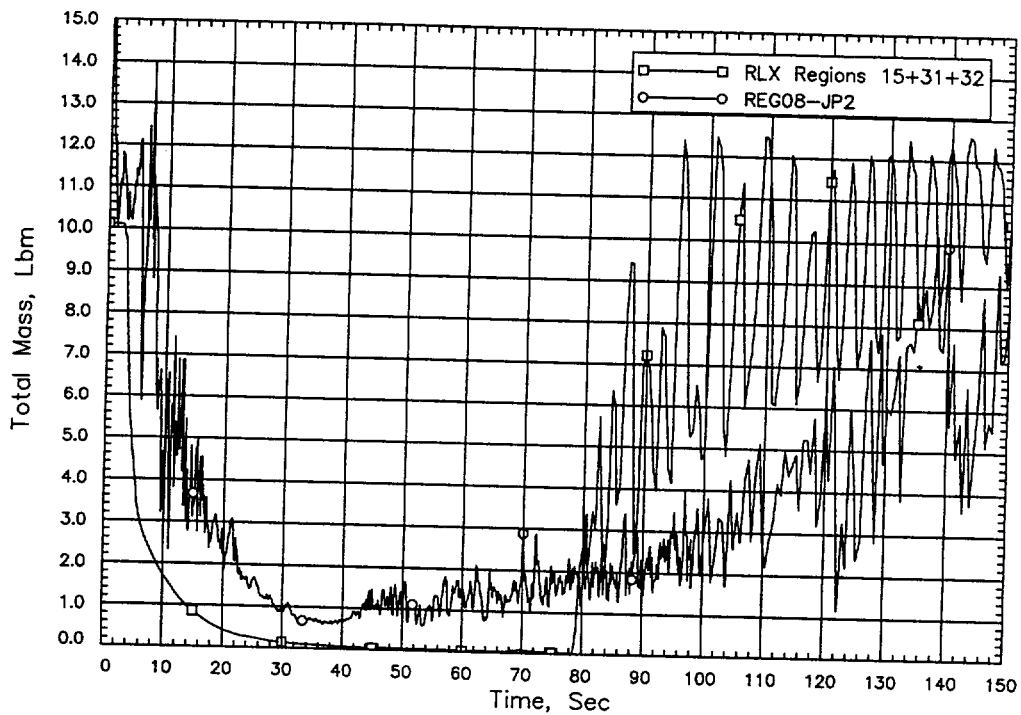
NQS 7289

**Figure 5.27 FIST BWR/4-DBA-1 Lower Downcomer Mass Inventory Response**



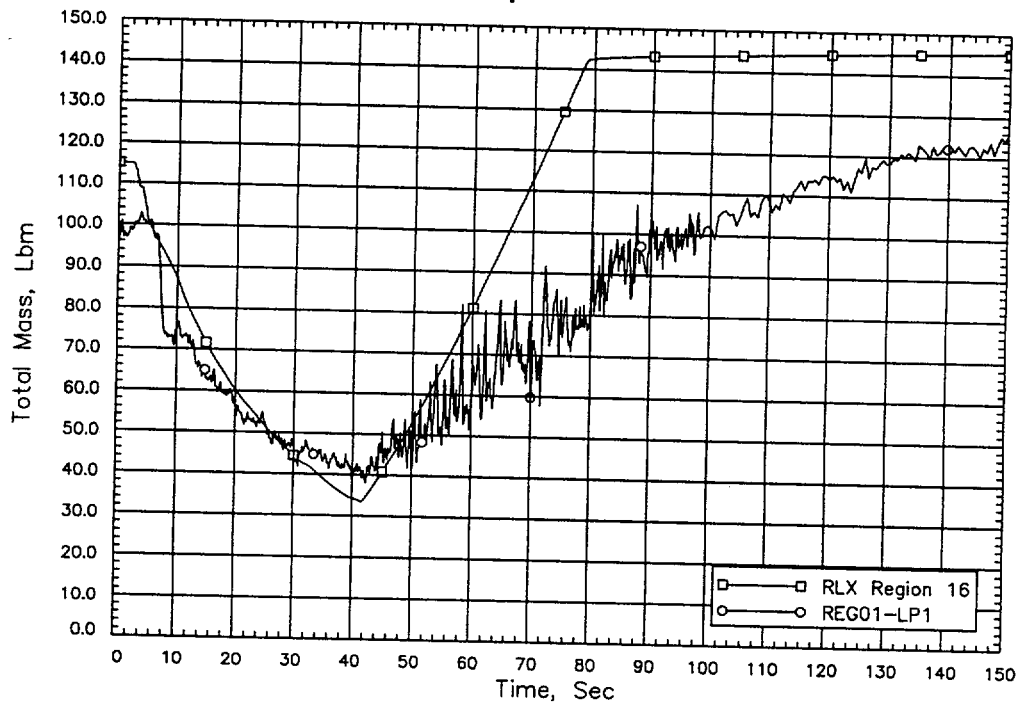
NQS 7289

**Figure 5.28 FIST BWR/4-DBA-1 Jet Pump 1 Mass Inventory Response**



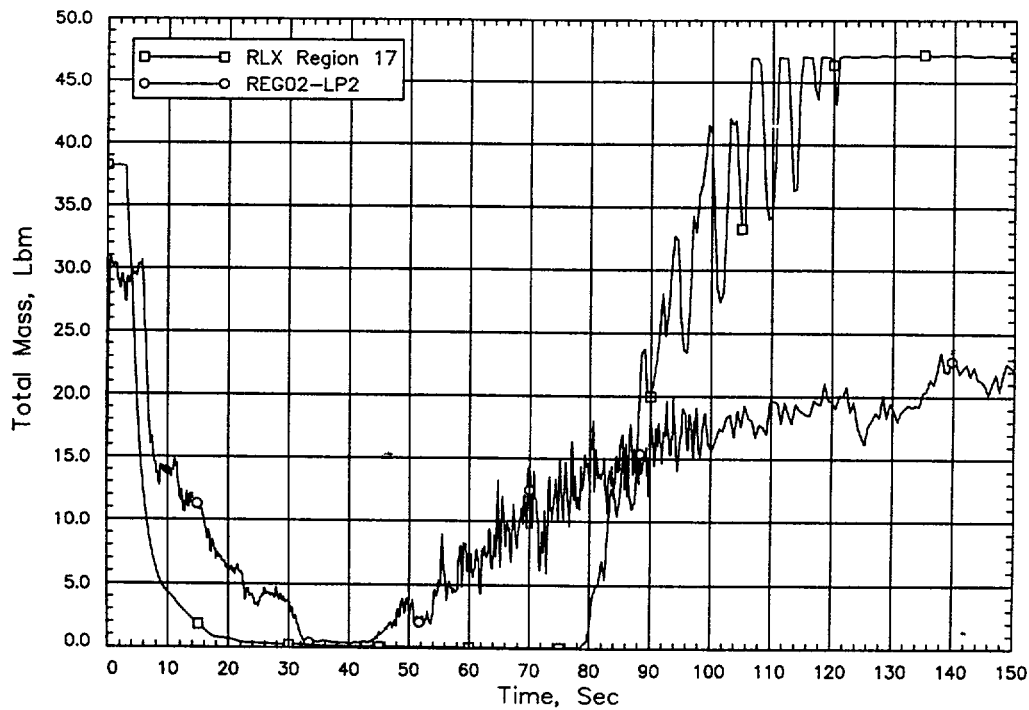
NQS 7289

**Figure 5.29 FIST BWR/4-DBA-1 Jet Pump 2 Mass Inventory Response**



NQS 7289

**Figure 5.30 FIST BWR/4-DBA-1 Lower Lower Plenum Mass Inventory Response**



NQS 7289

**Figure 5.31 FIST BWR/4-DBA-1 Upper Lower Plenum Mass Inventory Response**

**Figure 5.32 FIST BWR/4-DBA-1 Hot Assembly Mass Inventory Response**



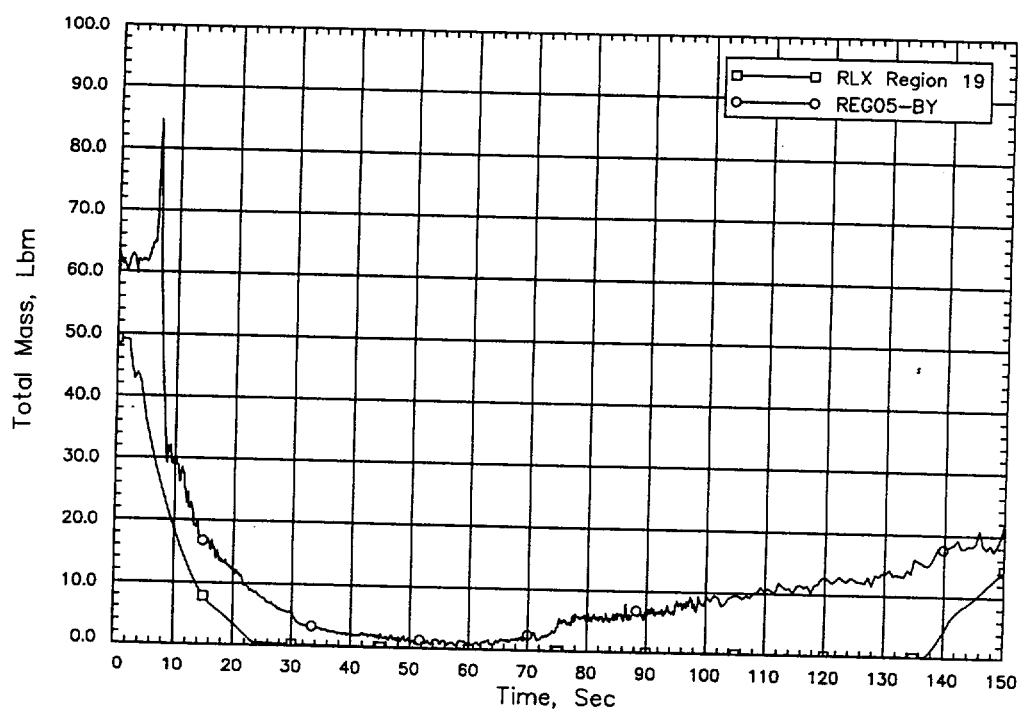


**Figure 5.33 FIST BWR/4-DBA-1 Bypass Region Mass Inventory Response**

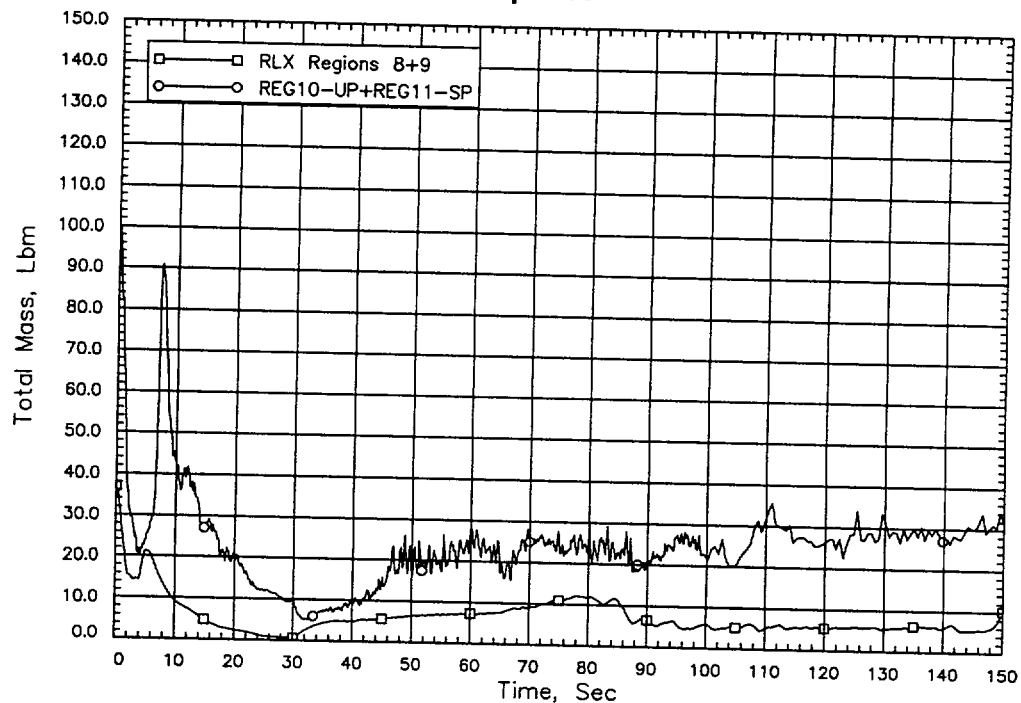


**Figure 5.34 FIST BWR/4-DBA-1 Upper Plenum Mass Inventory Response**

**Figure 5.35 FIST BWR/4-DBA-1 Bundle Mid-Plane Temperature Response**

**Figure 5.36 FIST BWR/4-DBA-1 87-Inch Elevation Temperature Response**

**Figure 5.37 FIST BWR/4-DBA-1 111-Inch Elevation Temperature Response**

### 5.1.3 Small-Break Test 6SB2C

This test simulated a BWR/6 recirculation suction line break of 0.05 ft<sup>2</sup> (0.01227 in<sup>2</sup> actual). The system is configured as in the large-break test with HPCS being injected into the upper plenum and LPCI into the bypass. The event is initiated by the “break” on the suction side of recirculation pump number 2 and coincident power scram, trip of the recirculation pumps, and feedwater flow. The pressure controller maintained the system pressure essentially constant until the MSIV was closed following the Level 1 trip. At approximately 50 seconds after event initiation, the power is essentially all generated by decay heat. The ADS is activated 120 seconds after the Level 1 trip, resulting in system flashing and level swell. As the flashing subsides, the mixture levels fall, uncovering the core region causing the bundle to heatup. In effect, the heatup is the result of the ADS activation.

This test simulated three LPCI systems available. The relatively large LPCI flow into the bypass region condenses sufficient vapor to allow CCFL breakdown at the top of the bypass. Liquid from the upper plenum drains through the bypass region into the lower lower plenum, while CCFL at the upper tie plate and orifice delay bundle reflood. Both top-down and bottom-up refilling (based on rod temperature responses) reflood the bundle. Table 5.3 compares calculated and measured key events.

Figure 5.38 compares the calculated and measured dome pressure response. During the 6-SB-2C test and before the MSIV trip, the dome pressure is controlled. RELAX does not have a similar control system, but by trial and error, a steam line flow as a function of time was specified as a boundary condition that maintained the dome pressure nearly constant at 1048.6 psia up to the time of the MSIV trip (Level 1). The calculated Level 1 trip is 11 seconds later than the measured trip (Table 5.3), resulting in delayed isolation, ADS activation, and depressurization. The reason for the 11 second delay is not known, but it is suspected that the initial water level used in the RELAX calculation, which is derived from a measured water level and corrected for the dryer pressure loss, could be the source. Reducing the initial water level by less than 6 inches could account for as much as a 10-second delay. This difference should have little impact on the calculation because the significant portion of the transient is caused by the ADS activation and, by that time, power and flow have reached steady conditions.

Figures 5.39 and 5.40 compare the measured and calculated jet pump exit flows. These figures show that RELAX accurately calculates the flow response.

Figures 5.41 through 5.48 compares the measured and calculated mass inventories. RELAX closely tracks the jet pump mass inventory response as shown in Figures 5.41 and 5.42. The lower downcomer and lower lower plenum mass inventory responses (Figures 5.43 and 5.44) should be considered together. Up to about 250 seconds, the RELAX and test lower downcomer mass inventories are consistent (Figure 5.43). Before ADS activation, both show a decrease as the mass is depleted through the break. ADS activation shows an increase in fluid mass in the lower downcomer as the depressurization causes a swell from the lower lower plenum (Figure 5.44). The test shows that the lower downcomer mass is relatively constant out to about 285 seconds, while the RELAX calculated mass decreases steadily. This phenomenon is attributed to two effects. First, during this period, the quality at the break is small ( $<0.12\%$ ). At low qualities, the Moody critical flow model is known to over predict the critical flow. Therefore, once saturated conditions exist at the break (post-ADS actuation), the mass depletion rate should be over predicted. Second, out to about 317 seconds, the jet pump suction (Junction 14) becomes vapor flow limited, i.e., essentially only vapor can escape from the lower lower plenum during the flashing period and the lower downcomer liquid mass is not replenished. This effect also is evident in the test data, wherein the lower lower plenum mass is essentially constant from 210 seconds to 280 seconds (Figure 5.44).

Figure 5.45 compares the mass inventory for the upper lower plenum region. The apparent drop in the mass observed in the test during the first 15 seconds is caused by the flow decay when the recirculation pumps are tripped. The offset between the test data and calculation from about 25 seconds to 200 seconds is caused by differences in the volumes modeled. The RELAX upper lower plenum region volume is nearly 32% larger than that defined in the test (the FIST bypass region is correspondingly larger). Except for these differences, the RELAX result compares closely with the test data.

Figure 5.46 provides the bundle mass comparison. The measured and calculated bundle mass agree quite closely, especially after ADS actuation at 200 seconds. Figure 5.46 also shows the hot node mass flow rate along with the reflood criterion and calculated time of reflood.

Figure 5.47 shows the bypass mass inventory comparison. Note that the test data initial mass is larger than that in RELAX. This accounts for the upper lower plenum mass difference

observed in Figure 5.45. The test and calculation show the same trends, with RELAX indicating a more rapid decrease in inventory after ADS actuation. The sudden increase in mass at 350 seconds is caused by CCFL breakdown at the bypass top guide. Once CCFL breakdown has occurred, the liquid mass passes to the lower lower plenum where the vapor begins to collapse. The lower lower plenum region remained full during the event although some voiding is calculated. Thus, with the CCFL breakdown at the top of the bypass, the mass in the upper lower plenum increased almost immediately at 350 seconds (Figure 5.45).

The upper plenum mass comparisons also are favorable, with both the data and RELAX exhibiting the same trends (Figure 5.48).

Figures 5.49 through 5.56 compare calculated and measure rod temperature responses at various elevations within the heated assembly. RELAX temperature responses are included at each elevation and are for information only. The HUXY results appear to be representative of the average of the thermocouples. HUXY applies conservative spray cooling coefficients during the refill or spray cooling period consistent with Appendix K. The spray cooling period is longest for the largest break sizes (most limiting PCTs) for BWRs and decreases for small breaks (significantly lower PCTs). The calculated temperature responses include only minimal conservatism and would not be expected to bound test result variations, particularly in small-break applications. A similar result was noted in Reference 36 when TRAC modeled the same small-break data. In Appendix K licensing-type calculations, two additional sources of conservatism would be available to provide bounding peak clad temperatures. First, 20% conservatism would be included in the decay heat. This would be very important for a break of this magnitude because by the time of ADS actuation all of the energy being generated within the rods is caused by the decay heat. Second, once the clad superheat exceeds 300 °F, a lockout occurs that precludes the reapplication of transition boiling heat transfer coefficients until the calculated time of reflood.

[

]

[

Figure 5.64

1

**Table 5.3 Comparison of SBLOCA Events**



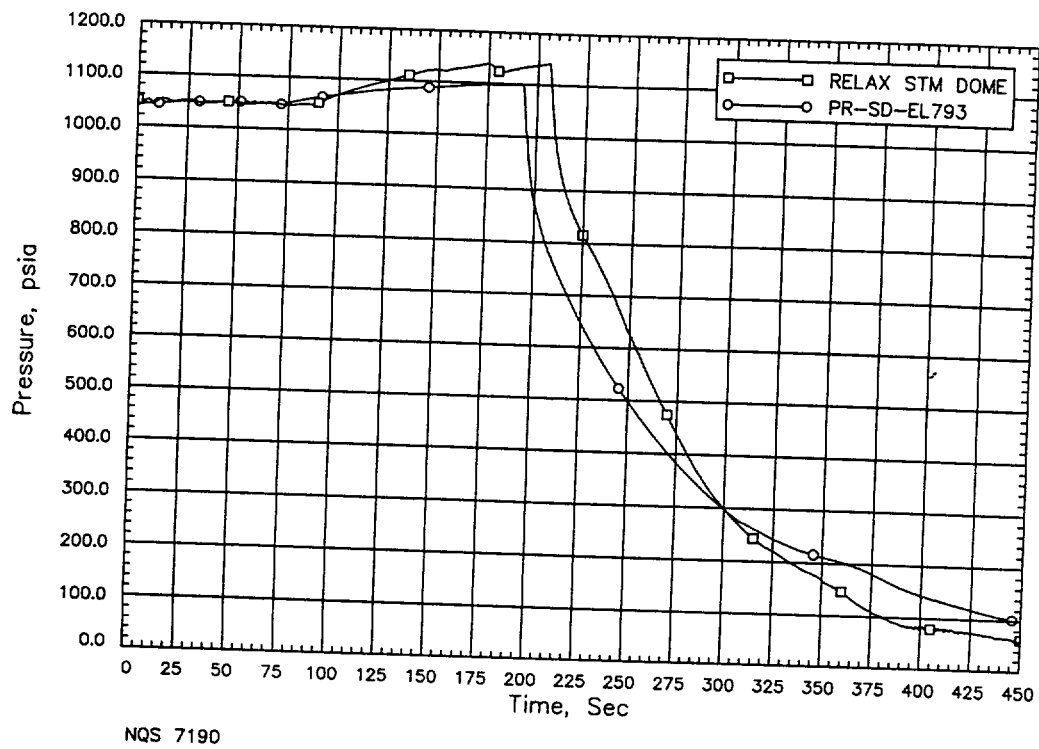


Figure 5.38 FIST BWR/6-SB2-C SBLOCA Dome Pressure Response

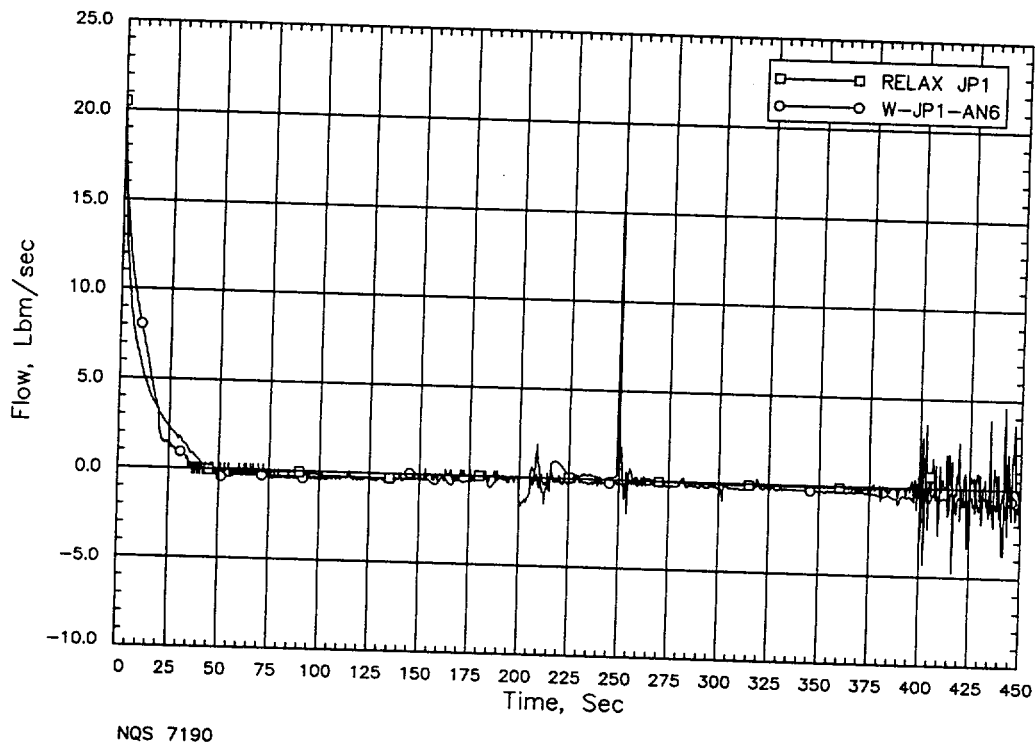
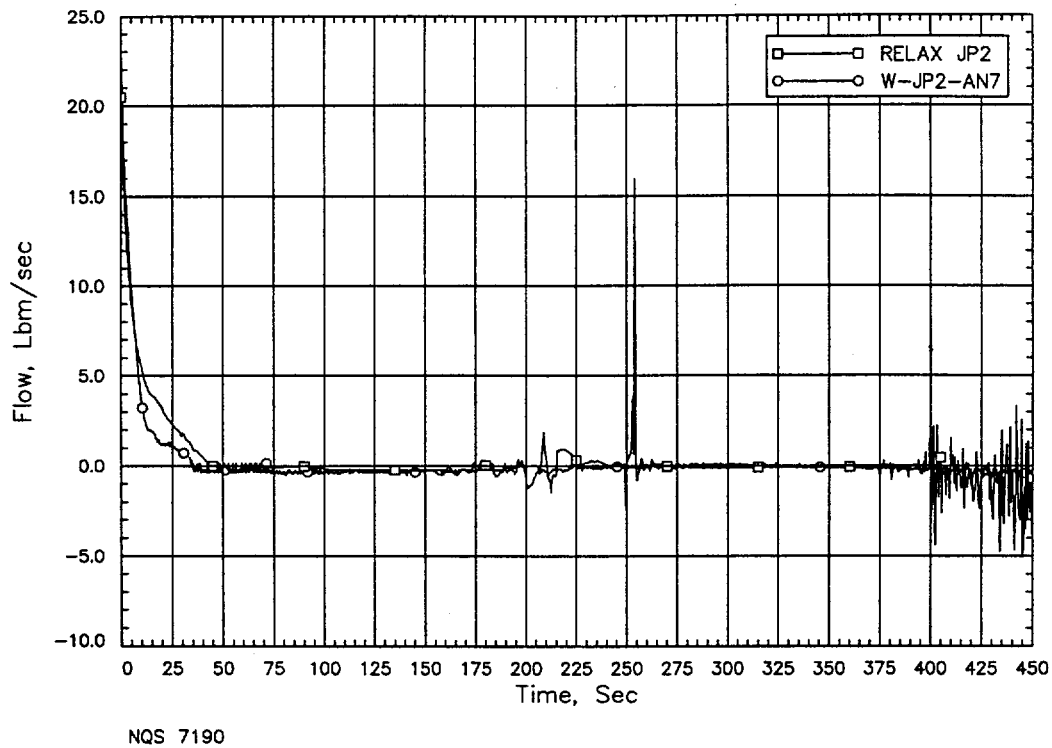
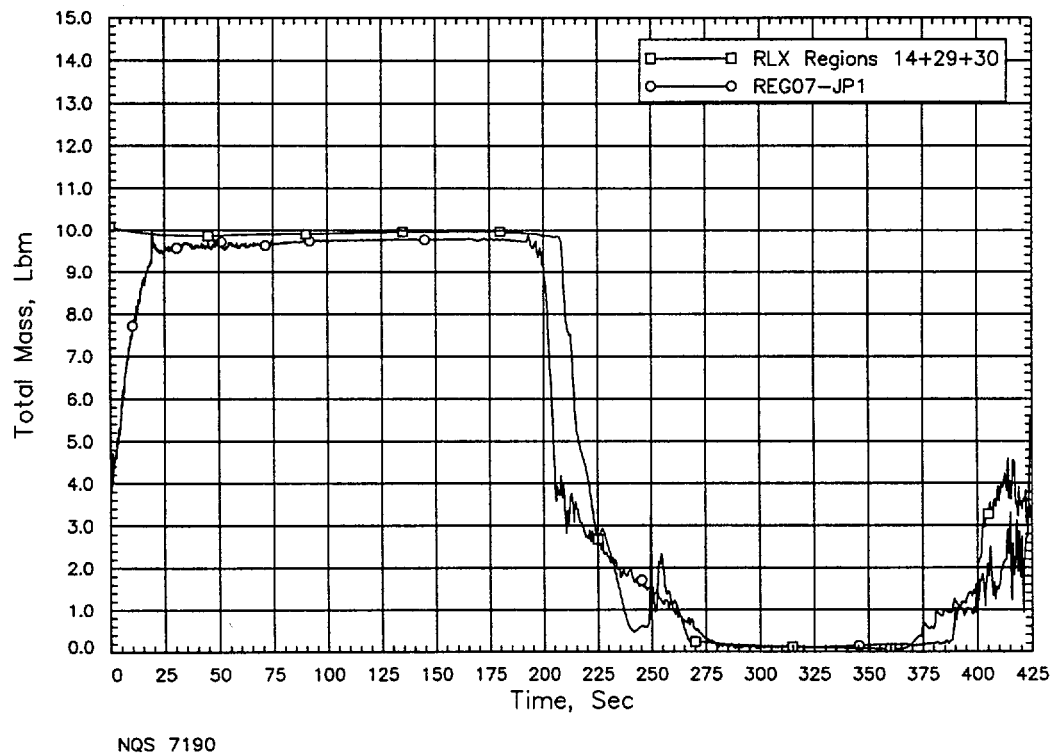


Figure 5.39 FIST BWR/6-SB2-C SBLOCA Jet Pump 1 Flow



**Figure 5.40 FIST BWR/6-SB2-C SBLOCA Jet Pump 2 Flow Response**



**Figure 5.41 FIST BWR/6-SB2-C SBLOCA Jet Pump 1 Mass Inventory**

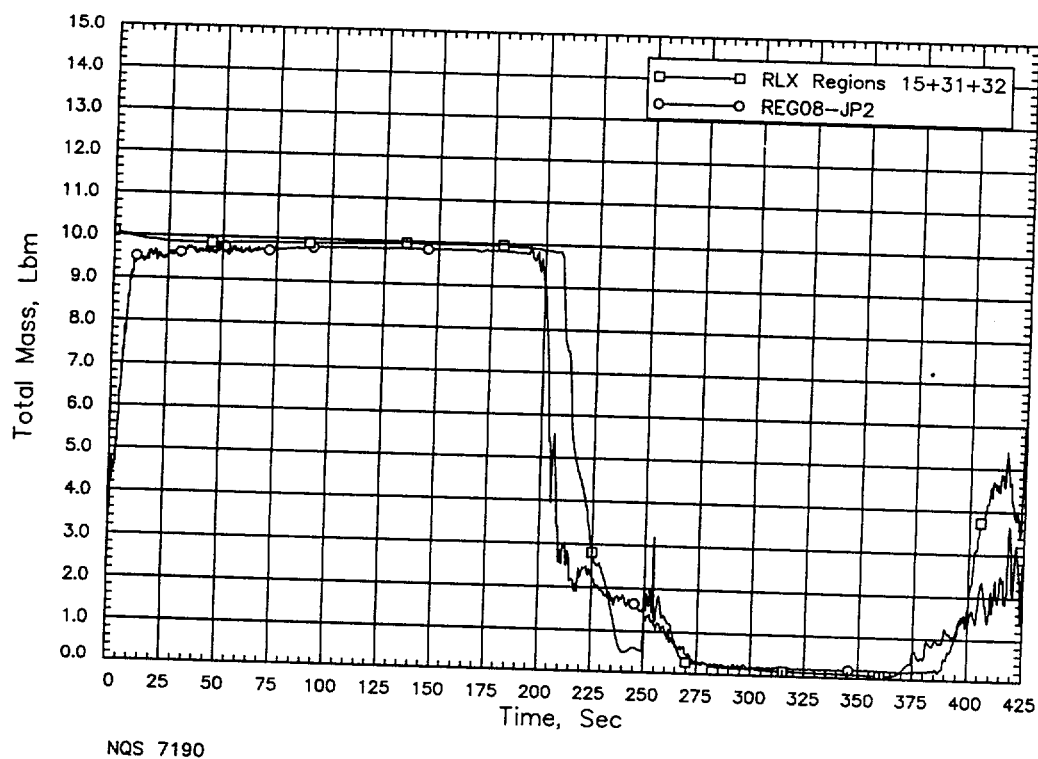


Figure 5.42 FIST BWR/6-SB2-C SBLOCA Jet Pump 2 Mass Inventory

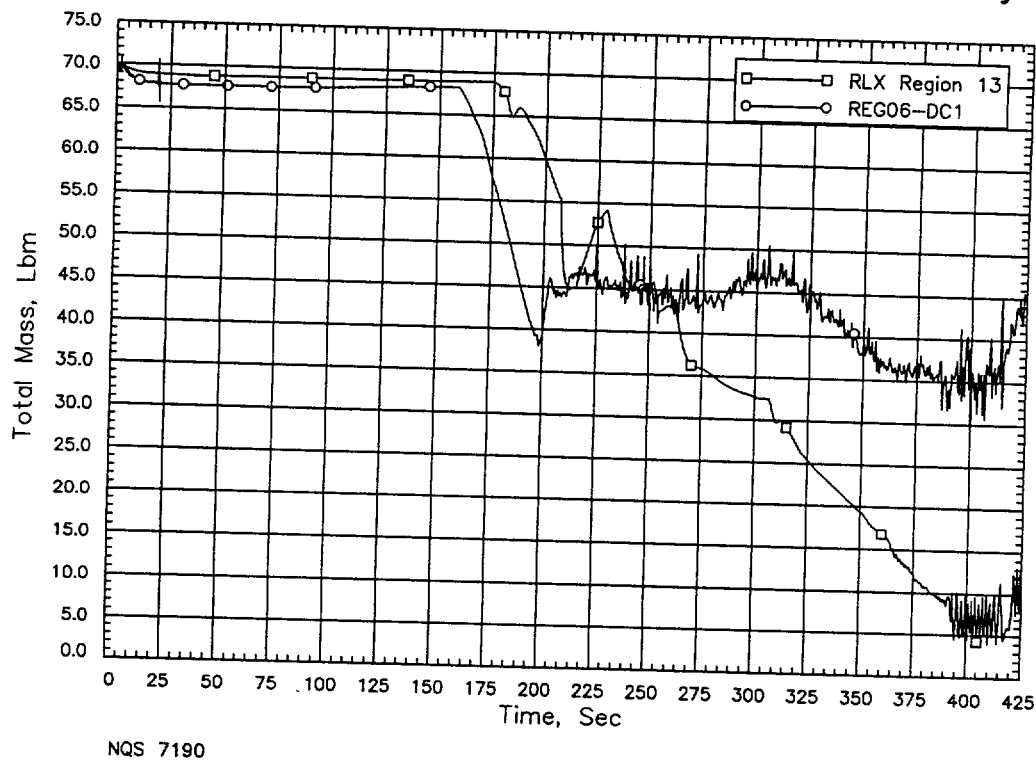
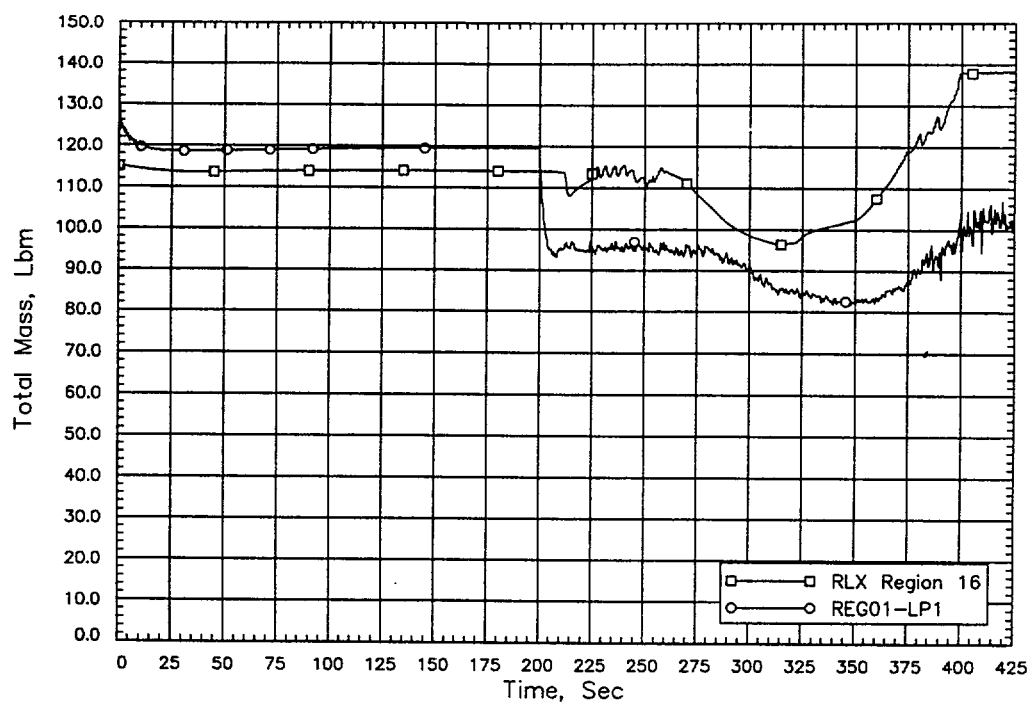
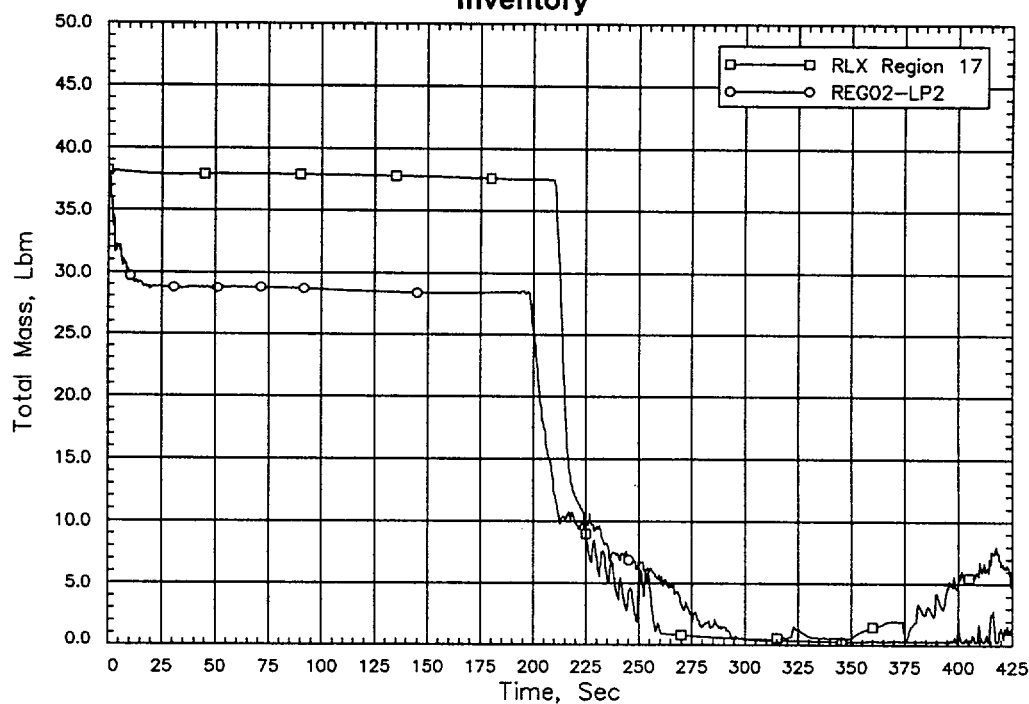


Figure 5.43 FIST BWR/6-SB2-C SBLOCA Lower Downcomer Mass Inventory



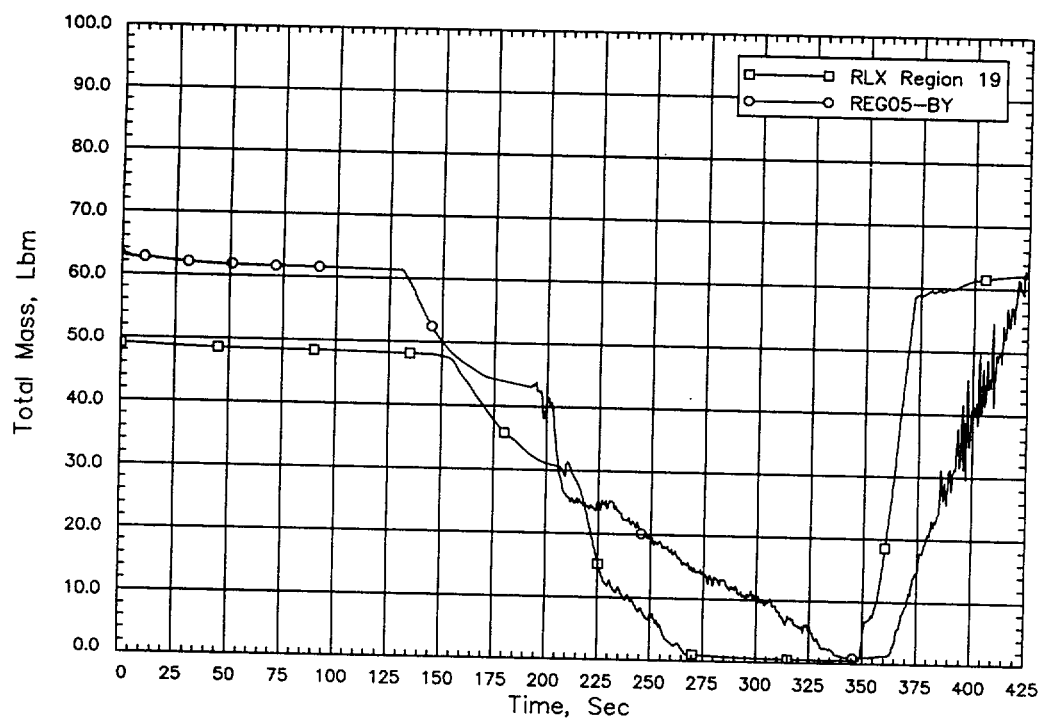
NQS 7190

**Figure 5.44 FIST BWR/6-SB2-C SBLOCA Lower Lower Plenum Mass Inventory**



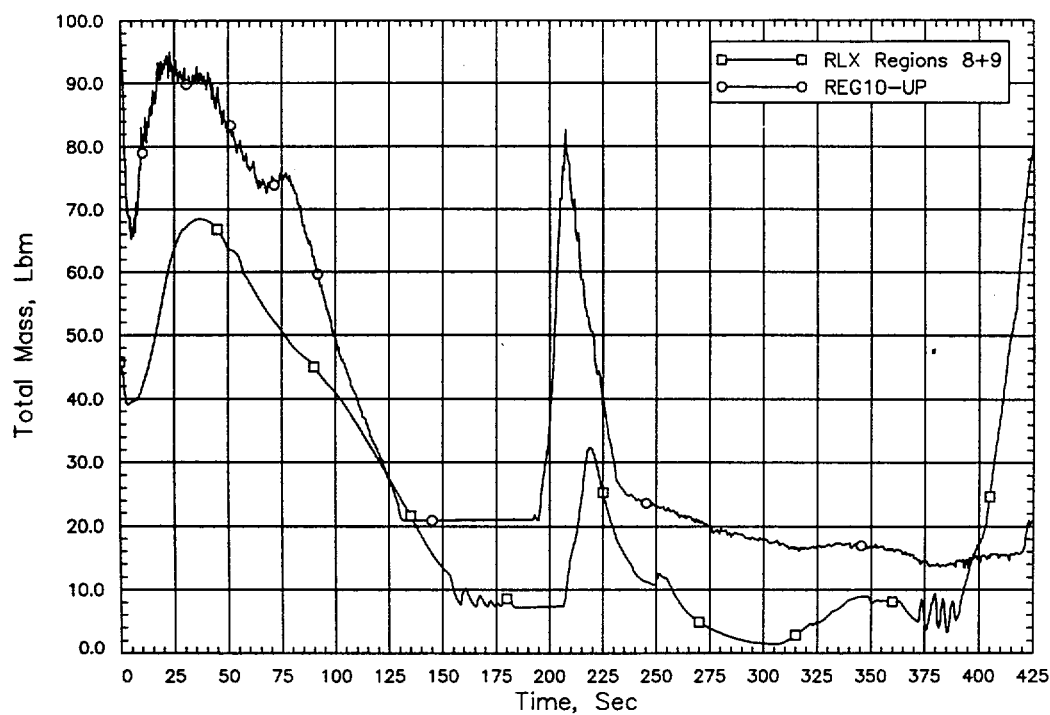
NQS 7190

**Figure 5.45 FIST BWR/6-SB2-C SBLOCA Upper Lower Plenum Mass Inventory**

**Figure 5.46 FIST BWR/6-SB2-C SBLOCA Bundle Mass Inventory**

NQS 7190

**Figure 5.47 FIST BWR/6-SB2-C SBLOCA Bypass Region Mass Inventory**



NQS 7190

**Figure 5.48 FIST BWR/6-SB2-C SBLOCA Upper Plenum Mass Inventory**

**Figure 5.49 FIST BWR/6-SB2-C SBLOCA Temperature Response  
75-Inch Elevation (1 of 3)**

**Figure 5.50 FIST BWR/6-SB2-C SBLOCA Temperature Response  
75-Inch Elevation (2 of 3)**

**Figure 5.51 FIST BWR/6-SB2-C SBLOCA Temperature Response  
75-Inch Elevation (3 of 3)**

**Figure 5.52 FIST BWR/6-SB2-C SBLOCA Temperature Response  
87-Inch Elevation (1 of 4)**

**Figure 5.53 FIST BWR/6-SB2-C SBLOCA Temperature Response  
87-Inch Elevation (2 of 4)**



**Figure 5.54 FIST BWR/6-SB2-C SBLOCA Temperature Response  
87-Inch Elevation (3 of 4)**

**Figure 5.55 FIST BWR/6-SB2-C SBLOCA Temperature Response  
87-Inch Elevation (4 of 4)**

**Figure 5.56 FIST BWR/6-SB2-C SBLOCA Temperature Response  
111-Inch Elevation**

**Figure 5.57 FIST BWR/6-SB2-C SBLOCA EM Temperature Response  
75-Inch Elevation (1 of 3)**

**Figure 5.58 EM Temperature Response 75-Inch Elevation (2 of 3)**

**Figure 5.59 FIST BWR/6-SB2-C SBLOCA EM Temperature Response  
75-Inch Elevation (3 of 3)**

**Figure 5.60 FIST BWR/6-SB2-C SBLOCA EM Temperature Response  
87-Inch Elevation (1 of 4)**

**Figure 5.61 FIST BWR/6-SB2-C SBLOCA EM Temperature Response  
87-Inch Elevation (2 of 4)**

**Figure 5.62 FIST BWR/6-SB2-C SBLOCA EM Temperature Response  
87-Inch Elevation (3 of 4)**

**Figure 5.63 FIST BWR/6-SB2-C SBLOCA EM Temperature Response  
87-Inch Elevation (4 of 4)**

**Figure 5.64 FIST BWR/6-SB2-C SBLOCA EM Temperature Response  
111-Inch Elevation**

#### 5.1.4 Summary of FIST Benchmarks

Best-estimate benchmark calculations of FIST tests 6DB1B, 4DBA1 and 6SB2C were performed using the RELAX code. The hydraulics and mass inventories were conservatively predicted. Large-break (DBA) PCTs are conservatively calculated using best-estimate methods.

SBLOCA PCTs are bound when the conservatism included in the EM methodology is applied. This result is acceptable because small break events are not limiting in BWRs and the test evaluated simulated an extremely small break in which core uncover and the resulting heat-up is minor such that the conservatism (Appendix K coefficients) are not allowed to raise fuel temperature to values of concern.

It is concluded that the SPC methodology using the RELAX code to simulate the blowdown and refill/reflood periods of a LOCA and the HUXY code for the heat-up period will produce conservative PCTs.

#### 5.2 **TLTA Benchmark**

SPC has used the TLTA benchmark to assess the blowdown behavior of RELAX. However, the EXEM BWR-2000 EM has several changes made to the RELAX code, as well as model changes. The latest TLTA benchmark input deck has been modified with the following items.

- Seven evenly spaced core nodes

[

•

]

- EPRI two-phase pump degradation model applied.

The benchmark was run to assess the impact of these changes along with the application of the EXEM BWR-2000 version of RELAX. Figures 5.65 through 5.70 show the results from the blowdown calculation.

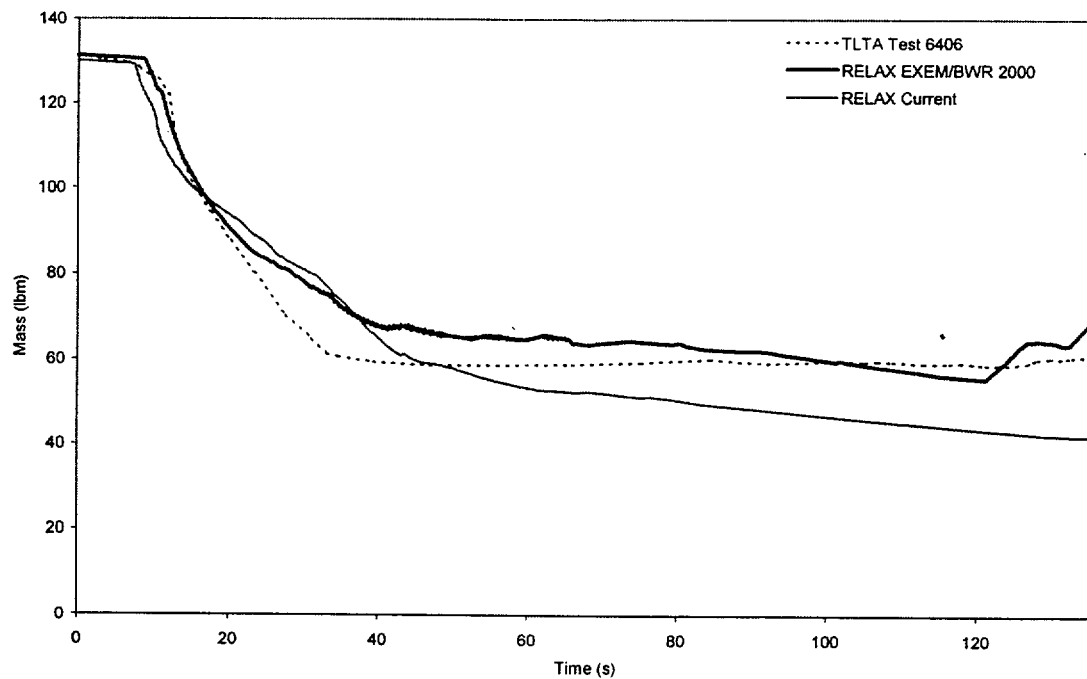


Figure 5.65 TLTA Lower Plenum Mass

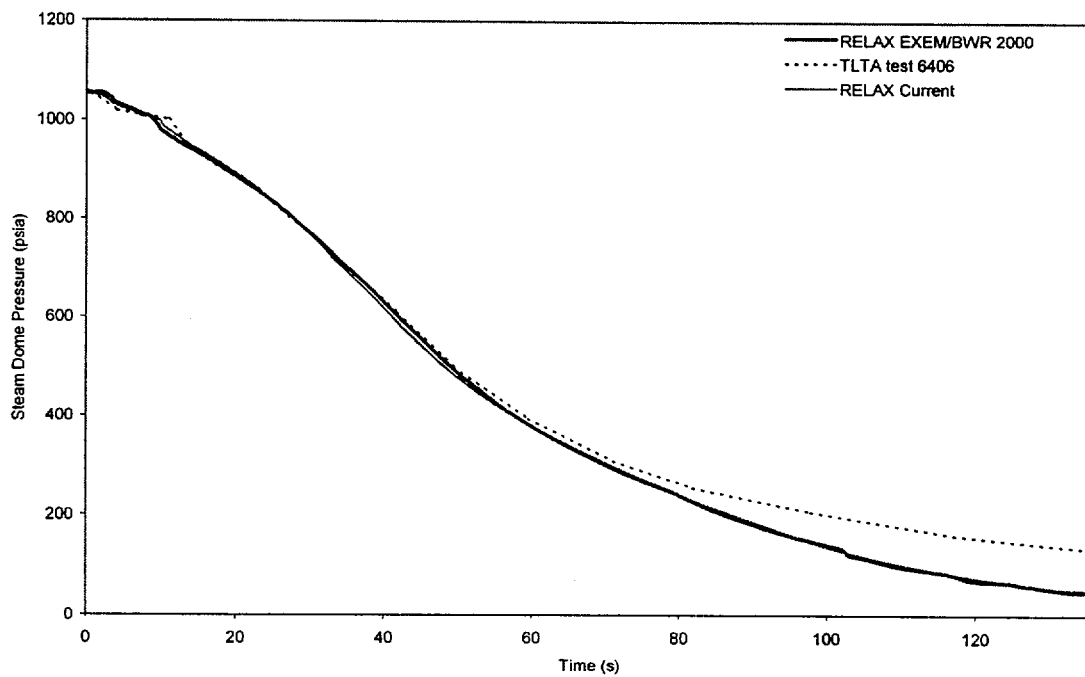


Figure 5.66 TLTA Steam Dome Pressure



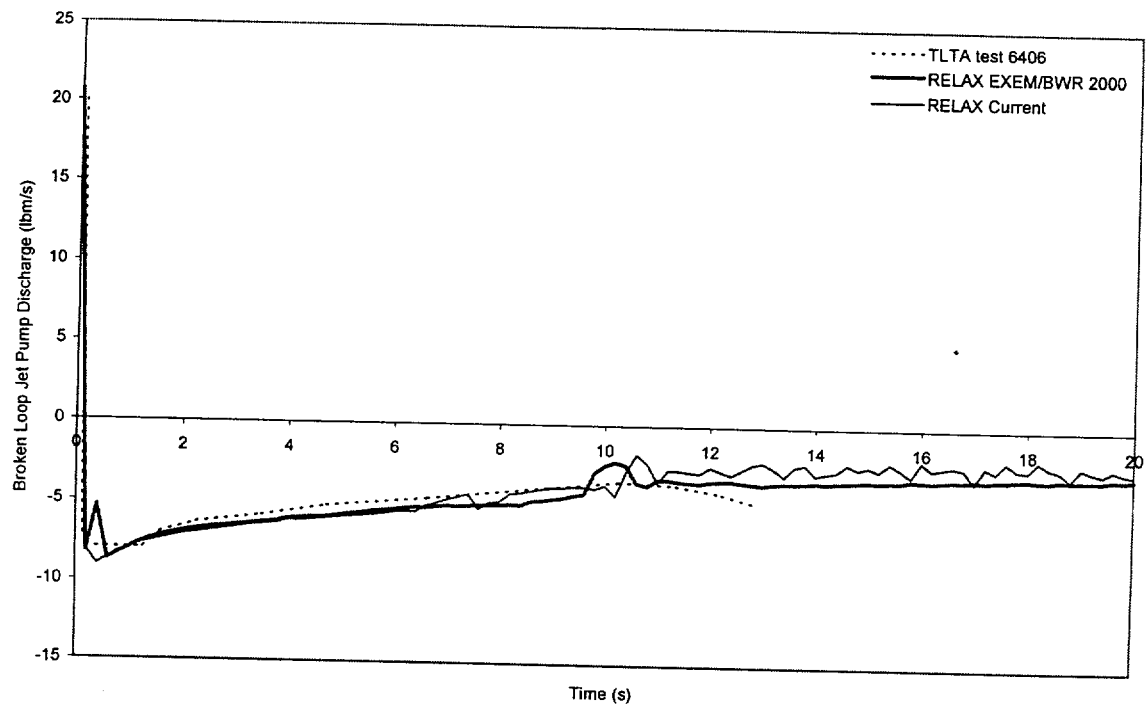


Figure 5.67 TLTA Broken Loop Jet Pump Discharge Flow

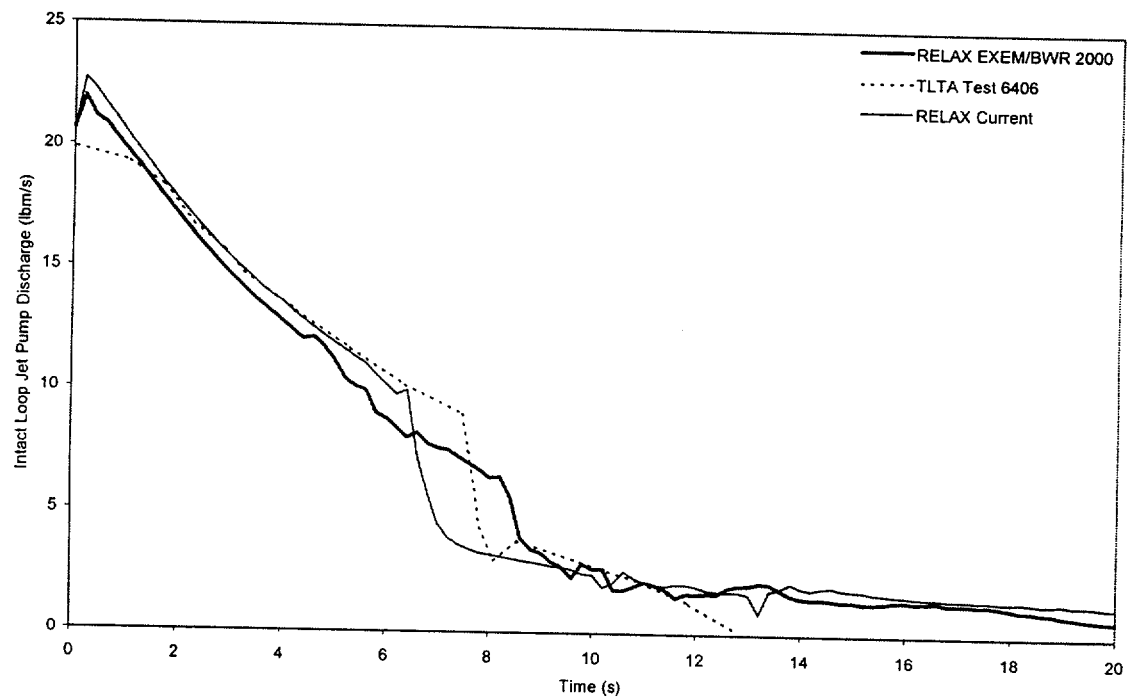
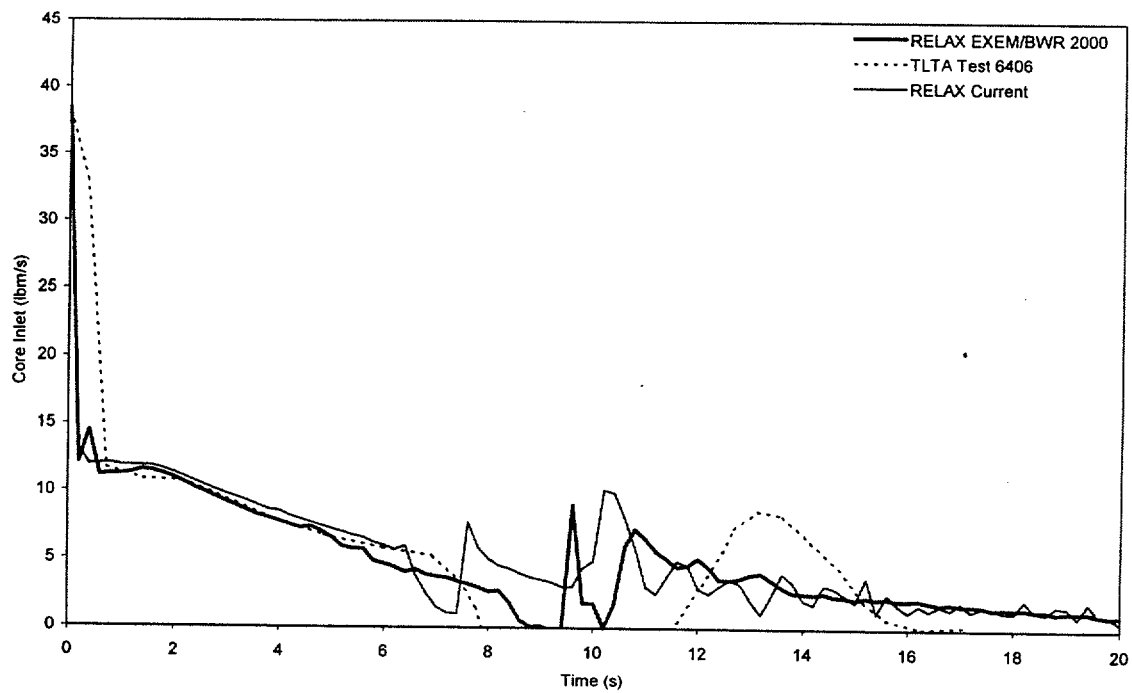
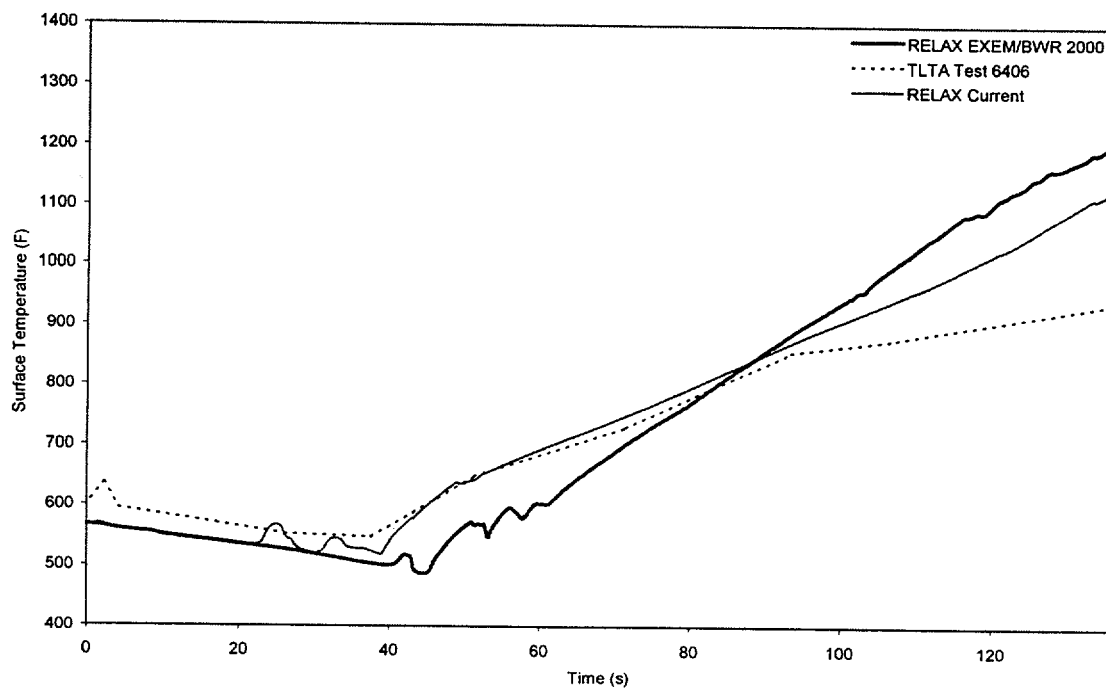


Figure 5.68 TLTA Intact Loop Jet Pump Discharge Flow

**Figure 5.69 Core Inlet Flow****Figure 5.70 Hottest Core Temperature**

The following conclusions can be drawn from the TLTA benchmark comparisons.

- EXEM BWR-2000 predicts measured behavior and trends as well or better than the EXEM/BWR evaluation model.
- The EXEM BWR-2000 predicts the lower plenum inventory closer to the data than EXEM/BWR.
- The EXEM BWR-2000 predicts steam dome pressure experimental data more accurately than EXEM/BWR.
- The figures show that the jet pump discharge flows are similar to the EXEM/BWR prediction and follow the trends of the measured data.
- The EXEM BWR-2000 predicts core inlet flow similar to the EXEM/BWR.
- The hottest core temperature predicted by the EXEM BWR-2000 shows a delayed heatup, but by the end of the blowdown, the final temperature is significantly more conservative than the test data.

The blowdown calculation of the TLTA benchmark produces the expected results. As mentioned, lower plenum inventory, as well as steam dome pressure, are predicted better by EXEM BWR-2000 than the EXEM/BWR EM. Other parameters are similar to, but show minor differences from, EXEM/BWR results, but the results exhibit acceptable physical trends. The hottest nodal temperature predicted by RELAX using EXEM BWR-2000 is conservative with respect to data.

## 6.0 References

### 6.1 Model References (Roadmap)

1. NUREG-1230, *Compendium of ECCS Research for Realistic LOCA Analysis*, U. S. Nuclear Regulatory Commission, December 1988.
2. XN-NF-929(P)(A) and Supplements 1 through 4, *Spray Heat Transfer Coefficients for Jet Pump BWR Fuel Assemblies with Water Rods*, Advanced Nuclear Fuels Corporation, March 1992.
3. XN-235(A), *Exxon Nuclear Evaluation Model for BWR Loss of Coolant Accidents*, Exxon Nuclear Company, January 1986.
4. XN-75-55(A) Revision 2 and Supplements 1 and 2, *The Exxon Nuclear Company WREM-Based NJP-BWR ECCS Evaluation Model and Application to the Oyster Creek Plant*, Exxon Nuclear Company, April 1976.
5. XN-NF-80-19(P)(A) Volumes 2, 2A, 2B, and 2C, *Exxon Nuclear Methodology for Boiling Water Reactors: EXEM BWR ECCS Evaluation Model*, Exxon Nuclear Company, September 1982.
6. ANF-91-048(P)(A), *Advanced Nuclear Fuels Corporation Methodology for Boiling Water Reactors EXEM BWR Evaluation Model*, Advanced Nuclear Fuels Corporation, January 1993.
7. ANF-91-048(P)(A) Supplements 1 and 2, *BWR Jet Pump Model Revision for RELAX*, Siemens Power Corporation, October 1997.
8. XN-76-44(A), *Revised Nucleate Boiling Lockout for ENC WREM-Based ECCS Evaluation Models*, Exxon Nuclear Company, February 1977.
9. XN-NF-82-07(P)(A) Revision 1, *Exxon Nuclear Company ECCS Cladding Swelling and Rupture Model*, Exxon Nuclear Company, November 1982.
10. XN-NF-81-58(P)(A) Revision 2 and Supplements 1 and 2, *RODEX2 Fuel Rod Thermal-Mechanical Response Evaluation Model*, Exxon Nuclear Company, March 1984.
11. 10 CFR 50.46, *Acceptance Criteria for Emergency Core Cooling Systems for Light Water Reactors*, Code of Federal Regulations, Title 10 "Energy," Part 50.46.
12. 10 CFR 50 Appendix K, *ECCS Evaluation Models*, Code of Federal Regulations, Title 10, "Energy," Part 50, Appendix K.
13. XN-CC-33(A) Revision 1, *HUXY: A Generalized Multirod Heatup Code with 10 CFR 50 Appendix K Heatup Option User's Manual*, Exxon Nuclear Company, November 1975.
14. XN-75-41(A) Volume 1, Volume II, Volume II Appendices, Volume III Revision 2, Supplements 1, 2, 3, 4, 5 Revisions 1, 6 and 7, *Exxon Nuclear Company WREM-Based PWR ECCS Evaluation Model*, Exxon Nuclear Company, February 1986.

15. NUREG-75/056 Revision 1, *WREM: Water Reactor Evaluation Model*, Nuclear Regulatory Commission, May 1975.
16. XN-NF-85-92(P)(A), *Exxon Nuclear Uranium Dioxide/Gadolinia Irradiation Examination and Thermal Conductivity Results*, Exxon Nuclear Company, November 1986.
17. ANCR-1127, *RELAP4 - A Computer Program for Transient Thermal-Hydraulic Analysis*, Aerojet Nuclear Company, December 1973.
18. "Evaluation of LOCA Hydrodynamics," Regulatory Staff: Technical Review, U. S. Atomic Energy Commission, November 1974.
19. ANF-CC-33(P)(A) Supplement 2, *HUXY: A Generalized Multirod Heatup Code with 10 CFR 50 Appendix K Heatup Option*, Advanced Nuclear Fuels Corporation, February 1991.
20. XN-NF-80-19(P)(A) Volume 1 and Supplements 1 and 2, *Exxon Nuclear Methodology for Boiling Water Reactors - Neutronic Methods for Design and Analysis*, Exxon Nuclear Company, March 1983.
21. XN-NF-80-19(P)(A) Volume 1 and Supplement 3, Supplement 3 Appendix F, and Supplement 4, *Advanced Nuclear Fuels Methodology for Boiling Water Reactors: Benchmark Results for the CASMO-3G/MICROBURN-B Calculation Methodology*, Advanced Nuclear Fuels Company, November 1990.
22. XN-75-32(P)(A) Supplements 1 through 4, *Computational Procedure for Evaluating Fuel Rod Bowing*, Exxon Nuclear Company, October 1983. (Base document not approved.)
23. K. Ohkawa and R. T. Lahey, Jr., "The Analysis of Proposed BWR Inlet Flow Blockage Experiments in PBF," NES-486, Rensselaer Polytechnic Institute, Troy, New York 12181, December 1978.
24. ANF-1125(P)(A) Supplement 1, Appendix E, *ANFB Critical Power Correlation Determination of ATRIUM-9B Additive Constant Uncertainties*, Siemens Power Corporation, September 1998.

## 6.2 Other References

25. Letter, J.H. Nordahl (SPC) to Director, Office of Environment (NRC), "Siemens Power Corporation - Nuclear Division Responses to the Demand for Information, Notice of Nonconformance and Unresolved Items (Inspection Report 99900081/97-01)," February 14, 1998.
26. EMF-2087(P)(A), *SEM/PWR-98: ECCS Evaluation Model for PWR LBLOCA Applications*, Siemens Power Corporation, June 1999.
27. EPRI NP-1556, Volumes 1 through 8, *Pump Two-Phase Performance Program*, September 1980.

28. W. Kastner and G. J. Seeberger, "Pump Behavior and Its Impact on a Loss-of-Coolant Accident in a Pressurized Water Reactor," *Nuclear Technology*, Volume 60, Jct. 1983, pp. 268-277.
29. EMF-CC-102(P), *HUXY: A Generalized Multirod Heatup Code, User's Manual Updated for ATRIUM-10 and Part Length Rod Fuel Designs*, Siemens Power Corporation, February 1995.
30. E-Q766-882-1, *Evaluation of FCTF 9x9Q Entrainment Tests*, Siemens Power Corporation – Nuclear Division, July 18, 1996.
31. EMF-SDR-129(P), *RELAX Users Manual ddec99*, Siemens Power Corporation, March 2000.
32. J. F. Wilson, R. J. Grenda, J. F. Patterson, "The Velocity of Rising Steam in a Bubbling Two-Phase Mixture," *Transactions of the American Nuclear Society, 1962 Annual Meeting*, Boston, Massachusetts, June 18-21, 1962.
33. P. G. Barnett, A Correlation of Rod Burnout Data for Uniformly Heated Annuli and Its Use for Predicting Burnout in Uniformly Heated Rod Bundles, AEEW-R 463 (1966).
34. E. D. Hughes, A Correlation of Rod Bundles Critical Heat Flux for Water in the Pressure Range of 150 to 725 psia, IN-1412 (July 1970).
35. NUREG/CR-2576, BWR (Boiling Water Reactor) Full Integral Simulation Test (FIST) Program Facility Description Report, General Electric Co., September 1984.
36. NUREG/CR-3711, BWR (Boiling Water Reactor) Full Integral Simulation Test (FIST) Phase 1 Test Results, General Electric Co., September 1984.
37. NUREG/CR-4128, BWR (Boiling Water Reactor) Full Integral Simulation Test (FIST) Phase 2 Test Results and TRAC-BWR (Transient Reactor Analysis Code) Model Qualification, General Electric Co., October 1985.
38. NUREG/CR-2229, Vol.2, *BWR Large Break Simulation Tests – BWR Blowdown*, Electric Power Research Institute, March 1981.

## **Distribution**

### **Controlled Distribution**

#### Richland

H. D. Curet  
S. C. Franz  
S. E. Jensen  
C. J. Lewis

### **E-Mail Notification**

#### Richland

D. G. Carr  
D. J. Denver  
R. L. Feuerbacher  
M. E. Garrett  
C. E. Hendrix  
J. G. Ingham  
J. F. Mallay  
R. S. Reynolds  
R. R. Schnepf